Natural Resources Canada Ressources naturelles Canada

GEOLOGICAL SURVEY OF CANADA
OPEN FILE 8390

Petroleum, mineral, and other resource potential in the offshore Pacific, British Columbia, Canada

R. Ferguson, H.M. King, K. Kublik, K.M.M. Rohr, L. Kung, C.J. Lister, M. Fustic, N. Hayward, T.A. Brent, and Y. Jassim

2018

Canada

GEOLOGICAL SURVEY OF CANADA
OPEN FILE 8390

Petroleum, mineral, and other resource potential in the offshore Pacific, British Columbia, Canada

R. Ferguson, H.M. King, K. Kublik, K.M.M. Rohr, L. Kung, C.J. Lister, M. Fustic, N. Hayward, T.A. Brent, and Y. Jassim

2018

Permanent link: https://doi.org/10.4095/308395

This publication is available for free download through GEOSCAN (http://geoscan.nrcan.gc.ca/).

Recommended citation
Ferguson, R., King, H.M., Kublik, K., Rohr, K.M.M., Kung, L., Lister, C.J., Fustic, M., Hayward, N., Brent, T.A., Jassim, Y., 2018. Petroleum, mineral, and other resource potential in the offshore Pacific, British Columbia, Canada; Geological Survey of Canada, Open File 8390, 82 p. https://doi.org/10.4095/308395

Publications in this series have not been edited; they are released as submitted by the author.

TABLE OF CONTENTS

EXECUTIVE SUMMARY

The Government of Canada is implementing marine conservation measures as part of its obligations under the United Nations Convention on Biodiversity. Canada has committed to conserve 10% of sovereign marine and coastal waters by 2020 under the Marine Conservation Targets[1] (MCT) initiative led by Fisheries and Oceans Canada (DFO). As part of this initiative, DFO requested that Natural Resources Canada (NRCan) conduct an assessment of petroleum resource potential for the proposed Pacific Offshore Marine Conservation Target (MCT) and surrounding regions. The NRCan study, by the Geological Survey of Canada (GSC), also identifies areas likely to contain mineral resources, geothermal potential, and capacity for carbon capture and storage in the offshore Pacific.

The study area encompasses approximately 200 000 km^2 west of Vancouver Island, in 150 to 3600 m water depth (Figures 1 and 2). Information compiled, produced and reviewed for this report are included in appendices, including: Glossary of Terms (Appendix A), Industry and Scientific Activities (Appendix B), Geological Detail (Appendix C), Qualitative assessment Detail: Petroleum, Minerals and Other Resources (Appendix D), and Reviewed or Referenced Documents (Appendix E). The NRCAN study was conducted between January 2017 and December 2017. The relatively short time available to evaluate this large, previously unassessed area impacted the depth of analyses. The evaluation relied heavily on existing literature for some aspects of the assessment where data coverage was sparse.

Conventional Petroleum Resource Potential

The 2017 GSC qualitative petroleum assessment of the offshore Pacific builds on previous quantitative petroleum potential studies done in the adjacent northwest areas of Winona and Tofino sedimentary basins (Hannigan et al, 2005). The present study summarises relative petroleum resource potential and does not provide a quantitative assessment of in-place petroleum resources. The petroleum assessment included evaluations of six petroleum play types in five tectonic regions: Pacific Plate, Explorer Plate, Juan de Fuca Plate, Winona Basin and the Cascadia Accretionary Complex (Figures 1 and 2). Data coverage, geological features, basin fill age and rock type in the study area are shown in Figures 3, 4, and 5, and discussed in Appendices B and C.

The interpretation of conventional petroleum resource potential, visually represented by a qualitative potential map (Figure 1), indicates the following:

A large part of the study area, including most of the **Pacific Plate,** has very low potential or no potential for conventional petroleum resources. Low petroleum potential occurs in the easternmost areas of the **Juan de Fuca Plate and Explorer Plate (**Figure 2**)**, where thicker Miocene and/or Pliocene to Recent sedimentary fill has potential for hydrocarbons in structural and stratigraphic plays. Areas of moderate petroleum potential occur in two regions (Figures 1 and 2): **Winona Basin,** which contains up to 10 km of Pliocene (or older) to Recent sedimentary fill with petroleum potential in structural and stratigraphic plays; and the **Accretionary Complex,** which contains up to 6 km of deformed Miocene to Recent sedimentary fill with petroleum potential in structural and stratigraphic plays.

Based on existing data, there are no parts of the study area with high potential for conventional petroleum resources.

[1] The Marine Conservation Targets (MCT) initiative provides targeted funding to Environment and Climate Change Canada (represented by the Parks Canada Agency), Fisheries and Oceans Canada (DFO), and Natural Resources Canada (NRCan) as part of the Government of Canada's commitment to conserve 10% of Canada's marine and coastal waters within the 200 nautical mile limit by 2020.

Unconventional Petroleum Resource Potential

Unconventional gas potential occurs in hydrate deposits in the Winona Basin and Accretionary Complex regions (Figures 2 and 6). Despite significant advances in marine gas hydrate geophysical characterization and gas production research, hydrates in marine settings remain a globally unproven exploitable natural gas source (see Appendix D).

Mineral Resource Potential

Advancements in the field of deep sea mining (e.g. first deep sea minerals mined in offshore Japan in September 2017) indicate that such activities are feasible in water depths encountered in the study area. Reviews of study area data indicate areas likely to contain one or more of the three marine mineral deposits types considered (Figure 7). These areas have the geological conditions suitable for the occurrence of significant concentrations of the specified mineral(s). Mineral grade, tonnage, and economic factors have not been determined or estimated in this report.

Volcanogenic Massive Sulphide (VMS) deposits

VMS deposits form around hydrothermal vents or hot springs at the seafloor and often contain high concentrations of iron, copper, zinc and precious metals. VMS deposits are present within the study area and areas likely to contain VMS deposits are identified where seafloor spreading centres and active or inactive hydrothermal vent fields are present (Figure 7). The only known active seafloor spreading centres with hydrothermal vent fields in Canada's offshore occur within the study area.

Ferromanganese and Manganese Crusts

Ferromanganese and manganese crusts often contain high concentrations of cobalt, nickel, other precious metals and rare earth elements. Areas likely to contain ferromanganese and manganese crust deposits are associated with seamounts in the study area (Figure 7), and in adjacent areas to the north and west.

Manganese Nodules

Manganese nodules contain high concentrations of copper, nickel and rare earth elements. A limited area that is likely to contain manganese nodule deposits occurs in the study area, where the seabed descends below 3500 m water depth (Figure 7). A much larger area with geologic conditions suitable for the presence of manganese nodules is identified in Canadian waters north of the study area.

Other Potential Geological Resources/Activities

Marine Geothermal Energy

Recent investigations in many countries indicate the potential for marine geothermal energy generation at sea floor spreading ridges. In 2017, Iceland, which has an aerially exposed seafloor spreading centre, granted its first marine geothermal exploration licences. Active seafloor spreading centres with conditions suitable for clean, green geothermal energy generation in the future (when the necessary technologies are developed), are present in the Pacific offshore study area (Figure 6). These seafloor spreading centres are the only known marine areas in Canada with geothermal energy potential. Hot springs with geothermal potential are present on land, but the electricity generation potential at seafloor spreading centres may be at least an order of magnitude larger than for onshore areas, when the technologies are developed.

Carbon Capture and Storage

Many countries are adopting or evaluating Carbon Capture and Storage (CCS) opportunities to offset carbon dioxide (CO_2) emissions from fossil fuel-powered plants, smelters and other high emission industries. In 2016, Iceland became the first country to reinject produced CO_2 from geothermal plants into basalt, where the carbon precipitates into a solid, nontoxic mineral. Studies have determined there are large areas of basaltic seafloor off the US west coast that might store as much as 150 years of US CO_2 production through CCS. Land-based CCS reservoirs more typically consist of porous sedimentary rocks where CO_2 stays in a gaseous form and requires long term monitoring to keep the gases from escaping.

Areas with geological conditions that are conducive to future CCS are identified in sediment covered regions of the Pacific, Explorer and Juan de Fuca plates in the study area (Figure 6). Further work to evaluate seabed and shallow sediment sealing capacity is needed. Suitability for CCS north of the study area has not been assessed, but the absence of young spreading centres suggests that the best young basaltic CCS reservoirs occur within the study area.

Final Comments

The findings of this report are based on existing data, reports and publications that were available to the team at the time of the study. Study findings might change when new or additional data become available. Issues of potential economic value in the study area cannot be fully assessed or evaluated based on current knowledge. That said, there is some Canadian and international academic work currently underway that is focused on emerging opportunities such as marine geothermal potential and CCS.

1.0 INTRODUCTION

This report summarizes the qualitative assessment of petroleum potential and identifies areas that are likely to contain minerals and other resources (geothermal energy, and capacity for carbon capture and storage) in the Pacific offshore study area proposed under the Marine Conservation Targets (MCT) initiative. The assessment studies were undertaken in 2017 by a team of geoscientists at the Geological Survey of Canada (GSC). Objectives were to: (a) review, analyze, and integrate relevant data from previous resource assessments and industry reports, existing scientific literature, and available geoscience databases (Appendices B and E); (b) conduct basin analysis, interpret and map petroleum system elements and regional petroleum plays to summarize the relative conventional and unconventional petroleum resource potential (Appendices C and D); and (c) consider potential for minerals and other resources in the study area (Appendix D). This study was conducted between January 2017 and December 2017. The relatively short time available to evaluate this large, previously unassessed area precluded the collection of new data and impacted the depth of analyses. The evaluation relied heavily on existing literature for some aspects of the assessment, where data coverage was sparse.

The study area is located in deep water (150 m to more than 3600 m water depth) west of Vancouver Island, British Columbia, and spans an area of approximately 200 000 km^2 (Figure 1). The study area is delimited by the shelf/slope break to the east, the exclusive economic zone (EEZ) boundary to the west, and the Canada – U.S. border to the south. The northern limit of the study area includes the Tuzo Wilson seamounts and the northern extension of Winona Basin. The study area encompasses five geodynamic regions: Pacific plate, Explorer plate, Juan-de Fuca plate, Winona Basin, and the Accretionary Complex (Figure 2). The Tofino, Hecate and Queen Charlotte sedimentary basins are located east of the study area in more shallow water depths.

The qualitative petroleum assessment was based on available offshore seismic reflection profiles and their integration with bathymetric surveys, potential field data, and well data accessed from the International Ocean Discovery Program (IODP) archives (Figures 3 and 4). The assessment was conducted over a larger area than requested by Department of Fisheries and Oceans to include thicker sedimentary deposits that occur to the east (Figure 1). This approach was implemented to improve the detail and accuracy of predictions in deep water areas where data are limited and no previous resource assessments exist. Additional information including petroleum industry well data obtained in shelf regions farther east, and geophysical and geological data from the U.S. Cascadia Basin and the U.S. Gulf of Alaska, located south and north of the Canada – U.S. border respectively, were also considered (Appendix B). The 2017 GSC qualitative petroleum assessment of the Pacific Offshore builds on previous quantitative petroleum potential studies done in the adjacent northwest areas of Winona and Tofino sedimentary basins (Hannigan et al., 2005). The current study does not provide a quantitative assessment of in-place petroleum resources.

2.0 REGIONAL GEOLOGICAL SETTING

The offshore Pacific study area spans an unusual and complex geologic setting that includes three oceanic plates: the Juan de Fuca, Explorer, and Pacific plates (Figures 2 and 3; Appendix C.1). The area has been the focus of many scientific studies that have furthered our understanding of the present day tectonic setting and how it has changed through time (e.g. Raff and Mason, 1961; Riddihough, 1984; Wilson, 1993; Botros and Johnson, 1988; Davis and Riddihough, 1982, McManus et al., 1972; Barr and Chase, 1974; Davis and Lister, 1977; Hyndman et al., 1979; Han et al., 2016; Cassidy et al., 1998; 2010; Riedel and Rohr, 2012; Milne and Smith, 1966; Audet et al., 2008;

Kao et al., 2009; Rohr and Furlong, 1994; Rohr, 2015). The west coast of Canada contains the continental-oceanic plate boundary indicated by the Cascadia subduction zone west of Vancouver Island and the Queen Charlotte fault, along which, the Pacific plate moves northward past Haida Gwaii, formerly known as the Queen Charlotte Islands. A number of high temperature seafloor spreading centres are also present in the study area where new oceanic crust is created and seabed ridges, valleys and hydrothermal vent fields are common (Figures 2, 3, and 4). Oceanic spreading centres commonly form far from continental margins (Underwood, 2005), whereas spreading centres in the study area, including Juan de Fuca spreading centres (Endeavor, Northern Symmetrical, West Valley and Middle Valley segments) and Explorer spreading centres (Southern and Northern Explorer segments), are within 150 to 300 km of the coast of British Columbia (Figure 2). The Endeavour Hydrothermal Vent Marine Protected Area (Figure 2), the first designated MPA under the Canada's Oceans Act (in 2003), straddles the Endeavor spreading ridge segment and contains hot (in excess of 300°C) mineralized black smoker chimney-like structures and unique ecosystems fueled by chemical energy from fluids emerging from the vents (NRCAN, 2017a). The study area encompasses the northern part of the Cascadia subduction zone, where dense oceanic crust collides with and is forced downward below the larger and less dense North American continental plate at a deformation front. A sediment-filled deep sea trench is present in front of the Cascadia subduction zone, and large strike slip faults (the Revere-Dellwood and Queen Charlotte faults) bound the Winona Basin. The three different kinds of plate boundaries meet in a triple junction region of complex deformation comprising the Explorer Plate and Winona Basin (Figure 2). Oceanic sediments scraped off down-going oceanic plates in a bulldozer-like fashion during subduction have accumulated through folding and faulting into a highly deformed sedimentary wedge known as the Accretionary Complex that occurs just landward of the deformation front (Figures 2, 3, and 4). The complex is comprised by long folded ridges (20 to 30 km long, a few kilometers wide) that rise up to 700 m above the surrounding seafloor (Appendix C, Figure C-5A; Davis and Hyndman, 1989). The youngest accreted sediments occur in the outermost parts of the complex near the deformation front, and accreted strata increase in age toward the east. In recognition of the differing tectonic, thermal and basin fill histories, the GSC assessment includes evaluations of five tectonic regions; the Winona Basin, Explorer Plate, Accretionary Complex, Juan de Fuca Plate, and the Pacific Plate (Figure 2). A more detailed tectonic overview and description of major tectonic elements and regions is provided in Appendix C.1.

The Pacific coast region is one of the most earthquake prone areas in Canada and one of the few areas in the world where all three types of plate movements (sea floor spreading, subduction and strike slip movements) take place, resulting in significant earthquake activity (NRCan, 2017b). The areas of highest seismicity are located in the Explorer microplate (Figure 2) and adjacent to the Revere-Dellwood and the Queen Charlotte faults where earthquakes with magnitudes greater than 4 are commonly observed (Cassidy et al., 1998; Riedel and Rohr, 2012). Frequent earthquakes of smaller magnitude occur across these regions and earthquakes of magnitude greater than 6 are common.

Underwood and others (2005) describe the Cascadia sedimentary system as being "in a class by itself". Submarine canyons and slope channels along the northern Cascadia margin deliver silt- and sand-rich gravity flows to the abyssal plain where the sediments accumulate in submarine fan deposits in a tectonically active setting where external controls on sedimentation include: subduction, accretion and uplift, earthquakes, glaciation related sea level fluctuations, volcanic eruptions; strike slip faulting, spreading ridge extension and volcanism. Seismic reflection profiles across the region image sedimentary deposits above oceanic crust that thin onto young seafloor ridges at spreading centres and thicken into the trough (or trench) of the Cascadia subduction zone (e.g. Figures 1B and C-2). At the onset of this study it was not known if basin fill in the study area has been buried deeply enough, and/or has warmed enough to generate, expel and migrate hydrocarbons.

The age and composition of sedimentary basin fill varies significantly from shelf to deepwater along this part of the Pacific margin (Figure 5). The coastal and shallow water regions east of the study area are part of the Insular Belt of the North American Plate, that includes Vancouver Island, Haida Gwaii, Queen Charlotte Basin, Hecate Basin and most of Hecate Strait and Queen Charlotte Sound (Monger et al., 1972) where rocks can be up to 200 Million years (Ma) old. The southern Queen Charlotte and Tofino basins occur adjacent to the study area, beneath the continental shelf on the outermost part of the North American Plate, where rocks can be up to 45 Ma. Within the study area (Figure 3), the seabed extends westward from the continental shelf edge (200 m water depth or less) across a steep and relatively narrow slope (between 200 m and 2000 m water depth) onto a deep-water abyssal plain (water depths greater than 2000 m). The deep water sedimentary deposits in this region are relatively young, mainly Pleistocene to Pliocene in age (0 to 5.3 Ma; Figure 5); with older Miocene strata (5.3 to 23 Ma) interpreted to be present in the western part of the Pacific Plate, in the Accretionary Complex and in the Tofino Basin. Submarine slope canyons, fan, channel levee deposits and slope failure deposits have been the focus of previous work on the Cascadia basin (Griggs and Kulm, 1970; Carson and McManus, 1971; McManus et al., 1972; Carson, 1973; Nelson, 1976; Hampton et al., 1989; Adams, 1990; Underwood, 2000, 2005, Kiyokawa and Yokowama, 2009, Atwater, 2014). Large earthquakes (greater than magnitude 6), can liquefy sediments and trigger large submarine landslides of older shelf and slope deposits that are then transported downslope and redeposited in deeper water (Pickering and Hiscott, 2016).

3.0 DATA

The geology of the deep-water study area is less well known than that of the adjacent upper slope, shelf and onshore Pacific Margin Basins, which have been the subject of many GSC, provincial, industry and National Energy Board (NEB) reports, as well as a wide range of academic publications. The deep water study area has not been previously evaluated for petroleum potential but the region has been the focus of many scientific research investigations on tectonic evolution, thermal conditions, seismicity, structure, and geohazard risks. Data consulted for this study came from a variety of public domain and research institution sources as detailed below.

3.1 Literature

Major sources of data were consulted for this assessment including data from the Deep Sea Drilling Program (DSDP), the Ocean Drilling Program (ODP) and the International Ocean Discovery Program (IODP). Refer to Sections 3.2 and 3.3 and Appendix B for more information. Industry well data from the Queen Charlotte and Tofino basins were considered and integrated into the gross depositional environment models.

GSC Bulletin 564 (Hannigan et al., 2001) and GSC Open File Report 4829 (Hannigan et al., 2005) provide information on previously assessed Pacific Margin basins, including the Tofino Basin and Winona basins, as well as the Cascadia Accretionary Complex. These studies provided a resource estimate (mean in-place volume of 265.7 billion m^3 gas) for a Tofino gas play that encompassed the continental shelf offshore Vancouver Island and adjacent deep-water slope and base of slope areas. A detailed list of supporting technical reports and scientific literature that are referenced in this report, or were consulted and contributed to background technical work that informed our maps, is provided in Appendix E.

3.2 Geophysical Data

Approximately 29 000 line-km of two-dimensional marine reflection seismic data were used in this qualitative assessment (Figure 3), much of which was collected by the GSC. Data quality varies from relatively high quality (e.g. multichannel seismic) to moderate-to-low quality (e.g. digital scans of paper plots). Many of the regional scale lines date from the 1970s when plate tectonic theories were becoming established, in large part due to exploration of the world's oceans. Other geophysical data integrated into this assessment include: seabed bathymetric data, (multibeam and side scan sonar surveys), potential field data (magnetics, gravity, and 3D inversion gravity models), heat flow data and seismicity data, much of which was collected by the GSC. Summary tables of sources for data that contributed to the sediment thickness mapping, and for bathymetry and gravity data, are provided in Appendix B (Tables B-1B and B-1C).

3.3 Geological Data

From 1973 to 2013, the DSDP/ ODP/ IODP scientific drilling programs completed eight expeditions, focused on 32 different sites. A total of 97 holes were drilled during the eight expeditions (Figure 4 and Appendix B, Figure B-1). Program objectives, year and outcomes are summarized in Appendix B (Table B-1A). Project-relevant information (lithological and grain size data, source rock geochemistry, gas analyses, temperature data, core descriptions, etc.) and related studies were reviewed and integrated into the geological interpretations (Appendix C; e.g. Expedition 311 Scientists, 2006 a, b, c, d, e, and f; Shipboard scientific party, 1997 a, b, and c; Shipboard scientific party, 1992 a, b, c, d, e, and f).

4.0 METHODOLOGY

4.1 Qualitative Petroleum Assessment

This section highlights the 4-step approach used to qualitatively assess petroleum potential in the study area. A more detailed description of the assessment approach utilized by the Marine Conservation Targets team is provided in Geological Survey of Canada Open File 8404 (Lister et al., *in press*).

The study area represents a frontier area that has not been targeted by the petroleum industry for exploration well tests and the majority of the area has never been assessed for petroleum potential. Available research data and analyses were reviewed for applicability to the petroleum resource assessment. The initial literature and data review concluded that the thickness, geological characteristics and evolution of sedimentary basin fill was not well understood away from well control (commonly the case in frontier settings with few well tests). Key uncertainties for petroleum system elements were identified and the following work plan (modified from the basin analysis and petroleum play assessment approach of Allan and Allan (1990)), was developed for the study:

Step 1. Basin Scale Analysis:

- plate tectonic framework *(Appendix C.1)*
- regional geologic conditions *(Appendix C.2)*
- thickness, age, characteristics of basin fill *(Appendices C.3, C.4, and C.5)*
- depositional environment models to help predict sand and organic richness of basin fill away from well control *(Appendices C.6 and C.7)*

Step 2. Petroleum Systems Element (PSE) Analysis *(see Appendices A and D):*

- Create "Chance of success" (COS) maps for each PSE:

Charge *(Appendices C.7 and D.1).*

- Compile hydrocarbon indicators *(Appendix C.7.3)*
- Potential presence of source rock characteristics needed for biogenic gas formation; predict away from well control on the basis of depositional environment models and sedimentation rate map
- Potential presence of source rock characteristics needed for thermogenic generation; predict away from well control on the basis of geological processes and predicted depositional environment models and areas where upwelling conditions were likely
- Test thermogenic maturation potential with 1D basin models

Reservoir *(Appendices C.6 and D.2)*

- Potential presence of porous deep water sandstones)

Seal *(Appendices C.6 and D.2)*

- Potential presence of fine grained, low permeability "cap rocks"

Trap *(Appendices C.1 and D.2)*

- Potential presence, structural and/or stratigraphic)

Step 3 Play Analysis:

- Play identification
- Create Geological Chance of Success (CCOS) maps, by play
- Apply subjective Global Scale factor
- Create Technical chance of success maps (TCCOS), by play

Step 4. Assessment of Petroleum Potential:

- Stacked Technical Cumulative (STCCOS) map

New work completed to inform the assessment, summarized in Appendices C and D, includes:

i) Seismic interpretation of top and base of sediments in 2D profiles (Figure C-1, Appendix C.1): *The seabed and base of sediments (top of oceanic crust or "basement") were interpreted, where possible, on available 2D seismic data which are recorded and displayed in two way travel time.*

ii) 3D inversion of gravity data in Winona Basin to constrain sediment thickness (Figure C-3, Appendix C.3): *Bouguer gravity data were used to evaluate density contrasts between sedimentary and underlying igneous basement rocks, which had a higher density contrast. 3-D inversion of the Bouguer gravity data with GRAV3D (Li and Oldenburg 1998) allowed estimation of the thickness and density of the Winona basin fill. The final model was chosen based on a good match to a depth-converted seismic reflection profile 88-02 (Figure C-3A, location of 88-02 in bold red on Figure C-2). More detail on the approach used is provided in Appendix C.3.*

iii) Creation of a sediment thickness map for the study area (Figure C-2, Appendix C.3): *A sediment thickness map was prepared for the study area to indicate where within the study area the sedimentary deposits might be thick enough and hot enough to mature any organic rich source rocks to generate and expel hydrocarbons. The thickness map was created using mostly 2D seismic data, and selected gravity profiles, and published depth cross sections were considered in areas where the seismic data available for this study were limited. The interpreted seismic horizons were converted from time to depth using a velocity gradient for the sediments from a refraction study (Horning et al., 2016). For further detail and a description of uncertainties inherent in this map see Appendix C.3.*

iv) Identification and mapping of possible seismic hydrocarbon indicators, including bright spots (Figures 4 and C-1C, Appendix C.7.3): *Bright spots were evaluated to distinguish possible gas responses from those related to volcanic rocks and preliminary amplitude versus offset (AVO) work was completed. More detail on the approach is provided in Appendix C.7.*

v) Review of seismic dataset for presence of possible traps, reservoirs (sand-prone facies), source rocks and/or seals (mud-prone facies) (Appendices C.6 and D.1)

vi) Integration of the above with available paleo-magnetic, seabed bathymetry and well data to: a) constrain basin fill age (Figure C-4, Appendix C.4) and b) propose gross depositional environment models at key time intervals to allow the prediction reservoir, source rock and seal potential away from well control (Figures C-5A, B, C, and D, Appendix C.6).

vii) 1D basin modelling at select locations (Figures D-1 and D-2, Appendix D.1): *Four 1D models were developed to evaluate petroleum maturation potential (at what burial depth and temperature a postulated source rock would be mature and able to generate and expel hydrocarbons). Models were located in areas of thicker sedimentary accumulations and a range of scenarios were considered to test sensitivity to temperature, sediment thickness and other local effects.*

viii) Creation of petroleum system element COS maps, play maps (geological chance of success maps (CCOS) shown in Figure D-3, Appendix D.1, and technical chance of success maps (TCCOS) shown in Figure D-4, Appendix D.1, and the petroleum systems potential map (stacked Technical Cumulative (STCCOS) map (Figure 1A).

In summary, plays in the study area were identified and defined based on geologic and tectonic trends, seismic interpretation, and analogue data (Table 1C). Each play was assessed individually and a chance of geologic success (CCOS) was assigned for each of its petroleum system elements (source, reservoir, trap, and seal). Biogenic and thermogenic plays were considered. Plays were weighted by an internally-developed global scale factor (a subjective estimate of how the volumetric potential of the play may compare to productive plays in other basins worldwide) to facilitate the creation of technical chance of success (TCCOS) maps for each play. The technical potential for all plays was summed to create a qualitative petroleum potential map (Figure 1A).

4.2 Assessment Approach for Unconventional and Other Resources

Literature reviews and consultations were undertaken for unconventional gas hydrate, and for emerging technology initiatives including carbon capture and sequestration (CCS) capacity and marine geothermal energy. Areas with highest potential to contain gas hydrate deposits were identified by isolating areas where Bottom Simulating Reflectors (BSRs) were observed, inferring gas hydrate to be present at the base of its stability zone in these locations, and extrapolating into adjacent areas where comparable geologic conditions are expected. Key criteria were identified and applied to available data sets to allow the identification of areas with geologically favourable conditions for CCS reservoirs and marine geothermal energy within the study area.

4.3 Mineral Assessment

A marine mineral resource literature review and consultations were undertaken and key criteria were identified and applied to available data sets to allow the identification of areas likely to contain three deep marine mineral deposit types (volcanogenic massive sulphides (VMS), ferro-manganese crust and manganese nodules) within the study area.

5.0 RESULTS AND INTERPRETATION

5.1 Petroleum Potential Map

Petroleum potential within the study area is summarized in Figure 1 and Tables 1A, B, and C. The presence of possible active petroleum systems in the Winona Basin and Accretionary Complex regions of the study area is supported by:

i) indications of gas hydrate deposits in seismic reflection data, seabed samples and wells;
ii) indications of local fluid escape/methane vent features at the seabed interpreted from seismic, bathymetry, well data and from Remote Operated Vehicle (ROV) images of the seabed; and,
iii) the presence of high amplitude seismic bright spots in areas with thicker sediments that might be indicative of gas in the subsurface.

There has been no petroleum exploration drilling in the study area and the interpretation and characterization of resource potential was based on indirect information from seismic data, scientific well data and basin modelling.

Subsurface interpretation, mapping and basin analysis of the Miocene and/or Pliocene to-Pleistocene sedimentary basin fill led to the identification of six play types (Table 1) in the study area (Appendices C and D). Petroleum migration between stratigraphic units or play areas is possible. The petroleum potential map created by evaluating and stacking identified plays indicates varying potential (Figure 1), with the eastern Winona Basin and Accretionary Complex regions considered as having moderate potential, the highest in the study area. The areas with the thickest sediments in the subduction trench on the Juan de Fuca plate and Explorer microplate have low potential. Most other parts of the study area have very low or no potential.

5.2 Unconventional Petroleum and Emerging Initiatives Map

5.2.1 Unconventional Gas Hydrates

Gas hydrate potential is identified in both the Winona Basin and Accretionary Complex regions of the study area (Figure 6). Natural gas in hydrates in the Accretionary Complex is sourced by a combination of shallow and deep sources (Riedel et al., 2010). Gas hydrate occurrences are laterally heterogeneous because the hydrate forms most commonly in coarser grained sandy or silty facies (Riedel, et al., 2010). In Winona Basin, bottom simulating reflections (BSRs) occur within isolated structural highs, which may indicate gas migration from a deeper thermogenic source (Riedel and Rohr, 2012). Natural gas potential from gas hydrates in the Canada Pacific offshore has been estimated to be 0.32-2.4 x 10^{13} m^3 (Majorowicz and Osadetz, 2001). This estimate included gas hydrates in the study area and those to the north adjacent to Haida Gwaii.

5.2.2 Carbon Capture and Sequestration (CCS)

Goldberg and Slagle (2009) identify the Juan de Fuca Ridge as one area that may offer large capacity CCS storage volumes within reasonable proximity to continental margins and potential industrial CO_2 sources. Study area data were screened using the following four criteria: i) presence of oceanic crust younger than 15 Ma, ii) sediment thickness greater than 200 m, iii) 20 km distance from possible recharge/discharge areas, and iv) water depths greater than 800 m (pers. comm.; Scherwath, Goldberg and Davis, 2017). Areas likely to contain CCS reservoirs (where geologic conditions required for CCS reservoirs were met) are shown in Figure 6. Porous basalts with very high permeability have been documented within the study area (Davis and Becker, 2002; Davis et al., 1989; Spinelli and

Fisher, 2004 and Fisher, 2005). The GSC did not assess seabed or shallow sediment porosity and permeability conditions due to limited data and expected local scale variability in mixed turbidite and pelagic sediments in the study area. Further work (beyond the scope of this study) is needed to determine where sediment cover is sufficiently low in permeability to allow for physical trapping to occur. A sediment cover of 150 m may be sufficient based on reports by Underwood and others (2005) that hemipelagic clays in ODP Leg 168 wells were effective hydrologic seals where basalt crust is buried by 100 to 150 m of strata.

5.2.3 Marine Geothermal Energy

Most seafloor spreading centres around the world are far from land. Like Iceland, active seafloor spreading centres are present in Canadian waters relatively close to onshore areas. Three areas of geothermal potential are identified within the study area (Figures 4 and 6). The only known active seafloor spreading centres with hydrothermal vent fields in Canada occur within the study area. Numerous hot springs with geothermal energy potential are present on land in British Columbia and British Columbia's geothermal resources from hot springs sources are currently estimated to be 3000-5000 MW (Energy B.C., 2017). The electricity generation potential at seafloor spreading centres may be an order of magnitude larger than that of geothermal sites in onshore areas. The unique location of spreading centres off the west coast of Canada indicate the study area could have significant geothermal clean-energy potential if/when the technologies are developed.

5.3 Mineral Resources

Areas with geological conditions favourable for the development of mineral occurrences, known as geologically permissive areas, are found throughout the study area. Types of mineral occurrences include:

i) VMS sulphide deposits: estimated total area of 93 000 km^2 within the study area (Figure 7). This interpretation is supported by the presence of seafloor spreading ridges, known high temperature conditions, active and inactive hydrothermal vent fields and proven occurrences of VMS within the study area (e.g. Endeavour and Explorer hydrothermal vents). Japan achieved a world first in September 2017, by successfully mining minerals from a deep sea hydrothermal vent field, which indicates there is potential in the future for similar mining activities to be proposed in or adjacent to the study area. The only known active hydrothermal vent fields in Canada occur within the study area.

ii) Ferromanganese Iron Crusts: estimated total area of 21 000 km^2 within the study area (Figure 7). This interpretation is supported by the presence of seamounts in the study area that occupy water depths between 500 and 2,800 m or deeper, and the reported presence of ferromanganese and/or manganese glassy rinds, pavement and crusts from seafloor samples. Geologically favourable conditions occur with numerous seamounts within the study area, a smaller number of seamounts in Canadian waters north of the study area as well as for seamounts that extend into international waters west of the study area.

iii) Manganese Nodules: estimated total area of 9,300 km^2 within the study area (Figure 7). This interpretation is supported by seabed with water depths greater than 3500 m and reports of manganese nodules from seabed dredge samples. Favorable conditions are identified over a limited area within the study area and over a much larger area north of the study area.

6.0 CONCLUSIONS

The findings of this report are based on existing data, new work, and previous reports and publications. Issues of potential economic value in the study area cannot be fully assessed or evaluated based on current knowledge. We conclude that within the study area:

i. A large part of the study area has very low potential or no potential for conventional petroleum resources and no areas with high potential for significant petroleum resources are predicted. Low to moderate conventional petroleum potential is predicted in Winona Basin and the Accretionary Complex, low conventional petroleum potential is predicted for the southeastern-most areas of the Juan de Fuca and Explorer plates. Potential exists for localized non-commercial occurrences of hydrothermally generated hydrocarbons (as documented in Middle Valley)
ii. Gas hydrate potential is identified in the Winona Basin and Accretionary Complex regions
iii. The study area contains marine minerals including proven VMS deposits as well as areas that are likely to contain additional undiscovered concentrations of: VMS deposits near seafloor spreading centres and active or inactive hydrothermal vent fields; Ferromanganese crusts that may contain rare earth elements on seamounts and Manganese nodules where the seabed is deeper than 3,500 m below sea level
iv. Conditions suitable for clean, green geothermal energy generation are expected to be present at active seafloor spreading centres
v. Conditions that may be suitable for future CCS are identified in sediment covered regions of the Pacific, Explorer and Juan de Fuca plates.

ACKNOWLEDGEMENTS

The authors sincerely thank Ulrike Schmidt and Will McCarthy for their valuable technical contributions, along with Robert Kung, Richard Nairn, and Christine Deblonde for assisting with GIS data. We particularly thank Jim Dietrich and Peter Hannigan, for their sustained efforts to support the project, including initial project design, team assembly, knowledge sharing, and critical reviews. Jim Dietrich, in particular, was instrumental in facilitating our success. We thank Marian Hanna, Elizabeth Atkinson, Andy Mort, Gary Sonnichsen, and Sonya Dehler for their support and review comments.

We thank the many regional and subject experts who shared their geological expertise and insights through consultations and/or workshops including: John Cassidy, Earl Davis and Roy Hyndman for their insights on offshore seismicity, structure and tectonic history and heatflow variations in the region; Laurence Coogan for insights on oceanic crust formation and hydrothermal vents at mid ocean spreading centres, Vaughn Barrie and Rod Smith for insights on regional Quaternary sedimentation history and processes; Zhiyong He for petroleum systems modelling considerations near young hot spreading centres, Vaughn Barrie and Martin Scherwath for insights on gas venting processes and features; Andy Mort, Martin Fowler and Michael Abrams for source rock geochemistry insights; Rick Hiscott for insights on deep marine environments, tectonics and sedimentation processes; Michael Riedel for guidance on gas hydrate evaluation; Arlene Drake, Mark Hannington, John Jamieson, Suzanne Paradis, Laurence Coogan and Keith Dewing for guidance on assessing potential for deep sea minerals; Laurence Coogan, Martin Scherwath, Dave Goldberg and Curtis Evans and Ocean Networks Canada for insights on carbon, capture and sequestration and Steve Grasby for insights on geothermal energy potential. We thank Rose Ann Weisser, Lamont Doherty Earth Observatory, and Ray Sliter, USGS, for their assistance in accessing data archives. Many other GSC colleagues and Emeritus scientists are thanked for directing us to information, and for sharing their knowledge. Their generosity greatly enriched this report.

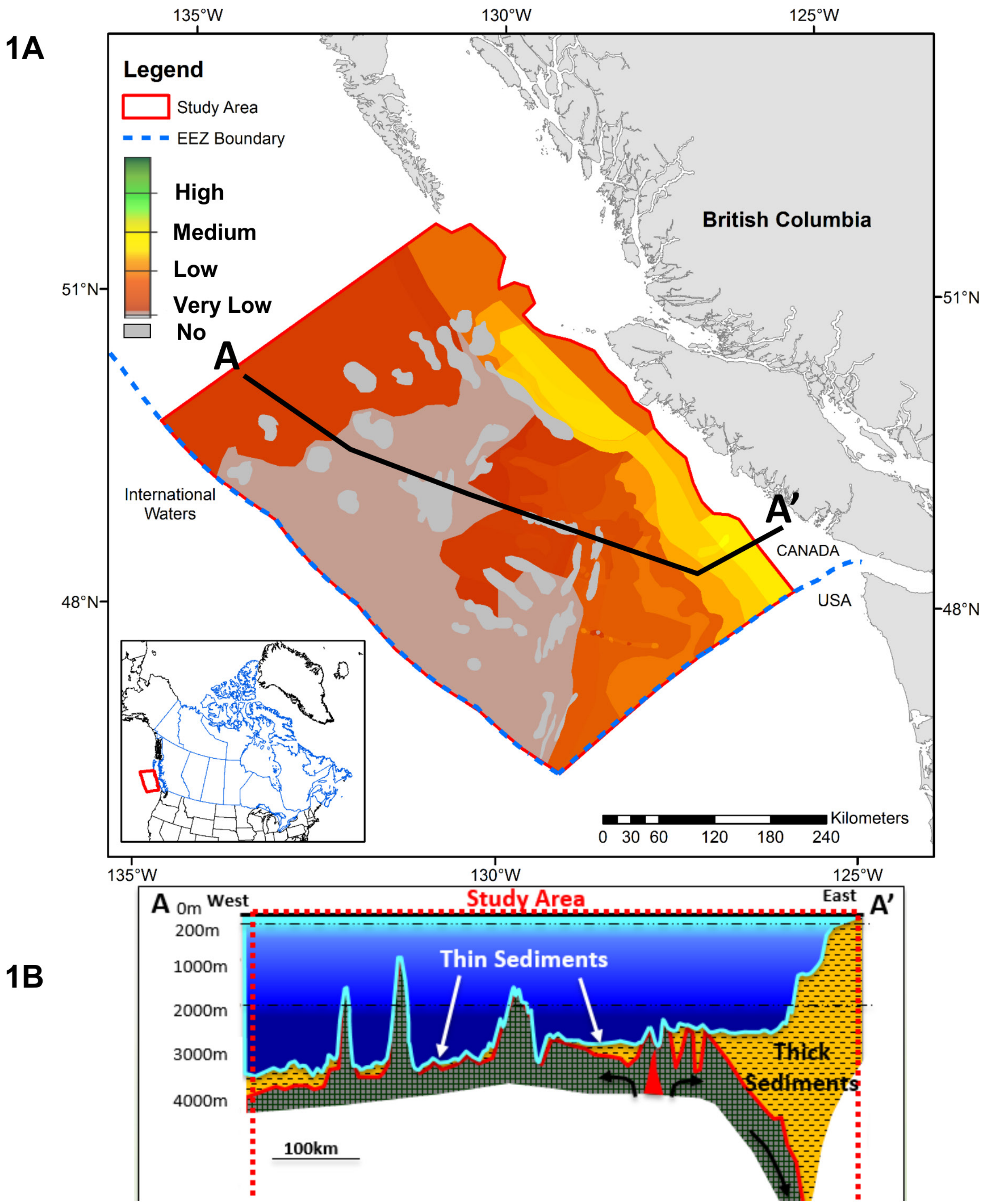

Figure 1. Petroleum Potential map and illustrative cross section, offshore Pacific study area.

(**A**) Petroleum Potential map of the offshore Pacific study area. Color code – gradation bar ranges from very low potential (red) to high potential (green, globally competitive for exploration). Grey polygons indicate areas of no petroleum potential. The Pacific offshore study area contains areas of no potential (grey), low potential (orange, red) and medium potential (yellow). There are no areas of high petroleum potential. (**B**) Cross section **A**-**A’** shows thin to no sediments across the majority of the study area and thick sediments in the east.

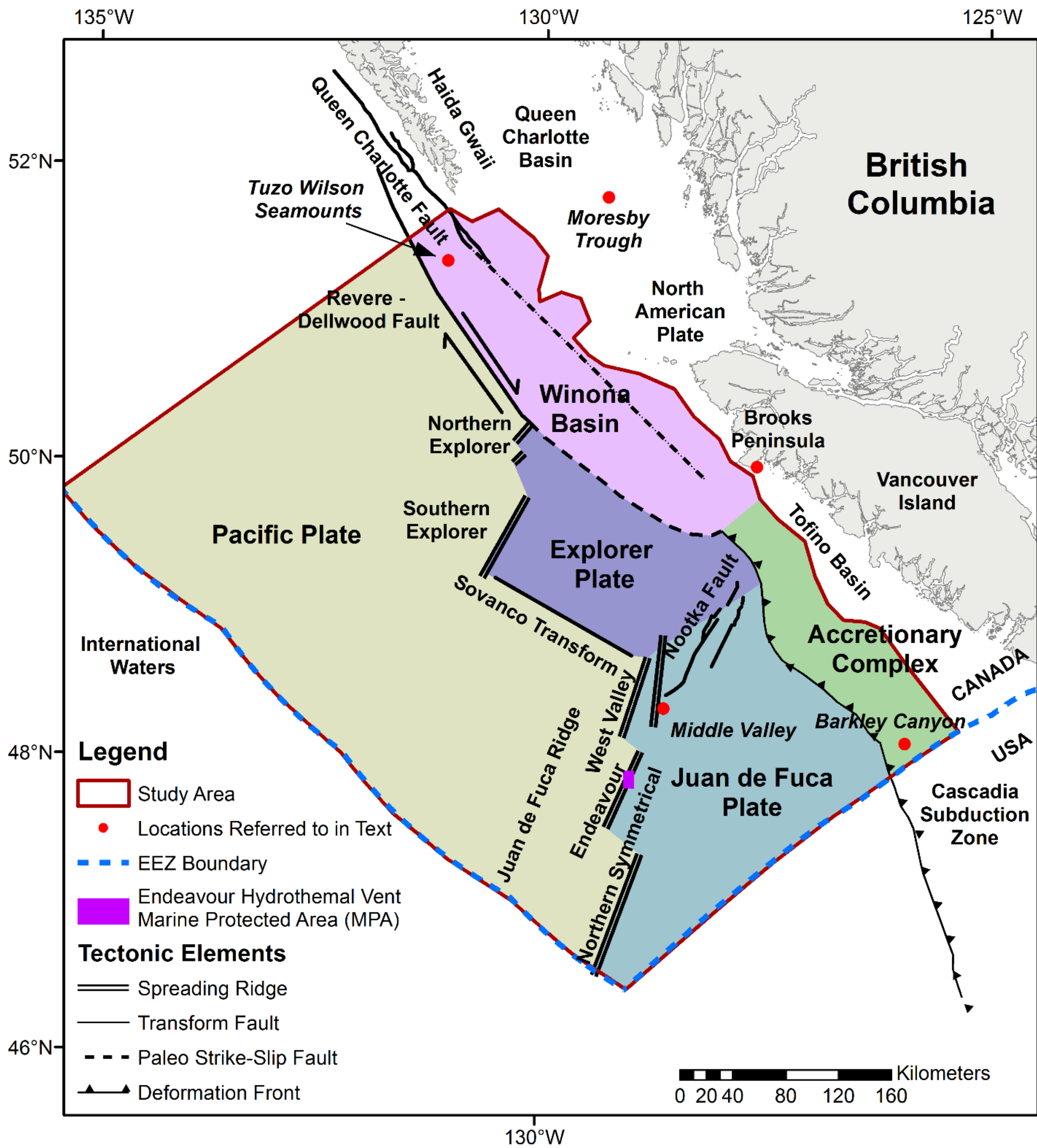

Figure 2. Tectonic regions and structural elements map

Tectonic regions (Juan de Fuca Plate, Explorer Plate, Pacific Plate, Winona Basin and Accretionary Complex) and structural elements (spreading ridges, transform faults, paleo strike slip faults and the deformation front associated with the Cascadia Subduction Zone) are present in the Pacific Offshore study area.

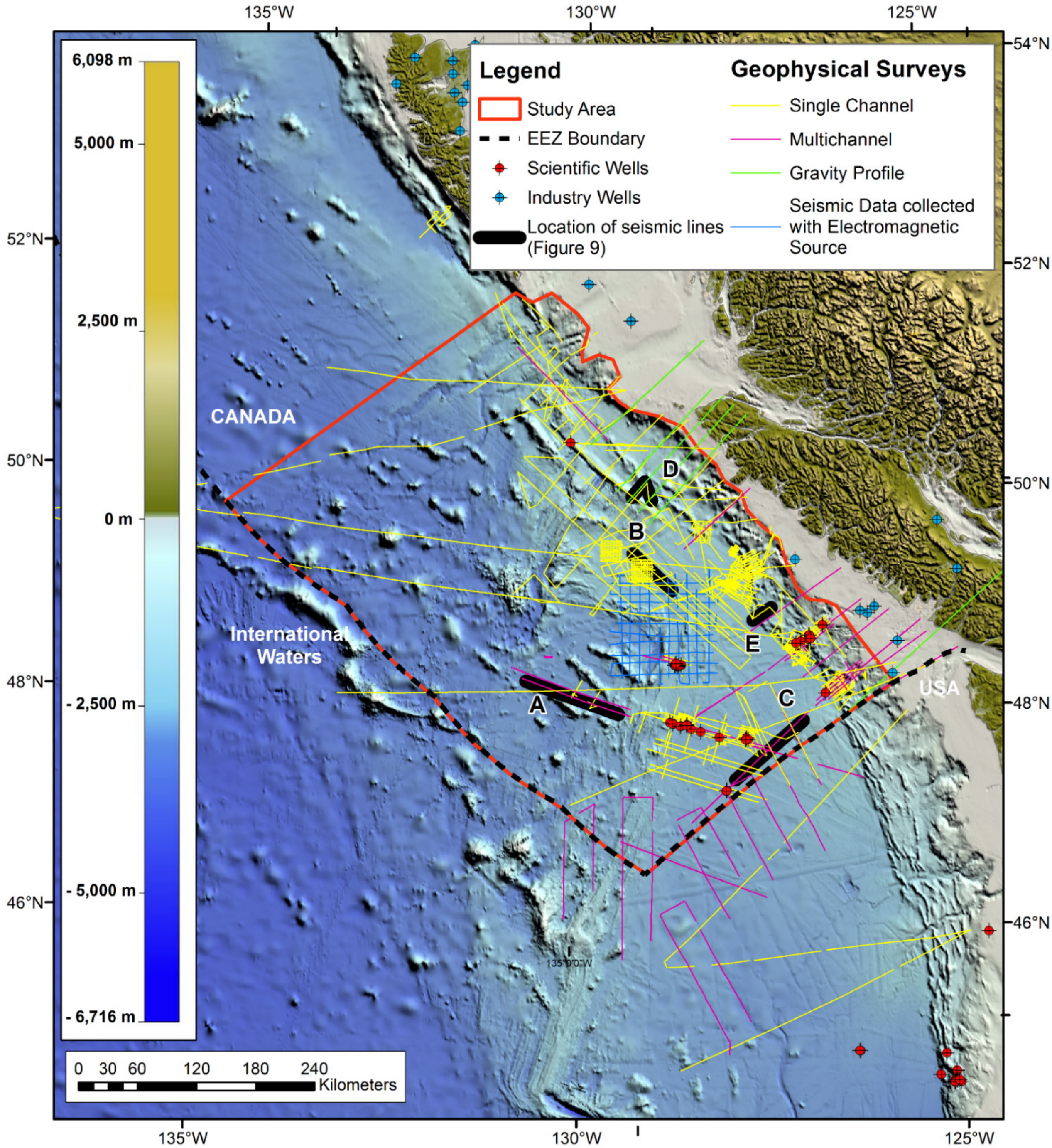

Figure 3. Geophysical data used to assess the study area.

Locations of available seismic reflection data (single channel, multichannel, and electromagnetic sourced data), gravity profiles and seismic images shown in this report (Figure C-1, Appendix C) are indicated. A summary of seismic data consulted in this study is provided in Appendix B, Table B-1B. Bathymetry data accessed from: http://www.geomapapp.org Global Multi-Resolution Topography (GMRT) Synthesis (Appendix B, Table B-1C; Ryan et al., 2009).

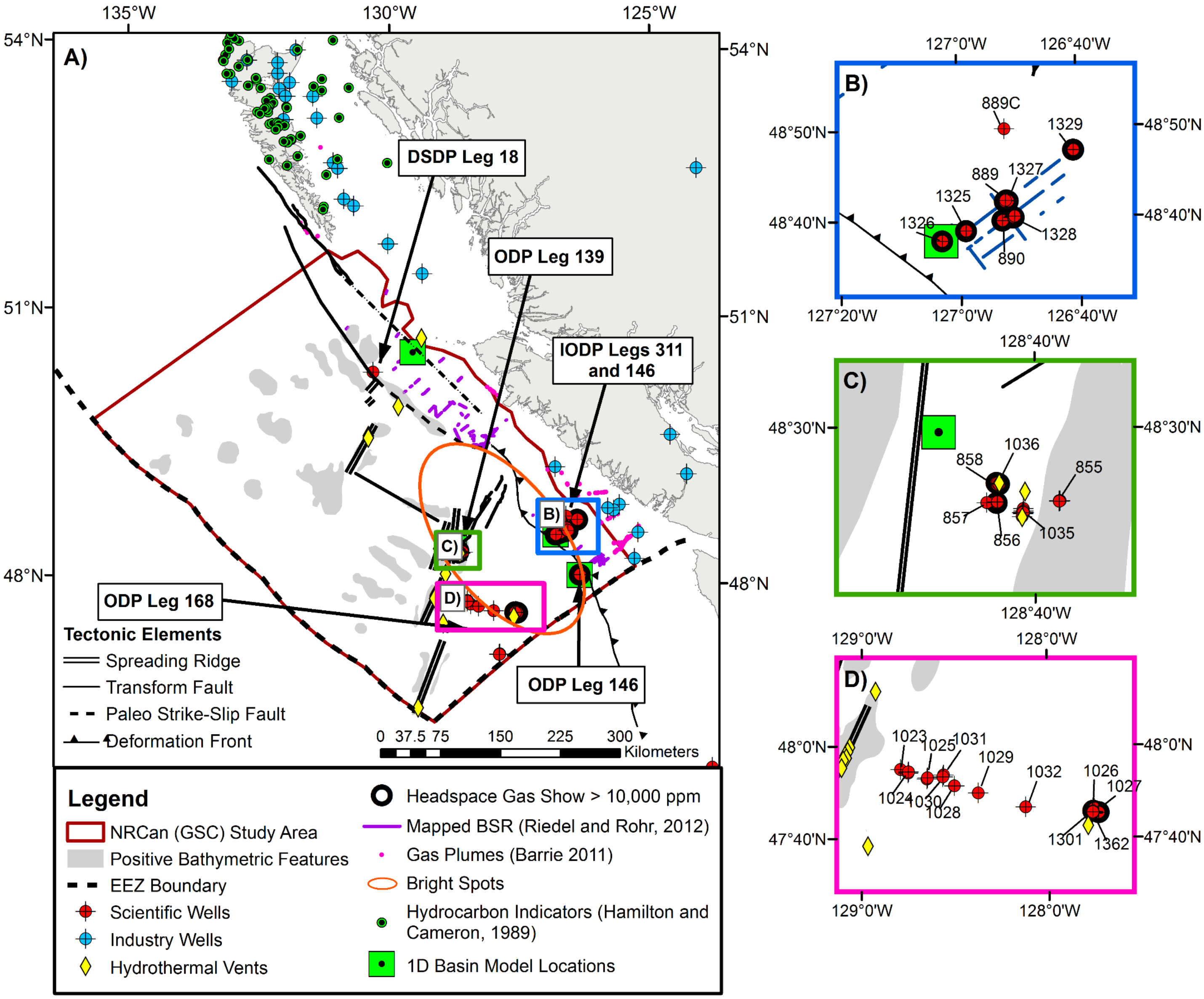

Figure 4. Well data, geological features and hydrocarbon indicators map.

(**A**) Well data, geological features and hydrocarbon indicators map. (**B**): Accretionary Complex ODP Leg 146, IODP Leg 311 wells. (**C**): Juan de Fuca (Middle Valley) ODP Leg 139 wells. (**D**): Juan de Fuca ODP Leg 168 wells. More information on data utilized in this study is provided in Section 3.0 and in Appendix B.

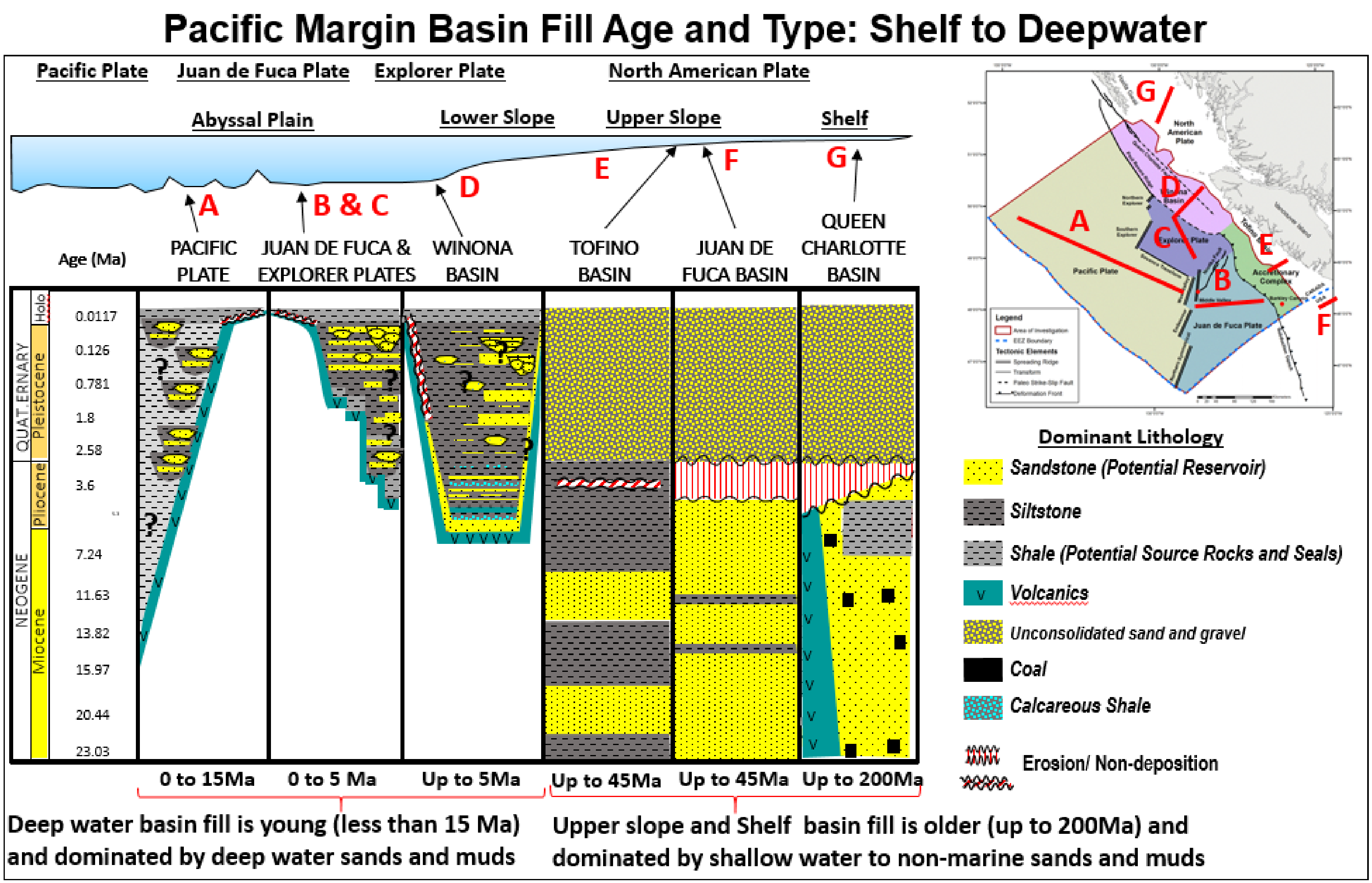

Figure 5. Generalized Pacific Margin Basin fill age and rock type from shelf to deepwater

Shelf stratigraphy adapted from Hannigan and others, 2001. Winona Basin, Juan de Fuca and Explorer and Pacific Plate stratigraphy based on available well data or inferred from paleomagnetic data, seismic interpretations and gross depositional environment models.

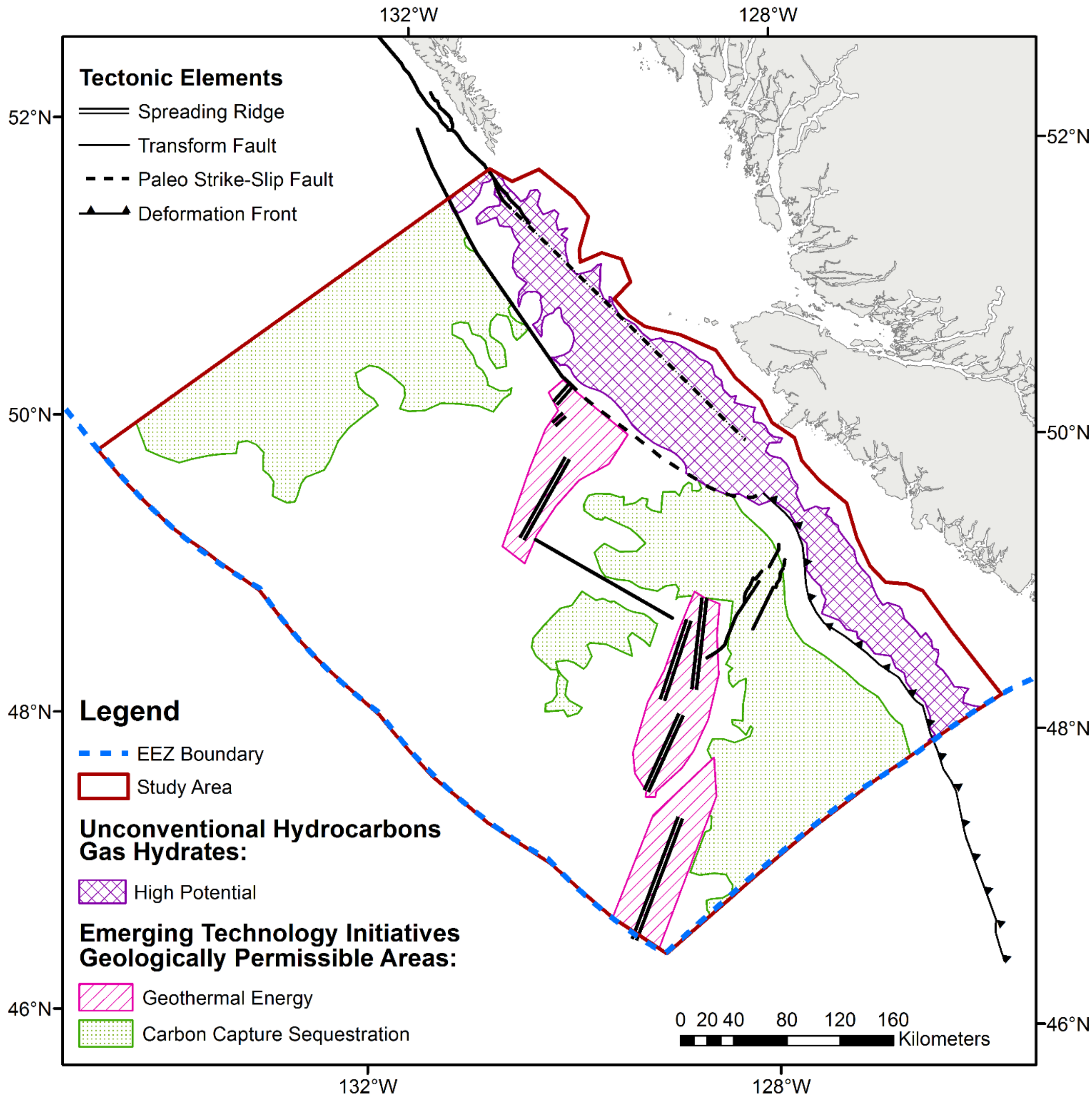

Figure 6. Unconventional and other potential geological resources and activities map.

Highest potential area for unconventional gas hydrate deposits and areas likely to contain geothermal energy and Carbon Capture and Storage (CCS) opportunities are indicated.

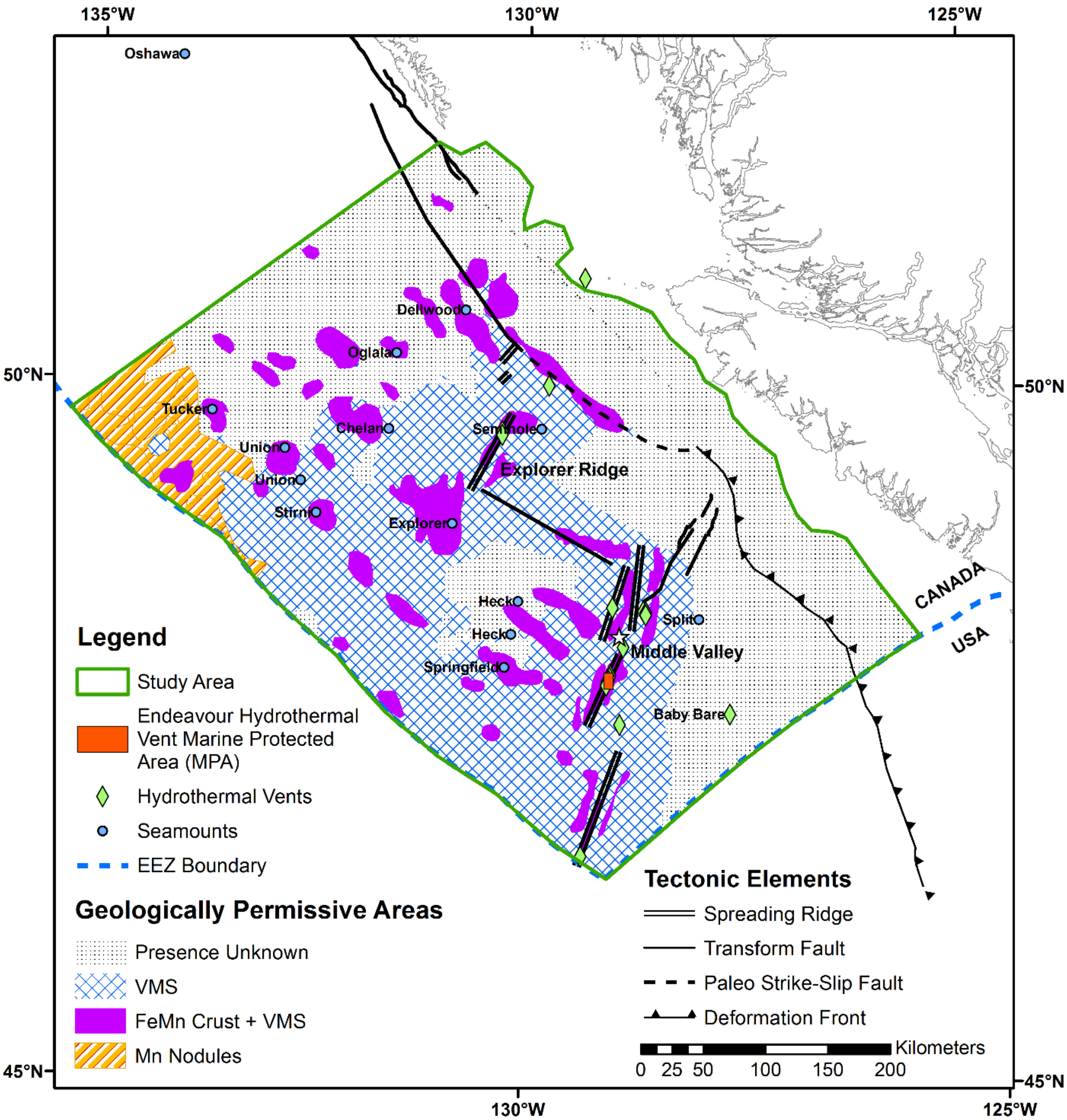

Figure 7. Marine minerals map showing areas with geologically favorable conditions for the presence of undiscovered VMS, Mn-Fe crust and Mn nodule deposits

Criteria for volcanogenic massive sulphide (VMS) deposits include: oceanic crust originating from seafloor spreading ridges, known hydrothermal vents and mineralization in the area, and less than 100 m sediment cover. Criteria for ferro-manganese (Mn-Fe) crust include: presence of basaltic oceanic crust on seamounts and/or ridges, in a water depth range of 400 m to 2500 m or greater. Criteria for manganese (Mn) nodules: water depth must be greater than 3500 m. The Endeavor Hydrothermal Vent Marine Protected Area (red box), seamounts, spreading ridges, Middle Valley, Explorer Ridge and known hydrothermal vent locations (green diamonds) are shown.

Table 1A: Summary of Petroleum Assessment Results for the Pacific Offshore study area.

Pacific offshore Hydrocarbon Assessment Results	Winona Basin	Accretionary Complex	Juan De Fuca Plate		Explorer MicroPlate		Pacific Plate
			Thick Trench and Valley Fill	Thinner Plate sediments	Thick Trench and Valley Fill	Thinner Plate sediments	
Thermogenic Potential	Moderate	Low to Moderate	Low	Very Low	Low	Very Low	Very Low
Biogenic Potential	Moderate	Moderate	Moderate	Very Low to Low	Moderate	Very Low to Low	Very Low to Low
Proposed MPA	Outside proposed Marine Conservation Target	Outside proposed Marine Conservation Target	Mostly outside proposed Marine Conservation Target	Within proposed Marine Conservation Target	Mostly outside proposed Marine Conservation Target	Within proposed Marine Conservation Target	Within proposed Marine Conservation

Table 1B: Summary of Qualitative Petroleum System Element Assessment Results by Region.

Pacific offshore Petroleum System Elements Assessment Results		PACIFIC OFFSHORE ASSESSMENT REGION						
		WINONA BASIN	ACCRETIONARY COMPLEX	JUAN DE FUCA PLATE		EXPLORER MICROPLATE		PACIFIC PLATE
				THICK TRENCH AND VALLEY FILL	THINNING SEDIMENTS	THICK TRENCH AND VALLEY FILL	THINNING SEDIMENTS	
Biogenic SOURCE	PRESENCE	SPECULATIVE: POSSIBLE	POSSIBLE to LIKELY	POSSIBLE	POSSIBLE	POSSIBLE	POSSIBLE	POSSIBLE
Thermogenic SOURCE ROCK	PRESENCE	SPECULATIVE: POSSIBLE	SPECULATIVE: POSSIBLE	SPECULATIVE: POSSIBLE	UNLIKELY	SPECULATIVE: POSSIBLE	UNLIKELY	UNLIKELY
	MATURITY	PREDICTION: OIL AND GAS GENERATION POSSIBLE IN FILL BURIED 2.2 km OR DEEPER.	PREDICTION: OIL GENERATION POSSIBLE IN FILL BURIED 2.3 km OR DEEPER	PREDICTION: OIL GENERATION POSSIBLE IN FILL BURIED 2.1 km OR DEEPER	PREDICTION: IMMATURE	PREDICTION: OIL GENERATION POSSIBLE IN FILL BURIED 2.1 km OR DEEPER	PREDICTION: IMMATURE	PREDICTION: IMMATURE
RESERVOIR	PRESENCE	VERY LIKELY	POSSIBLE	VERY LIKELY	VERY LIKELY	VERY LIKELY	LIKELY	POSSIBLE
TRAP	STRUCTURAL	VERY LIKELY	VERY LIKELY	LIKELY	LIKELY	VERY LIKELY	VERY LIKELY	UNLIKELY
	STRATIGRAPHIC	MORE LIKELY THAN NOT	MORE LIKELY THAN NOT	VERY LIKELY	VERY LIKELY	VERY LIKELY	VERY LIKELY	POSSIBLE
SEAL	PRESENCE	UNCERTAIN: POSSIBLE	UNCERTAIN: POSSIBLE TO UNLIKELY	UNCERTAIN: POSSIBLE?	UNCERTAIN: POSSIBLE TO UNLIKELY	UNCERTAIN: POSSIBLE TO UNLIKELY	UNCERTAIN: UNLIKELY	UNLIKELY
KEY UNCERTAINTY (IES)		SOURCE ROCK PRESENCE	SOURCE ROCK PRESENCE, MATURITY and SEAL	SOURCE ROCK PRESENCE, MATURITY	SOURCE ROCK PRESENCE, SEAL	SOURCE ROCK PRESENCE, MATURITY and SEAL	SOURCE ROCK PRESENCE, MATURITY and SEAL	SOURCE ROCK PRESENCE, MATURITY

Qualitative Ranking	Positive	Possible	Negative

Table 1C: Summary of Petroleum Plays by region within the Pacific offshore study area.

Play age, Play type (Structural or stratigraphic), Petroleum system elements (trap, source rock, reservoir, seal) and Data Coverage are summarized by region. A global scale factor (Section 4.1, Main report) was applied as thermogenic where potential for a thermogenic petroleum source was highest (Winona Basin, Accretionary Complex, and deeper parts of trench fill deposits west of the deformation front) and as biogenic everywhere else. The global scale factor is a subjective estimate of global competitiveness based on professional experience.

Petroleum Plays in the Pacific offshore study area							
			Juan De Fuca Plate		Explorer MicroPlate		
Play Region	Winona Basin	Accretionary Complex	Thick Trench and Valley Fill	Thinner Plate sediments	Thick Trench and Valley Fill	Thinner Plate sediments	Pacific Plate
Play Age	Plio-Pleistocene	Miocene to Pleistocene	Miocene to Pleistocene	Plio-Pleistocene	Miocene to Pleistocene	Pliocene to Pleistocene	Miocene to Pleistocene
Structural Trap Plays	Compression & strike slip dominated anticlines and folds	Compressional anticlines and folds	Extensional fault blocks	Extensional fault blocks	Strike Slip dominated structures	Strike Slip dominated structures	None Identified
Stratigraphic Trap Plays	Turbidite Channel fill & submarine fan pinch outs	Turbidite Channel fill & submarine fan pinch outs	Turbidite Channel fill & submarine fan pinch outs	Turbidite Channel fill & submarine fan pinch outs	Turbidite Channel fill & submarine fan pinch outs	Turbidite Channel fill & submarine fan pinch outs	Turbidite Channel fill & submarine fan pinch outs
Source Rock	Hemipelagic Type II, Turbidite Type III Potential for Upwelling enrichment	Hemipelagic Type II, Turbidite Type III Potential for Upwelling enrichment	Hemipelagic Type II, Turbidite Type III Potential for Upwelling enrichment	Hemipelagic Type II, Turbidite Type III	Hemipelagic Type II, Turbidite Type III Potential for Upwelling enrichment	Hemipelagic Type II, Turbidite Type III	Hemipelagic Type II, Turbidite Type III
Reservoir	Sandy Turbidites	Sandy Turbidites	Sandy Turbidites	Sandy Turbidites	Sandy Turbidites	Sandy Turbidites	Sandy Turbidites
Seal	Hemipelagic shales Glacial turbidite shales Mass transport deposits	Hemipelagic shales Glacial turbidite shales Mass transport deposits	Hemipelagic shales Glacial turbidite shales Mass transport deposits	Hemipelagic shales Glacial turbidite shales Mass transport deposits	Hemipelagic shales Glacial turbidite shales Mass transport deposits	Hemipelagic shales Glacial turbidite shales Mass transport deposits	Hemipelagic shales Glacial turbidite shales Mass transport deposits
Data Coverage							
Wells	ODP well at downdip basin margin	Multiple shallow ODP wells No deep ODP wells	1 shallow ODP well no deep ODP wells	Multiple ODP wells	No ODP wells	No ODP wells	No wells
2D Seismic	Moderate	Moderate	Limited	Moderate	Limited to moderate	Limited to moderate	Minimal
Global Scale Factor							
Thermogenic	0.6 (Structural Traps) 0.5 (Stratigraphic Traps)	0.6 (Structural Traps) 0.5 (Stratigraphic Traps)	0.6 (Structural Traps) 0.5 (Stratigraphic Traps)	N/A (Structural traps) 0.5 (Stratigraphic Traps)	0.6 (Structural Traps) 0.5 (Stratigraphic Traps)	0.6 (Structural Traps) 0.5 (Stratigraphic Traps)	N/A
Biogenic	N/A	N/A	0.25	0.25	0.25	0.25	0.25

APPENDIX A – GLOSSARY OF TERMS

(*1 from or modified from Schlumberger Limited's on-line dictionary, The Oilfield Glossary: http://www.glossary.oilfield.slb.com)
(*2 from or modified from the Canadian Association of Petroleum Producers Glossary: https://www.capp.ca/publications-and-statistics/glossary)
(*3 from or modified from National Energy Board's Glossary: https://www.neb-one.gc.ca/nrg/tl/glssr-eng.html)
(*4 from or modified from the Geology Dictionary.com: https://geology.com/dictionary/glossary-s.shtml)
(*5 from or modified from Doust, 2010: https://doi.org/10.1306/06301009168)

Accretionary Complex: A dynamically deforming fold and thrust belt that forms when sediments on a subducting oceanic plate are scraped off above a detachment surface in a bulldozer-like manner. Younger sediments form the outermost parts of the complex or prism, and sediments become older in the innermost parts of the complex.

Basalt*4**:** Formed from cooled, hardened molten rock, often associated with volcanic processes. It forms the bedrock of the ocean floor and also occurs on land in extensive lava flows.

Biogenic gas: Gas produced by biological activity as microorganisms attempt to decompose the remains of marine life, typically at shallow depths and lower temperatures (less than 70°C).

Carbon Capture and Storage*2: The process of taking waste carbon dioxide and transporting it to a storage site, normally underground in a specific type of geological formation.

Conventional Petroleum*4**:** an umbrella term for oil and natural gas that can flow into a well at commercial rates without the extensive use of technology after the well is drilled.

Deep Water Play*1: Conceptual model for a type of hydrocarbon accumulation in offshore areas where water depths exceed approximately 600 feet [200 m], the approximate water depth at the edge of the continental shelf. While deep-water reservoir targets are geologically similar to reservoirs drilled both in shallower present-day water depths as well as onshore, the logistics of producing hydrocarbons from reservoirs located below such water depths presents a considerable technical challenge.

DSDP: Deep Sea Drilling Project. An ocean drilling project that operated from 1968 to 1983.

Gas Hydrate*1: An unusual occurrence of hydrocarbon in which molecules of natural gas, typically methane, are trapped in ice molecules. More generally, hydrates are compounds in which gas molecules are trapped within a crystal structure. Hydrates form in cold climates, such as permafrost zones and in deep water. To date, economic liberation of hydrocarbon gases from hydrates has not occurred, but hydrates contain quantities of hydrocarbons that could be of great economic significance.

Geothermal Energy*3: The use of geothermal heat from the earth's molten core to generate electricity.

Hydrocarbon*1**:** A naturally occurring organic compound comprising hydrogen and carbon. Hydrocarbons can be as simple as methane [CH_4], but many are highly complex molecules, and can occur as gases, liquids or solids. The molecules can have the shape of chains, branching chains, rings or other structures. Petroleum is a complex mixture of hydrocarbons. The most common hydrocarbons are natural gas, oil and coal.

Hydrothermal Vent: A hot spring on the sea floor, usually near mid-ocean ridges, that discharges hot water laden with dissolved metals and dissolved gases. When these hot fluids contact the cold ocean water the dissolved materials precipitate, producing a dark plume of suspended material. The water discharged from these springs is sea water that percolates down into the earth through fissures in the sea floor. This water is heated and picks up dissolved gases and metals as it interacts with the hot rocks and magma at depth. Also known as a "black smoker."

IODP: The Integrated Ocean Drilling Program is an international marine research program.

Maturation*[1]: The process of a source rock becoming capable of generating oil or gas when exposed to appropriate pressures and temperatures. As a source rock begins to mature, it generates hydrocarbons.

Migration*[1]: The movement of hydrocarbons from their source into reservoir rocks. Migration typically occurs from a structurally low area to a higher area because of the relative buoyancy of hydrocarbons in comparison to the surrounding rock.

Miocene: Geological Epoch approximately 23 to 5.3 million years before present.

ODP: The Ocean Drilling Program was established in 1985 as an international cooperative effort to explore and study the composition and structure of the Earth's ocean basins. In 2004, it transformed into the IODP.

Oligocene: Geological Epoch approximately 33.9 to 23 million years before present.

Petroleum*[2]: A naturally occurring mixture composed predominantly of hydrocarbons in the gaseous, liquid or solid phase.

Petroleum System*[1]**:** Geologic components and processes necessary to generate and store hydrocarbons, including a mature source rock, migration pathway, reservoir rock, trap and seal.
Appropriate relative timing of formation of these elements and the processes of generation, migration and accumulation are necessary for hydrocarbons to accumulate and be preserved.

Play*[1&5]: A conceptual model for a style of hydrocarbon accumulation used by explorationists to evaluate petroleum opportunities in a basin, region or trend. Plays can are best defined by defining the petroleum source rock, the reservoir and the trap type. In areas where few accumulations are in an individual play, meaningful statistical analyses may have to be conducted at higher levels.

Pleistocene: Geological Epoch approximately 2,588 to 11.7 thousand years before present.

Pliocene: Geological Epoch approximately 5.333 to 2.58 million years before present.

Reservoir*[1]**:** A subsurface body of rock having sufficient porosity and permeability to store and transmit fluids. Sedimentary rocks are the most common reservoir rocks as they have more porosity than most igneous and metamorphic rocks and form under temperature conditions at which hydrocarbons can be preserved. A reservoir is a critical component of a complete petroleum system.

Sandstone*[2]: A compacted sedimentary rock composed mainly of quartz or feldspar; a common rock in which oil, natural gas and/or water accumulate.

Seal*[1]**:** A relatively impermeable rock, commonly shale, anhydrite or salt that forms a barrier or cap above and around reservoir rock such that fluids cannot migrate beyond the reservoir. A seal is a critical component of a complete petroleum system.

Seamount*[4]**:** A mountain on the sea floor that has at least 1000 meters of local relief. Most seamounts are shield volcanoes.

Sedimentary: rock formed from the consolidation of sediments transported by water, wind or ice.

Shelf: The area of seabed around a large landmass where the sea is relatively shallow compared with the open ocean. The continental shelf is geologically part of the continental crust.

Slope: The slope between the outer edge of the continental shelf and the deep ocean floor.

Source rock*[1]**:** A rock rich in organic matter which, if heated sufficiently, will generate oil or gas. Typical source rocks, usually shales or limestones, contain about 1% organic matter and at least 0.5% total organic carbon (TOC), although a rich source rock might have as much as 10% organic matter.

Seafloor Spreading Centre: A divergent plate boundary. In this context, two oceanic plates are moving apart and magma is coming to the surface to create new oceanic crust.

Stratigraphic Trap*[1]**:** A variety of sealed geologic container capable of retaining hydrocarbons, formed by changes in rock type or pinch-outs, unconformities, or sedimentary features such as reefs.

Strike-slip: A fault where two plates are moving parallel to each other in opposite directions. Movement is parallel to the line of the fault.

Structural Trap*[1]**:** Structural traps, in contrast, consist of geologic structures in deformed strata such as faults and folds whose geometries permit retention of hydrocarbons.

Subduction: A tectonic process where one plate slides underneath another as they move towards each other.

Tectonic Plate*[4]**:** The crust and the uppermost mantle, consists of a number of pieces or tectonic plates that are composed of oceanic crust or continental crust. The movement of the plates toward each can form mountains and oceanic crust will move under continental crust (subduction). When plates move away from each other, hot magma can be released at the Earth's surface (seafloor spreading) to form new oceanic crust.

Thermogenic: Organic matter is heated to a temperature that allows for the production of hydrocarbons.

Trap*[1]**:** A configuration of rocks suitable for containing hydrocarbons and sealed by a relatively impermeable formation through which hydrocarbons will not migrate. Traps are described as structural traps (in deformed strata such as folds and faults) or stratigraphic traps (in areas where rock types change, such as unconformities, pinch-outs and reefs). A trap is an essential part of a petroleum system.

Triple junction: A place where three different plate boundaries meet. They were initially thought to occupy points but mapping over the years shows that, in fact areas hundreds of km wide can be affected.

Unconventional Petroleum Resource*[3]: An umbrella term for oil and natural gas that is cannot be produced without mining; the extensive use of technology; or without altering the natural viscosity of the oil. Examples include: coalbed methane, shale gas and gas hydrates.

APPENDIX B – INDUSTRY AND SCIENTIFIC ACTIVITIES

B.1 Petroleum industry activity: shelf and deepwater exploration

Petroleum exploration in the west coast region occurred intermittently between 1913 and 1984 (B.C. Ministry of Energy, Mines and Natural Gas). Shell Canada Ltd. drilled 14 offshore wells between 1965 and 1969, which included eight wells in the Queen Charlotte Basin and six in the Tofino Basin (Figure B-1); no wells have been drilled in the Winona Basin (Hannigan et al., 2001). No oil or gas field discoveries have been made to date but several wells encountered oil or gas shows, (e.g. Sockeye B-10, Pluto I-87, and Prometheus H-68 (see Appendix C.7.3 for detail). Dry biogenic gas shows have been encountered in Pleistocene sands and gravels on the Fraser river delta and in 8 wells drilled in the Bellingham sub-basin (NW Washington (Hannigan et al., 2001). Previous work on hydrocarbon occurrences, petroleum source rocks, organic geochemistry data, and petroleum systems models include: McIver (1973), Macauley (1983), Hamilton and Cameron (1989), Vellutini (1988), Fowler and others (1988 & 1987), Vellutini and Bustin (1993a and b), Lyatsky and Haggard (1993), Bustin (1997), Snowden (2002), Schümann and others (2013 and 2008).

An indefinite moratorium was imposed on petroleum exploration in the Pacific offshore by the Canadian federal government in 1972. No offshore drilling has occurred since the moratorium was established; exploration licenses issued prior to the moratorium are in abeyance (B.C. Ministry of Energy, Mines and Natural Gas).

B.2 Scientific drilling, geophysical surveys and observatory research in Northern Cascadia Basin

Since 1973, the Deep Sea Drilling Program (DSDP), Ocean Drilling Program (ODP), and Integrated Ocean Drilling Program (IODP) have undertaken eight expeditions within the study area. These programs drilled 97 holes at 32 different sites to study a wide range of topics, including subduction zones and the triple junction of the Juan de Fuca, North American and Pacific plates, massive sulfides, hydrothermal circulation of the ocean crust, and Cascadia margin gas hydrates (Table B-1A). Approximately 29 000 line-km of seismic data as well as bathymetry and gravity data were available for appraisal in this study. Table B-1B references a subset of the seismic data, specifically those lines where returning seismic energy allowed, in whole or in part, interpretation of the top of oceanic crust (approximately 21 000 line-km). Data types, originating institutions/survey years, and key reference information are summarized for seismic data (Table B-1B) and for bathymetry and gravity data (Table B-1C).

The Geological Survey of Canada has previously assessed petroleum resource potential in the Gwaii Hannas (Dietrich and others (1992) Open File Report 2557), Scott Islands (Hannigan and others, (2005) Open File Report 4829) and Hecate Strait (Hannigan and Dietrich (2011) Open File Report 6860) areas in support of marine conservation activities. The locations for these assessments are shown in Appendix B, Figure B-1. Additional resource assessment works consulted during the study includes works by: Hannigan and others (2001 & 1998), Dietrich (1995) and Carson and Nelson (1987).

Seabed installations related to ongoing research activities within the study area, by Ocean Networks Canada, NEPTUNE Canada and various Canadian and International academic investigators,include:
i) the North-east Pacific Time-series Undersea Networked Experiments (NEPTUNE) cable and,
ii) Circulating Obviation Retrofit Kits (CORK) borehole seals (Best et al., 2015; Figure B-1).

i) NEPTUNE cable: The 800 km long fibre-optic Neptune Cable was installed by the University of Victoria in 2007. The cable forms a loop and connects five active nodes that include the ODP site 889, Barkley Canyon, ODP site 1027, and the Endeavor segment on Juan de Fuca Ridge (Moran, 2013).

ii) CORKs: these permanent seabed installations seal boreholes from the surface to allow for long term monitoring of in situ temperature and pressure measurements. Data obtained from CORK stations can provide important information on heat flow, chemical exchange between the ocean and crust, methane hydrate formation and ore deposition (Becker and Davis, 2005). CORKs need to be revisited occasionally for data collection and maintenance.

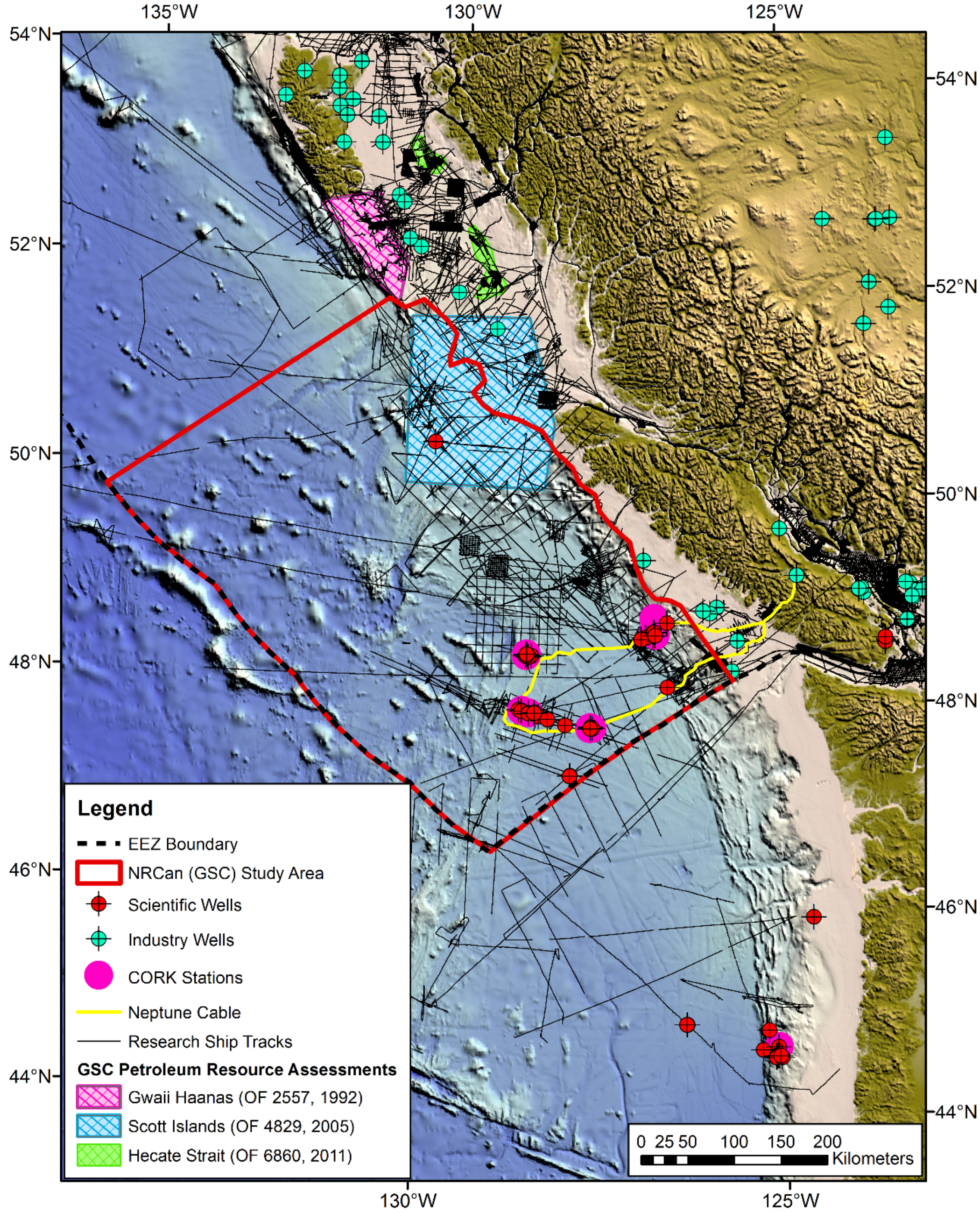

Figure B-1. Petroleum Industry and Scientific Activity map. Summary of Industry wells, scientific data (wells, seismic, Cork stations and Neptune Cable) and previous GSC petroleum resource assessment areas within the Offshore Pacific region. A summary of seismic data consulted in this study is provided in Appendix B, Table B-1B. Bathymetry data accessed from: http://www.geomapapp.org Global Multi-Resolution Topography (GMRT) Synthesis (Appendix B, Table B-1C; Ryan et al., 2009).More information on the locations of exploration licenses under moratorium can be found at http://webmap.em.gov.bc.ca/mapplace/minpot/offshore.cfm.

Table B-1A. Scientific drilling research programs.

Program details (objectives, wells count and program year) are summarized for programs in the study area (DSDP Leg 18, ODP Legs 139, 146, 168, 169, IODP Legs 301, 311, 327 and 341S).

Leg	Basic Objective	No. Wells in AOI	Year
18	Study subduction zones and Paul Revere Ridge (triple junction of Juan de Fuca, North American, Pacific plates)	2	1973
139	Massive sulfides, and hydrothermal vents	23	1992
146	Understand mechanism of diffuse and channel flow within the wedge, and to study the relationship between BSR's and the occurrence of gas hydrate and free gas	9	1993
168	Hydrothermal circulation in oceanic crust: Eastern flank of the Juan de Fuca Ridge	19	1997
169	Continuation of Leg 139, investigation of massive sulfides	14	1998
301	Juan de Fuca Hydrogeology	4	2004
311	Cascadia Margin Gas Hydrates	23	2005
327	Hydrogeologic architecture of basaltic oceanic crust	11	2010
341S	SCIMPI (Simple Cabled Instrument for Measuring Parameters In situ) deployment and Hole 858G CORK replacement	1	2013

Table B-1B

Overview of seismic datasets used in this study to map sediment thickness. The reader is referred to Appendix E for citations associated with reference papers or principal investigators acknowledged in this summary table.

Data Type	Source Organisation and year-cruise	Reference paper or principal investigator
Single Channel	Geological Survey of Canada - Pacific 1971	Davis and Lister, 1977
Single Channel	Geological Survey of Canada - Pacific 1972-28	Geological Survey of Canada Open File Report 751, E. E. Davis and D. A. Seemann, 1981
Single Channel	Geological Survey of Canada - Pacific 1973	Geological Survey of Canada Open File Report 751, E. E. Davis and D. A. Seemann, 1981
Single Channel	Geological Survey of Canada - Pacific 1977	Hyndman et al., 1981
Multichannel	Geological Survey of Canada - Pacific 1985	Geological Survey of Canada Open File 1661, Yorath et al., 1987
Single Channel	Geological Survey of Canada - Pacific 1987-04	PI: Rohr GSC archive
Multichannel	Geological Survey of Canada - Pacific 1988	Geological Survey of Canada Open File 2258, Rohr and Dietrich, 1990
Single Channel	Geological Survey of Canada - Pacific 1988-09	Davis et al., 1992
Multichannel	Geological Survey of Canada - Pacific 1989	Geological Survey of Canada Open File 2391, Spence et al 1991
Single Channel	Geological Survey of Canada - Pacific 1989-05	Geological Survey of Canada Open File 2391, Spence et al 1991
Single Channel	Geological Survey of Canada - Pacific 1994-04	PI: Rohr, Hamilton
Single Channel	Geological Survey of Canada - Pacific 1995-04	PI: V. Barrie, B. Bornhold, K. Rohr
Single Channel	Geological Survey of Canada - Pacific 1996-03	PI: K. Rohr
Single Channel	Geological Survey of Canada - Pacific 1999-02	PI: Ross Chapman and George Spence
Single Channel	Geological Survey of Canada - Pacific 2001-03	PI: George Spence and Rick Coffin (Naval Research Lab)
Single Channel	Geological Survey of Canada - Pacific 2003-04	PI: E. Willoughby
Single Channel	Geological Survey of Canada - Pacific 2004-08	PI: George Spence and Ele Willoughby
Single Channel	Geological Survey of Canada - Pacific 2010-05	Geological Survey of Canada, Open File 7558, G. D. Spence and M. Riedel, 2014
Single Channel	Geological Survey of Canada - Pacific 2013-08	Geological Survey of Canada, Open File 7716, Riedel et al., 2014
Single Channel	Geological Survey of Canada - Pacific 2014-06	Geological Survey of Canada, Open File 7715, Riedel et al., 2014
Single Channel	Lamont-Doherty Earth Observatory, Columbia University 1966	PI: Charles Fray
Single Channel	Lamont-Doherty Earth Observatory, Columbia University 1967	PI: Walter Pitman
Single Channel	Lamont-Doherty Earth Observatory, Columbia University 1971	PI: Robert Embley
Multichannel	Lamont-Doherty Earth Observatory, Columbia University 2002	Canales et al., 2005; Carbotte et al., 2008; Carbotte et al.,2006; Carbotte et al.,2004
Multichannel	Lamont-Doherty Earth Observatory, Columbia University 2012	Han et al., 2016
Multichannel	United States Geological Survey (USGS)	Hampton et al., 1989; Triezenberg et al., 2016; https://walrus.wr.usgs.gov/NAMSS/
Multichannel	University of Bremen, Bremen, Germany	Zühlsdorff et al., 1999
Multichannel	University of Victoria, British Columbia, Canada 1996	C. R. Fink and G. D. Spence, 1999; Ganguly et al., 2000

Table B-1C

Overview of other data sets (bathymetry, gravity, well data, dredge samples, and gas seep) datasets used in this study. The reader is referred to Appendix E for citations associated with reference papers or principal investigators acknowledged in this summary table.

Data Type	Source Organisation	Reference paper or principal investigator
Bathymetry Data	GeoMapApp: Global Multi-Resolution Topography (GMRT) Synthesis	http://www.geomapapp.org Ryan, W.B.F., S.M. Carbotte, J.O. Coplan, S. O'Hara, A. Melkonian, R. Arko, R.A. Weissel, V. Ferrini, A. Goodwillie, F. Nitsche, J. Bonczkowski, and R. Zemsky (2009), Global Multi-Resolution Topography synthesis, Geochem. Geophys. Geosyst., 10, Q03014, doi:10.1029/2008GC002332. Data DOI: 10.1594/IEDA.0001000
Gravity Data	Natural Resources Canada Geological Survey of Canada., 2014. Geoscience Data Repository for Geophysical Data	http://gdr.agg.nrcan.gc.ca/gdrdap/dap/info-eng.php Geological Survey of Canada., 2014. Geoscience Data Repository for Geophysical Data, Gravity, Point Data, Natural Resources Canada. http://gdr.agg.nrcan.gc.ca/gdrdap/dap/searcheng.php1.
ODP Well data (Lithology, grain size, biostratigraphy, geochemiistry, heat flow data and more)	International Ocean Discovery Program (http://web.iodp.tamu.edu/OVERVIEW/)	(http://web.iodp.tamu.edu/OVERVIEW/) Deep Sea Drilling Project, 1989. Archive of Core and Site/Hole Data and Photographs from the Deep Sea Drilling Project (DSDP). NOAA National Centers for Environmental Information. doi:10.7289/V54M92G2 Integrated Ocean Drilling Program, 2010. Archive of Core and Site/Hole Data and Photographs from the Integrated Ocean Drilling Program (IODP). NOAA National Centers for Environmental Information. doi:10.7289/V58913SM. Ocean Drilling Program, 2005. Archive of Core and Site/Hole Data and Photographs from the Ocean Drilling Program (ODP). NOAA National Centers for Environmental Information. doi:10.7289/V5W37T8C
Seabed Dredge Samples	National Geophysical Data Center, NOAA.	Curators of Marine and Lacustrine Geological Samples Consortium (2013). The Index to Marine and Lacustrine Geological Samples (IMLGS). National Geophysical Data Center, NOAA. doi:10.7289/V5H41PB8 [2017-07-05].
Gas Seep Data	Data shown in Figure 4 provided by Natural Resources Canada Geological Survey of Canada, (Barrie, 2011) Additional data consulted during the study were provided by Ocean Networks Canada.	Barrie, J.V., 2011. Hydrocarbon Gas Seep Sightings – Marine Expeditions 2011001PGC and 2011002PGC. Ocean Networks Canada Data Archive, http://www.oceannetworks.ca, University of Victoria, Canada.
Seamount data	Seamount Biogeosciences Network (via EarthRef.org)	https://earthref.org/SC/
Seabed Imagery	Ocean Networks Canada Data Archive	Ocean Networks Canada Data Archive, http://www.oceannetworks.ca, University of Victoria, Canada. Seabed Imagery

APPENDIX C – GEOLOGICAL AND GEOPHYSICAL OVERVIEW AND DETAIL

C.1 Tectonic Setting

C.1.1 Overview and Major Tectonic Elements

The study area contains three tectonic boundaries: the Juan de Fuca spreading centre (separating the Pacific and Juan de Fuca plates), the Cascadia subduction zone (the zone where the Juan de Fuca Plate is subducting beneath the North American Plate) and the strike-slip Revere-Dellwood and Queen Charlotte faults (separating the Pacific and North American plates; Figure 2). These three tectonic boundaries separate three tectonic plates (Pacific, North American and Juan de Fuca) that intersect at a triple junction. The recent evolution of the triple junction includes the formation of a microplate (Explorer), and a ‘block’ (the Winona Basin), the reorientation of the Northern Juan de Fuca ridge and along-strike propagation of the strike-slip faults. While the main plate boundaries are well defined, many aspects of the recent evolution of the triple junction region are not.

The pattern of linear magnetic anomalies on either side of the spreading centre (Raff and Mason, 1961) provide the framework for the Pacific and Juan de Fuca plate relative motion history (Riddihough, 1984; Wilson, 1993). The various segments of the spreading centre mostly exhibit small lateral offsets; but there is also a major transform fault, the Sovanco Fracture Zone, that forms the southwestern boundary of the Explorer microplate. The along-strike propagation of these rift valleys have left in their wake disrupted crustal structure and magnetic signatures (Wilson, 1993). The triple junction region does not show the typical pattern of linear magnetic stripes. Rapid western migration and jumps of the Explorer spreading centre (Botros and Johnson, 1988) as well as later shearing appears to have disrupted or destroyed most of the original lineation pattern. The absence of magnetic lineations in the Winona Basin is in part because a blanket of thick sediments has sufficiently raised crustal temperatures to overprint the original magnetisation (Davis and Riddihough, 1982).

Seismic reflection profiles across the region image the top of oceanic crust, seafloor spreading centres, seamounts and Quaternary sediments that thicken into the trough (or trench) of the Cascadia subduction zone on the Juan de Fuca Plate. Numerous small offset faults were also imaged around the northern Juan de Fuca Ridge (McManus et al., 1972; Barr and Chase, 1974; Davis and Lister, 1977), in the Explorer microplate (Barr and Chase, 1974; Davis and Lister, 1977), Nootka Fault Zone (Hyndman et al., 1979) and the Juan de Fuca Plate itself (Han et al., 2016). In the latter region, the faults may be the result of a small internal shear from Pacific-North America oblique interactions, as well as bending stresses from glacial outwash sediments and flexure into the subduction zone (Han et al., 2016).

Canada’s most seismogenic zone occurs within the Explorer microplate (Figure 2), and adjacent to the Revere-Dellwood and the Queen Charlotte faults (Cassidy et al. 1998, Geoscience Canada, 2010). Earthquakes of magnitude greater than 4 are commonly observed along the Queen Charlotte Fault, Revere-Dellwood Fault, within the Explorer microplate and on the northernmost extent of the Juan de Fuca spreading centre (e.g. Riedel and Rohr, 2012). Frequent earthquakes of smaller magnitude occur broadly scattered across these regions. They are less accurately located but can also occur on smaller structures. Events of magnitude greater than 6 are common in this region and were identified even when only a few seismometers were located on Vancouver Island (e.g. Milne and Smith, 1966). By 1992, the distribution of seismometers was considered sufficient to locate the larger offshore earthquakes with approximately +/- 10 km accuracy (G. Rogers and J. Cassidy, pers. comm. 2009).

Plate tectonic illustrations of the last 30 years have typically shown the Cascadia subduction zone continuing past Vancouver Island to the southern tip of the Queen Charlotte fault and treats the volcanic edifices of the Dellwood Knolls and the Tuzo Wilson seamounts as spreading centres. However, north of Brooks Peninsula on Vancouver Island the lack of a visible subducting slab (Audet et al., 2008) or episodic seismic tremor (Kao, et al., 2009) under Vancouver Island indicate that subduction does not continue past that point. Multibeam bathymetry of the Dellwood Knolls and the Tuzo Wilson seamounts shows that they are better characterised as coalescing volcanic cones and sills that lack the dominant signature of extensional faults seen at spreading centres (Rohr and Furlong, 1995). Significant seismicity has been observed along the northward trend of the Revere-Dellwood Fault and side-scan sonar and seismic reflection data indicate that this fault overlaps the Queen Charlotte fault by 120 km. The Dellwood Knolls and the Tuzo Wilson seamounts are interpreted to be the result of limited extension on a right step between two right-lateral strike slip faults (Rohr, 2015; Rohr and Furlong, 1995). This zone of overlap has propagated northward in the last 2 Ma (Davis and Riddihough, 1982).

C.1.2 Tectonic Regions

Five distinct regions are identified in the study area based on the tectonic setting and associated structural style (Figures 2 and C-1):

1. **Pacific Plate** This rugged, tectonically quiet region is dominated by relatively thin, flat-lying sediments, limited structure and occasional seamounts (Figure C-1A).

2. **Explorer Microplate** This highly seismogenic region is dominated by pervasive small-offset, high-angle faults formed by shearing of the microplate during the evolution of the triple junction (Figure C-1B).

3. **Juan de Fuca Plate** Small-offset extensional fault-blocks are visible in the seismic data throughout this region in the study area (Figure C-1C). Most cannot be mapped and the true sense of movement on individual faults is not known. These faults may have a shear component (Han et al., 2016) and are enhanced by bending stresses. Middle Valley, a graben containing thicker sediments is mapped near the spreading centre.

4. **Winona Basin** The Winona Basin is characterized in its southern portion by compressional structures including anticlinal ridges and folds; some appear to be positive flower structures (e.g. Rohr and Tryon, 2010; Figure C-1D). Deformation increases southward where several sedimentary ridges with bathymetric expression have been mapped. The northern portion of the basin is characterized by transtension between two strike-slip faults that resulted in the formation of volcanic edifices and sills.

5. **Accretionary Complex** The modern accretionary wedge extends northeastward from the deformation front to the shelf edge and is dominated by compressional structures that include ramp anticlines on imbricate thrusts and back-thrusts as well as fault-propagation folds in the accreted sediments (Figure C-1E).

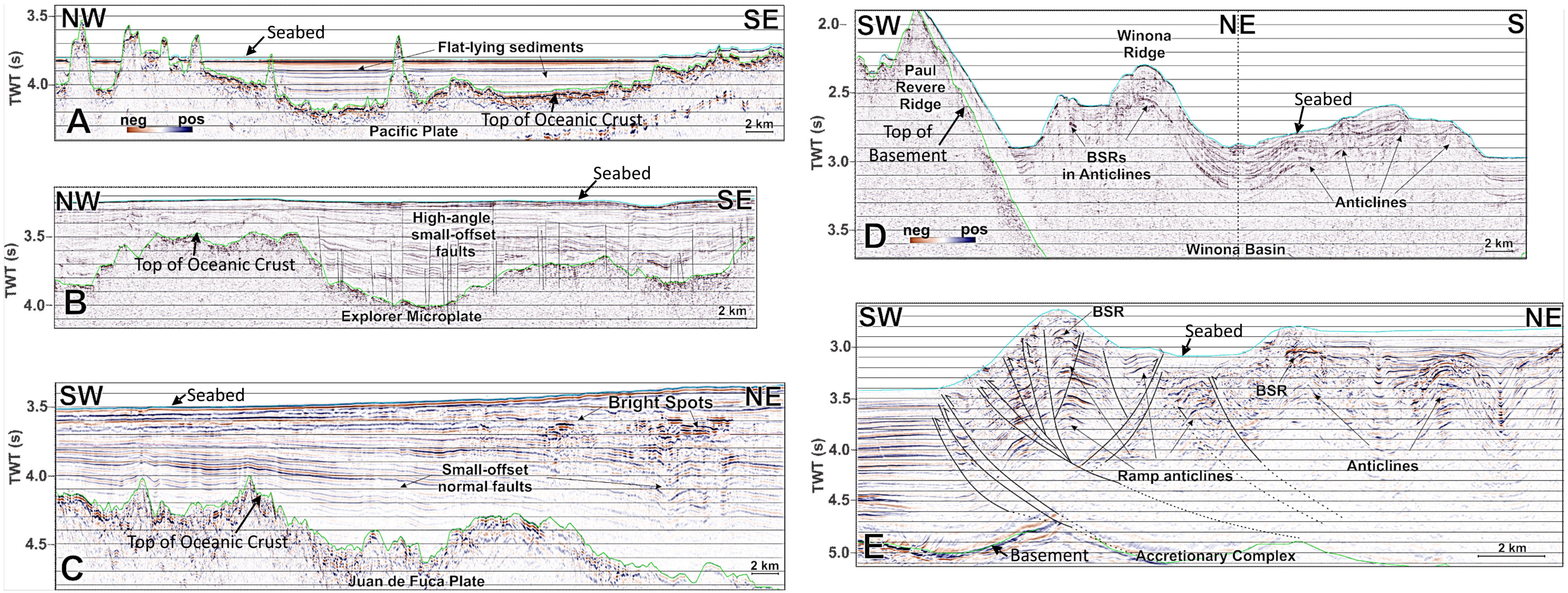

Figure C-1. 2D seismic profiles showing dominant structures by tectonic region.

Refer to Figure 3 for 2D Line locations. Seabed (light blue) and top of basement (bright green) are shown; all sections have the same reflection polarity); A. Pacific Plate: sedimentary strata are thin or absent; Original data source: Line EW0207-20, Lamont-Doherty Earth Observatory, 2002; B. Explorer Plate: pervasive, high-angle, small-offset strike-slip faults; Original data source: PGC9404_EX08_line2, Geological Survey of Canada – Pacific, 1994-04; C. Juan de Fuca Plate: small-offset normal fault blocks and direct hydrocarbon indicators (bright spots); Original data source: Line 85-09, Geological Survey of Canada – Pacific, 1985; D. Winona Basin: anticlinal ridges, folds, and BSRs; Original data source: Line PGC9404_EX20_line34to38, Geological Survey of Canada – Pacific, 1994-04; E. Accretionary Complex: thrust faults, anticlines and BSRs; Original data source: Line 8909B, Geological Survey of Canada – Pacific, 1989.

C.2 Thermal Conditions

The study area is characterized by highly variable geothermal gradients controlled by a range of tectonic features (spreading ridge, accretionary prism, transform basin, and multiple plate boundaries) and, at a local scale, by hydrothermal activities and basalt extrusions. Temperature data including shallow temperature measurements (from Bullard, Lister, or Ewing probes) were obtained during DSDP/OPD/IODP research expeditions and heat flow variability within the study area has been the focus of numerous scientific investigations (e.g. Davis et. al., 1989; Davis and Villinger, 1992; Hyndman and Wang, 1993; Davis and Becker, 2002). Geothermal gradients predictions involving calibration with heat probe measurements can have errors of less than 10 per cent; uncertainties as high as 50 to 60% of calculated values can occur if calibration data are not available (Grevemeyer and Villinger, 2001).

Measured heat flow values in Winona Basin range between 23 to 147 mWm^{-2} with lower values occurring in the inner part of the basin as a result of higher sedimentation rates (Davis and Riddihough, 1981). In the Accretionary Complex heat flow decreases landward across the continental margin. This predictable trend is a result of a thickening accretionary prism overlying a cooling subducting oceanic crust. (Davis et al, 1990). Thermal conditions at the Juan de Fuca Trench are influenced by frictional heat of accreting sediments and oceanic crust of the Juan de Fuca plate subducting beneath the North American Plate (Hyndman and Wang, 1993). Middle Valley rests on young crust (<1 Ma) resulting in very high heat flows. Measured data do not yield trends coherent with basin structure and are likely complicated as a result of influence from hydrothermal circulation and basalt sill extrusions.

C.3 Thickness of Sedimentary Basin Fill

A sediment thickness map for the study area was created using mostly 2D seismic data, a few gravity profiles, and some published depth cross sections (Figure C-2). The top and base of sediments (represented by the seabed and sediment-basement interface) were picked, where possible, on the available 2D time seismic data and converted to approximate thickness using a velocity gradient for the sediments from a refraction study (Horning et al., 2016). In the Winona Basin, the base of sediments was not easily interpreted due to a lack of acoustic penetration under thick sediments. A 3D gravity inversion model was generated in Winona Basin to estimate sediment thickness (see below). Results of the modeling suggest sedimentary basin fill is likely in excess of 8.6 km thick in the deepest part of Winona Basin. In the Accretionary Complex, a simple velocity gradient was not valid due to complex velocity fields in the accreted sediments (e.g. Yuan et al., 1994). Therefore, a published depth-converted multichannel seismic section was integrated to help constrain depth in this area. Previous velocity model work in the Tofino Basin were also consulted (Hayward and Calvert, 2007). The entire study area also contains numerous seamounts and ridges where sediment cover is minimal. For the purposes of this study, these areas were constrained as having zero sediment thickness.

The map depicted in Figure C-2 is our best current estimate of sediment thickness in the study area, which ranges from 0 to ~8.6+ kilometers. Uncertainty remains for the thickness of sediments in Middle Valley, the Juan de Fuca Trench, Winona Basin, and Accretionary Complex, where base of sediments is not resolvable or imaged on seismic profiles. In Middle Valley, a minimum value was computed from the thickness of imaged sediments. Another source of uncertainty arises from the use of a regional refraction velocity function, which does not account for local variations in velocity. Various velocity functions were tested; the gradient function ultimately used was chosen because it matched observations of drilled thickness at IODP site 1027 and the time to basement reflector on a seismic profile over the drill site.

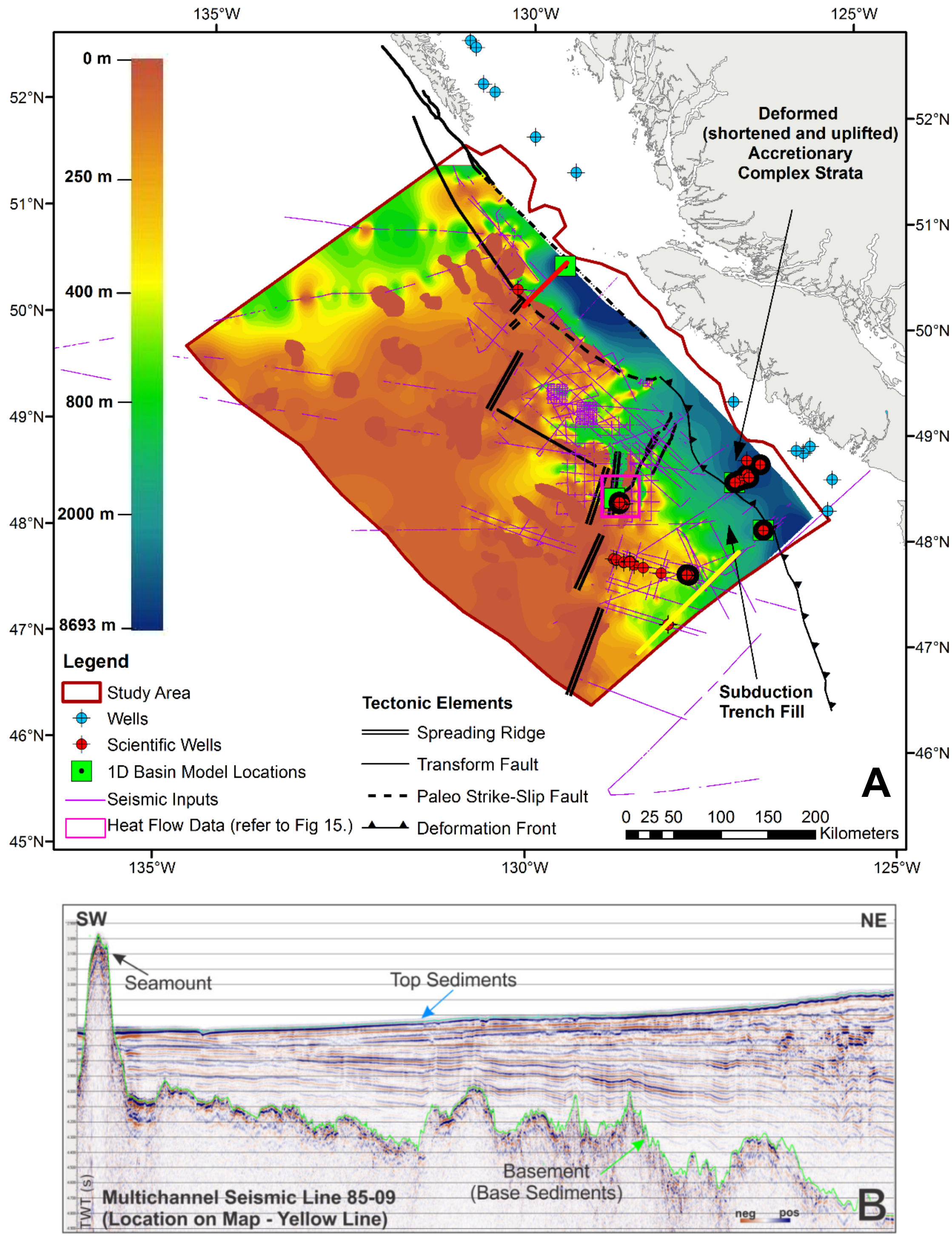

Figure C-2. Sediment thickness map (A) and illustrative seismic line (B).
Line location is shown in yellow. Original data source: Line 85-09, Geological Survey of Canada – Pacific, 1985. Sediment thickness shown in (**A**) represents the thickness between blue horizon (Seabed or top sediments) and green horizon (Basement or base of sediments). Note the seamount on the SW end of the line. Thickness map was generated using seabed and base of sediments interpretations (K.Rohr, this study), and utilizing seabed data from the Global Multi-Resolution Topography (GMRT) Synthesis from variable data density and interpolation issues (especially on the Pacific plate, in Winona Basin, and within the Accretionary Complex).

Other velocity functions computed lower sediment thicknesses (e.g. Gardner et al., 1993); actual thicknesses likely fall somewhere between. Further sources of uncertainty arise (Ryan et al., 2009). Thickness in depth was approximated by using a velocity gradient for sediments based on a refraction study by Horning and others, 2016.

Gravity model: Sediment thickness in the Winona Basin is estimated from the 3D inversion of marine Bouguer gravity data (Geological Survey of Canada, 2014). Sediment in the Winona Basin has a lower density than the underlying igneous, oceanic crustal, basement. Thus, the low Bouguer anomaly observed over the basin is an indication of the basin's sedimentary fill, as well as variations in density and thickness. A 3-D inversion of the Bouguer gravity data with GRAV3D (Li and Oldenburg 1998) provides a tool for estimation of these two unknowns. Model input parameters were varied within reasonable limits to form a suite of density contrast models. The final model was chosen based on a good match to a depth-converted seismic reflection profile 88-02 (Figure C-3A, location of 88-02 in bold red on Figure C-2). The model predicts the lowest sediment densities (Figure C-3A) to be associated with a region of relatively low seismic reflectivity and gently NE-dipping seismic reflections between shot points 12 700 and 13 000. Below, at a depth of approximately 6 km, model density contours align with higher amplitude, NE-dipping, reflections. The density model also reflects the zone of deformation to the southwest of shot point 13 000 (Figure C-3A). The 3D density contrast model (Figure C-3B) suggests that the Winona Basin is much broader and deeper to the southeast of line 88-02. Internally its structure appears complex with local depocenters, but greatest basement depths of approximately 12 km occur within the center of the basin.

C.4 Basin Fill Age Constraints and Stratigraphy

The recognition of magnetic anomaly isochrons (Figure C-4A) and the work that followed to identify spreading ridges, fracture zones and propagating ridges has resulted in a good understanding of oceanic crust age in the northwest Pacific region (Atwater and Menard, 1970; Wilson, 1988; 2002; Riddihough, 1984). Oceanic crust forms at spreading ridges and its age increases away from the spreading centre to a maximum age of 16 Ma in the northwest corner of the Pacific Plate, and 9 Ma in the southeast corner of the Juan de Fuca Plate (Figures C-4A and C-4B; Wilson, 2002). These crustal ages provide useful constraints for the dating of overlying sediments where age dating from wells is sparse (Figure C-4C). Basin fill within the study area is expected to be Pleistocene or younger in the vicinity of crustal spreading ridges, Pliocene and younger over parts of the Juan de Fuca Plate, Pacific Plate and Explorer microplate, and Miocene and younger in the thickest areas of trench fill on the Juan de Fuca plate, in the Accretionary complex region and along the western side of the study area on the Pacific Plate. Magnetic isochron data are not available to constrain basin fill age in the Winona Basin. The DSDP Leg 18, Site 177 well located just east of the Revere- Dellwood Transform Fault reached Total depth (TD) in Pliocene sediments, which suggests the Winona Basin fill could be at least Pliocene and younger in age. The age of oceanic crust beneath TD at Site 177 is not known, and overlying basin fill away from well control may be different.

Research well data within the region provide some constraints to the age of basin fill (Figure C-4C). Basin fill above the Juan de Fuca Plate ranges in age from Pliocene to Recent (Underwood et al, 2005). No wells have been drilled in the thicker basin fill of the Pacific Plate, the Explorer microplate or the Winona Basin, and the only well in the Juan de Fuca Trench (Leg 146, Site 888) tests the upper 600 m of a 2500 m thick section. Sediment age at depth in thicker untested basin fill of the study area are unknown. Industry exploration wells in the Tofino Basin encountered Eocene to Recent stratigraphy in the eastern portion of the Accretionary Complex (Johns et al., 2012, Johns et al., 2015). The western region of the Accretionary Complex is younger, with an expected age range from Miocene to Recent.

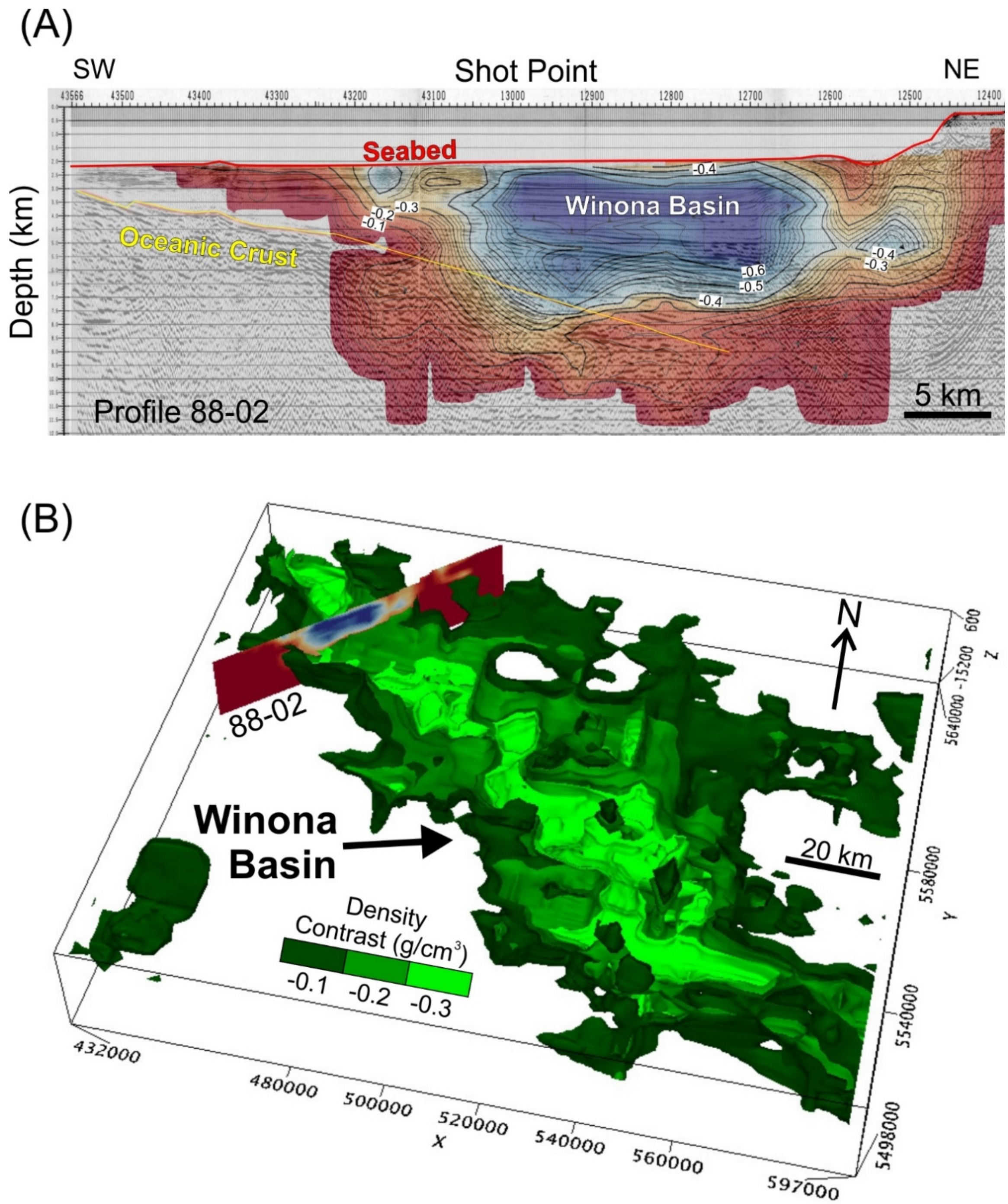

Figure C-3. Winona Basin Density contrast model.
Model is derived from a 3-D inversion of the Bouguer gravity anomaly. (**A**) Comparison of a section through the density contrast model with the lowest densities in blue, and seismic reflection profile QC88-02B (original data source: Geological Survey of Canada – Pacific, 1988). (**B**) 3-D distribution of low density contrast, interpreted to be associated with the Winona Basin's sedimentary fill. Nested density contrast isosurfaces are shown in green. Density contrast model along seismic reflection profile 88-02 is shown crossing the northwestern part of the basin.

Age Constraints for Basin Fill

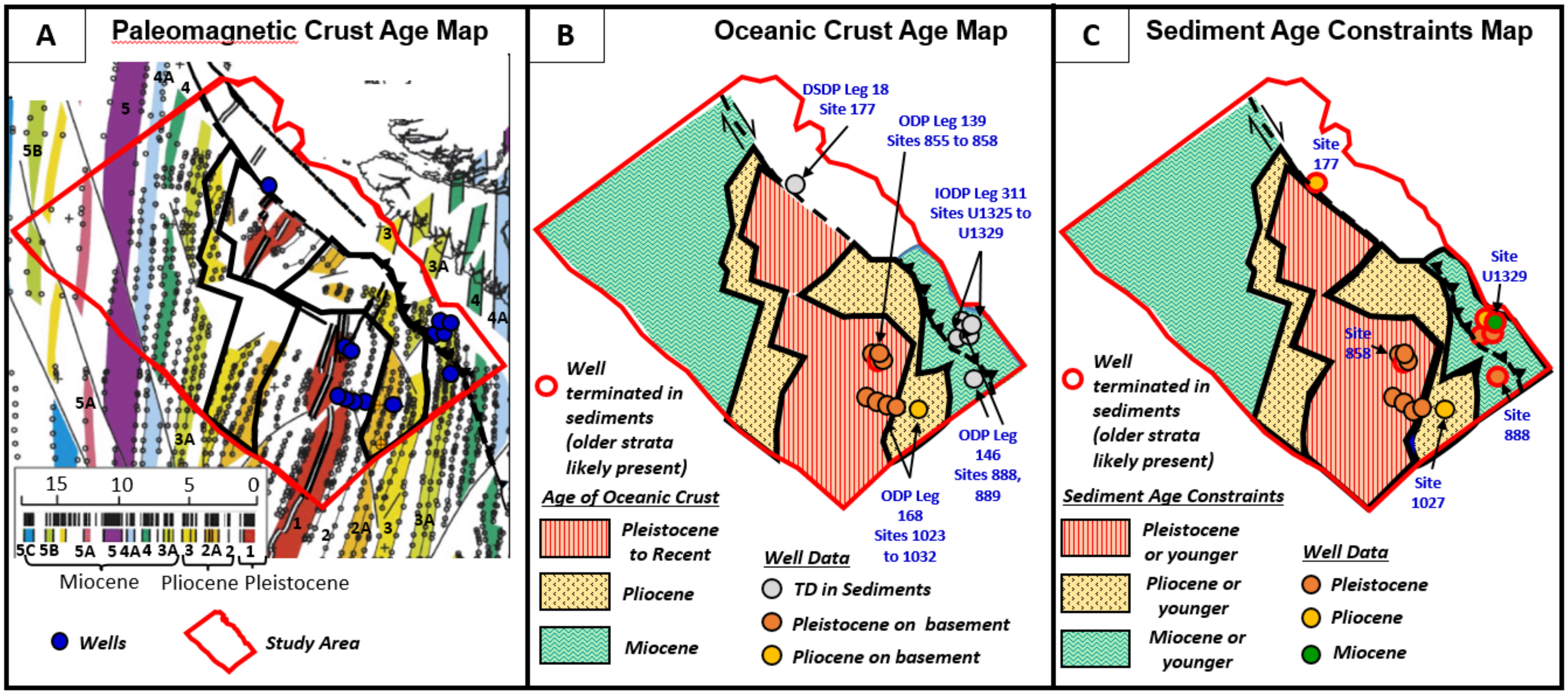

Figure C-4. Paleo-magnetic data (A), oceanic crust age (B), and sediment age constraints (C) maps.

(**A**). Paleo-magnetic Isochron map (*modified from* Wilson, 2002, Fig. 2) indicates oceanic crust within study area (red polygon) is young, ranging from 0 to 1 million years (Ma) (red "1" stripes) at spreading ridges to 16 Ma (Green "5B" stripes) in the northwest; (**B**) Simplified Ocean crust age map (based on Paleo-magnetic isochron in A) and age of sediments resting on basement; (**C**) Age of deepest sediments tested superimposed on crust age constraints map.

Sedimentary sections in the adjacent coastal, shelf and slope regions east of the study area include strata that are much older than basin fill in the study area, with ages ranging from 0 to 45 Ma in the Tofino basin, and from 0 to 200 Ma in Queen Charlotte Basin (Hannigan et al., 2001; 2005; Johns et al., 2012; 2015, Narayan et al., 2005; Figure 5). Many of the documented hydrocarbon plays and petroleum system elements (source rocks, reservoirs, traps and seals) identified in these basins are not present in the study area, because the age equivalent basin fill is not present. Age equivalent Miocene to Recent deposits are present and a limited review of these data was conducted.

C.5 Factors controlling sediment supply

C.5.1 Climate

Climate change can exert significant controls on the nature and rate of sediment supply to oceanic basins along continental margins. Investigations of climate change over the past 5 million years reveal oscillations between glacial and interglacial conditions that involved 3 phases:

Middle/Late Pleistocene to Recent (0.8 to 0 Ma): this was a time interval dominated by major glaciation-interglaciation cycles, occurring every 100, 000 years (Lambeck et al., 2002; Lisiecki and Raymo, 2005), where major ice sheet growth during glaciation events resulted in lower sea levels and colder climate conditions. There is potential in the Pacific offshore for eight or more major glaciations to be recorded in the deep water basin fill. Major ice sheet growth led to significantly lower sea levels (by as much as 130 m below current levels), and at times these ice sheets extended to the continental shelf edge (Barrie et al., 2014; Barrie and Conway, 2002; James et al., 2000) and high volumes of glacial melt waters had potential to transport and deliver sediments directly into deep water regions (Shaw et al., 2017). Deepwater deposits are likely to be dominated by thicker rapidly deposited accumulations of glacially derived sediment gravity flow (SGF) deposits, including debris flow and turbidite deposits, as well as SGF deposits generated by earthquakes) and pelagic deposits. Well data in and adjacent to the study area indicate cool ocean surface temperatures, sand and gravel rich deposits with possible drop stones (e.g. DSDP Leg 18, Site 177 (Ingle, 1973); and ODP Leg 146, Site 888 (Knudson and Hendy, 2009); as well as in Tofino Basin wells (Johns et al., 2015; 2012).

Middle/Late Pliocene to Middle/Late Pleistocene (2.7 to 0.8Ma): this time interval was dominated by moderate amplitude climate oscillations punctuated by glacial conditions every 40 000 years (Lambeck et al., 2002). Lower sea levels during glaciation episodes would result in less space for sediments to accumulate on the shelf and increased potential for transport of glaciogenic sediments into deep water, and conversely, higher sea levels during interglacial periods would create more accommodation space on the shelf, so less sediment might be transported beyond the shelf edge into deep water. Deep water deposits are likely to be a mix of finer-grained, turbidite and pelagic deposits and coarser grained glacially derived sediments. Well data in and adjacent to the study area confirm shallowing sea level conditions and a shift to cooler ocean surface temperatures in the middle to late Pliocene to Pleistocene (e.g. DSDP Leg 18, Site 177 (Ingle, 1973) and Tofino Basin wells (Johns et al., 2015; 2012)).

Miocene to Middle/Late Pliocene (5 to 2.7Ma): a time interval dominated by small amplitude glacial-interglacial oscillations where globally warm conditions resulted in higher sea levels with no major ice sheets in the Northern Hemisphere (Lambeck et al., 2002). Accommodation space on the shelf was likely high and the transfer of coarse clastics to deep water was likely reduced.

Deep water deposits are finer-grained and dominated by a combination of sediment gravity flow turbidite processes and pelagic settling of fine grained particles in the water column. Well data in and adjacent to the study area confirm higher sea level conditions and warm ocean surface temperatures in the Miocene through the Pliocene (e.g. DSDP Leg 18, Site 177 (Ingle, 1973); and Tofino Basin wells (Johns et al., 2015; 2012).

C.5.2 Water Depth

Present day water depths range from 200 m or less along the easternmost edge of the study area to more than 3,500 m in the northwest corner. The seabed over the majority of the study area occurs in abyssal water depths of greater than 2,000 m, with the exceptions of seamounts that rise to various heights above the abyssal plain, and the upper/lower continental slope (200 to 2,000 m) along the eastern edge of the study area.

Paleo-water depth analyses were outside the scope of this study. However, global sea level fluctuations related to major oscillations between glacial and interglacial climate conditions are observed to be on the order of 130 m (Lambeck et al, 2002). A relative lowering of sea level of 130-140 m observed in Queen Charlotte Sound and central Hecate Strait (Barrie et al., 2014) during the Wisconsinan glaciation probably coincided with a significant basinward movement of the shoreline and subaerial exposure of areas of the continental shelf (Barrie et al., 2014; Barrie and Conway, 2002; James et al., 2000). A vertical lowering of 130 m would have little impact on water depth zones at lower bathyal to abyssal water depths, where deep water conditions would have persisted throughout the Quaternary. Shelf areas with less than 130 m water depth would be exposed and susceptible to the effects of erosion and non-deposition.

C.5.3 Shelf Edge Processes

High quality bathymetry data reveal a variety of slope features including submarine canyon heads, erosional gullies and submarine channels (e.g. Davis and Hyndman, 1989; Riedel and Rohr, 2012; Ryan et al., 2009). Kendall and Deptuck (2012) report similar features on the Scotian Slope, Offshore Nova Scotia, where they provide sediment transport paths for the transfer of fine to coarse clastics from the shelf to deep water (Figure C-5A). Steeply dipping upper slope regions that are incised by canyons, gullies and/or submarine channels represent potential sediment bypass zones that are dominated by erosion and non-deposition as sediments are transported and deposited further basinward. The base of slope and areas of variable seabed morphology (e.g. the anticline ridge topography of the accretionary complex) represent potential sediment accumulation sites, where changes in seabed slope can impede turbidity current flow and reduce flow velocities, which lowers the flows ability to carry sediment in suspension and may result in the deposition of coarser grained sediments (Pickering and Hiscott, 2016). Lower sea levels associated with glacial maxima, combined with maximum ice coverage close to the shelf edge created conditions where sediment laden glacial meltwaters would potentially bypass the shelf and deposit their sediments directly into deeper waters.

C.6 Depositional environment models

The assessment of the hydrocarbon potential in the study area requires geological predictions for the presence and quality of lithology, source rock, reservoir and seal in and away from well control. Industry wells on the continental shelf confirm the presence of Pliocene and Pleistocene fine and coarse grained clastics (muds, silts, sands and gravels) in the Queen Charlotte and Tofino basins (Hannigan et al., 2001; Johns et al., 2015; 2012). Regional and study area data that were used to gain further insights on the age, lithology and characteristics of the sedimentary basin fill within the study area include: i) research well data, including lithology, biostratigraphy, and geochemistry data from the continental slope and abyssal plain (Expedition 311 Scientists, 2006 a, b, c, d, e, and f;

Akiba et al, 2009; Johns et al., 2015, 2012, Goldfinger et al., 2012; Knudson and Hendy, 2009); Kiyokawa and Yokoyama, 2009; Hashimoto and Minamizawa, 2009; Narayan, et al., 2005; Underwood et al., 2005; Nelson et al., 2000; Su, 2000; Su et al., 2000; Underwood and Hoke, 2000; Mao et al., 1994; Shipboard scientific party, 1997 a, b & c; Westbrook et al., 1994; Shipboard scientific party, 1992 a, b, c, d, e, and f; Davis et al., 1991; Hayes, 1973; Ingle, 1973; Kulm et al., 1973) ii) seabed structure and geomorphology interpretations from slope bathymetry data (Davis and Hyndman, 1989; Riedel and Rhor, 2012; Hampton et al., 1989; Atwater et al., 2014), and iii) geophysical data interpretations, including regional tectonic elements, study area sediment thickness map as well as local seismic facies and hydrocarbon indicators (Rohr, 2015; Riedel and Rohr, 2012; Walton et al., 2014; Hayward and Calvert, 2007; Zuhlsdorff and Spiess, 2001; Zuhlsdorff et al., 1999; Cassidy et al., 1998; Yuan et al., 1994; Gardner et al., 1993; Davis and Hyndman, 1989; Davis and Villanger, 1989; Hampton and Kenyon, 1989; Botros and Johnson, 1988; Caron and Nelson, 1987; Davis and Clowes, 1986; Davis and Riddihough, 1982; Clowes et al., 1997; Davis and Lister, 1977; Barr and Chase, 1974; Carson, 1973, McManus, et al., 1973; Carson, 1971; Griggs and Kulm, 1970). Volcanic complexes were largely excluded from these maps. It is possible to subdivide the Pacific offshore basin fill at some well locations (e.g. ODP Leg 168, Site 1027) and attempts were made on test lines to extend interpretations away from well control throughout the seismic grid. Further seismic stratigraphic analysis and mapping of the basin fill was not possible in the time available, but may be the focus of future work. In the absence of more detailed geological maps, we considered the data described above and geological principles to predict gross depositional environment models for the Upper Pleistocene, Lower Pleistocene and Pliocene to Miocene time periods (Figure C-5). Miocene strata were encountered in the Accretionary Complex region (Figures 2 and C-4) in IODP Leg 311, Site U1329, Pliocene strata were encountered in DSDP Leg 18, Site 177, ODP Leg 146, Site 889 and ODP Leg 168, Site 1027.

C.6.1 Submarine Fans

Three submarine fans are interpreted to be present within the study area (Figures C-5B, C, and D). This interpretation is supported by: i) the presence of locally thickened sedimentary accumulations mapped along the base of slope, and in areas of the abyssal plain (Figure C-2A), ii) the presence of sediment delivery systems including shelf indenting canyons, slope and seabed channels evident in bathymetry and seismic data (Figure C-5A; Underwood et al., 2005; Zuhlsdorff and Speiss, 2001; Davis and Hyndman, 1989; Hampton et al., 1989), iii) the presence of localized erosional channels and high amplitude reflection packet (HARP) seismic facies commonly associated with sand-rich submarine fan channel complexes, and iv) the presence of interbedded deep marine silt- and sand-rich sediment gravity flow deposits including turbidites and debris flow deposits encountered in research wells (ODP Leg 168, Sites 1023 to 1032; ODP Leg 139 Site 855-858; ODP Leg 146 Site 888, DSDP Leg 18, Site 177; Underwood, 2005, Kiyokawa and Yokoyama, 2009). The fans in the study area include: i) the Nitinat Fan, located immediately west of the Cascadia deformation front on the Juan de Fuca Plate that appears to have been controlled, in part, by subduction margin related tectonic processes, ii) a fan that covers parts of the Explorer, Juan de Fuca and Pacific plates that appears to have been controlled, in part, by tectonic movements in a triple junction setting, and a fan, referred to as the “Queen Charlotte” Fan in some previous work (e.g. Dehlinger et al., 1971; Shaw, 2017) on the Pacific Plate that appears to have been controlled, in part, by “strike slip tectonic movements”.

Nitinat Fan: Juan de Fuca Plate, along the southern boundary of the study area (Figures C-5A and B):

The Nitinat Fan straddles the Canada-US boundary in the southeastern region the study area, and covers an estimated area of more than 50 000 km^2 (this study). This fan developed approximately 760 000 years before present (Andrews et al., 2012) and is sourced mainly by the Fraser River (Kiyokawa and Yokoyama, 2009). Channels, including the Vancouver Valley and Juan de Fuca Channel, are evident at the seabed in the bathymetry data (Hampton et al., 1989). Pleistocene channel.

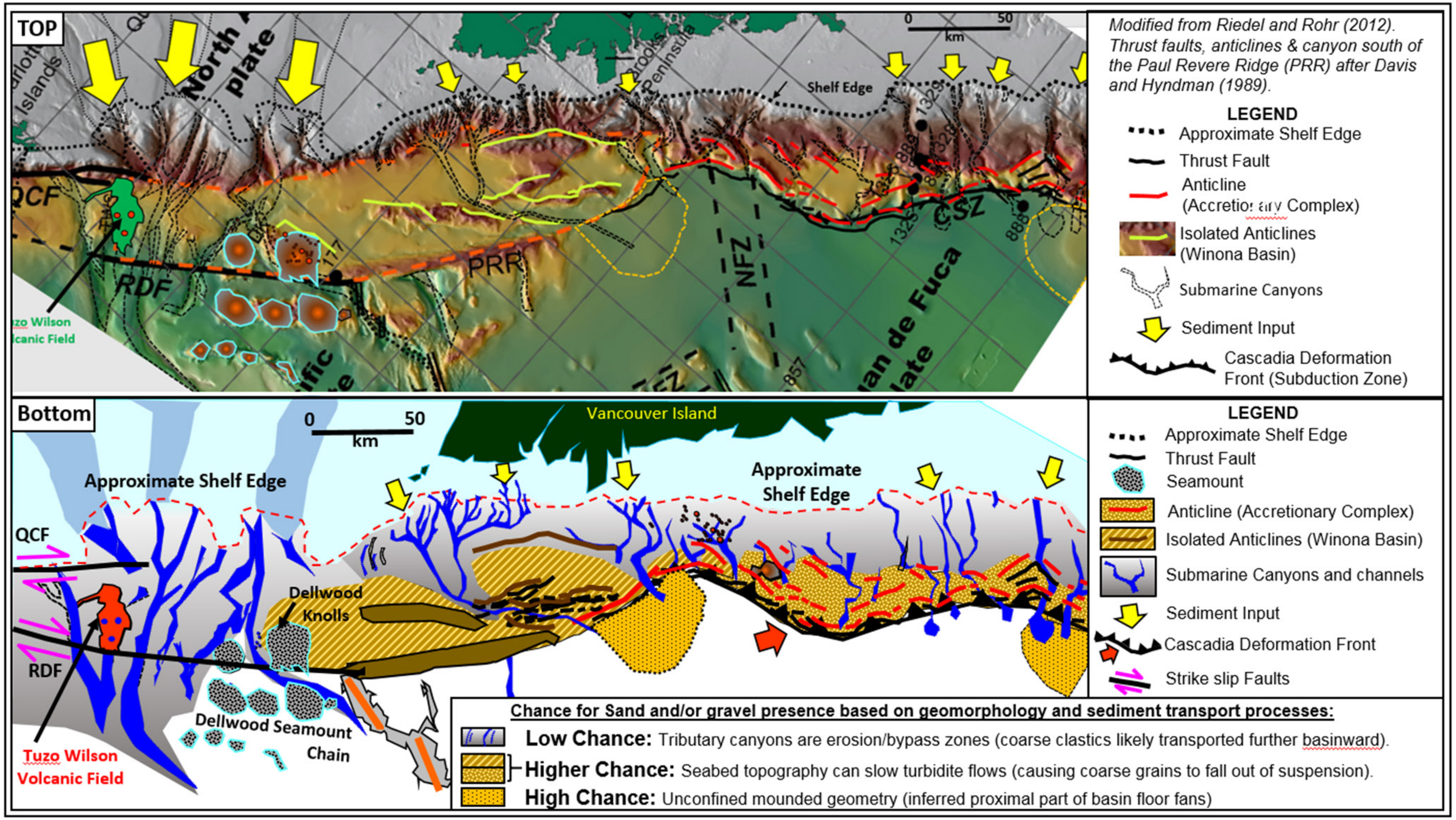

Figure C-5A. Seabed bathymetry, structure and sediment transport features of the offshore Pacific continental slope. **Top:** Composite seabed bathymetry, structure and submarine channel interpretations for the continental slope west of Vancouver Island (*modified from* Riedel and Rohr, 2012, Fig. 1, with thrust faults, anticline traces and submarine channel interpretations south of the Dellwood Knolls *modified from* Davis and Hyndman, 1989, Fig. 5b. **Bottom:** Implications for downslope sediment transport and predictions for areas with higher and lower likelihood for coarse clastics (sands/gravels) to be present in deep water (from this study, building on structural and/or submarine channel interpretations from Davis and Hyndman, 1989 and Riedel and Rohr, 2012).

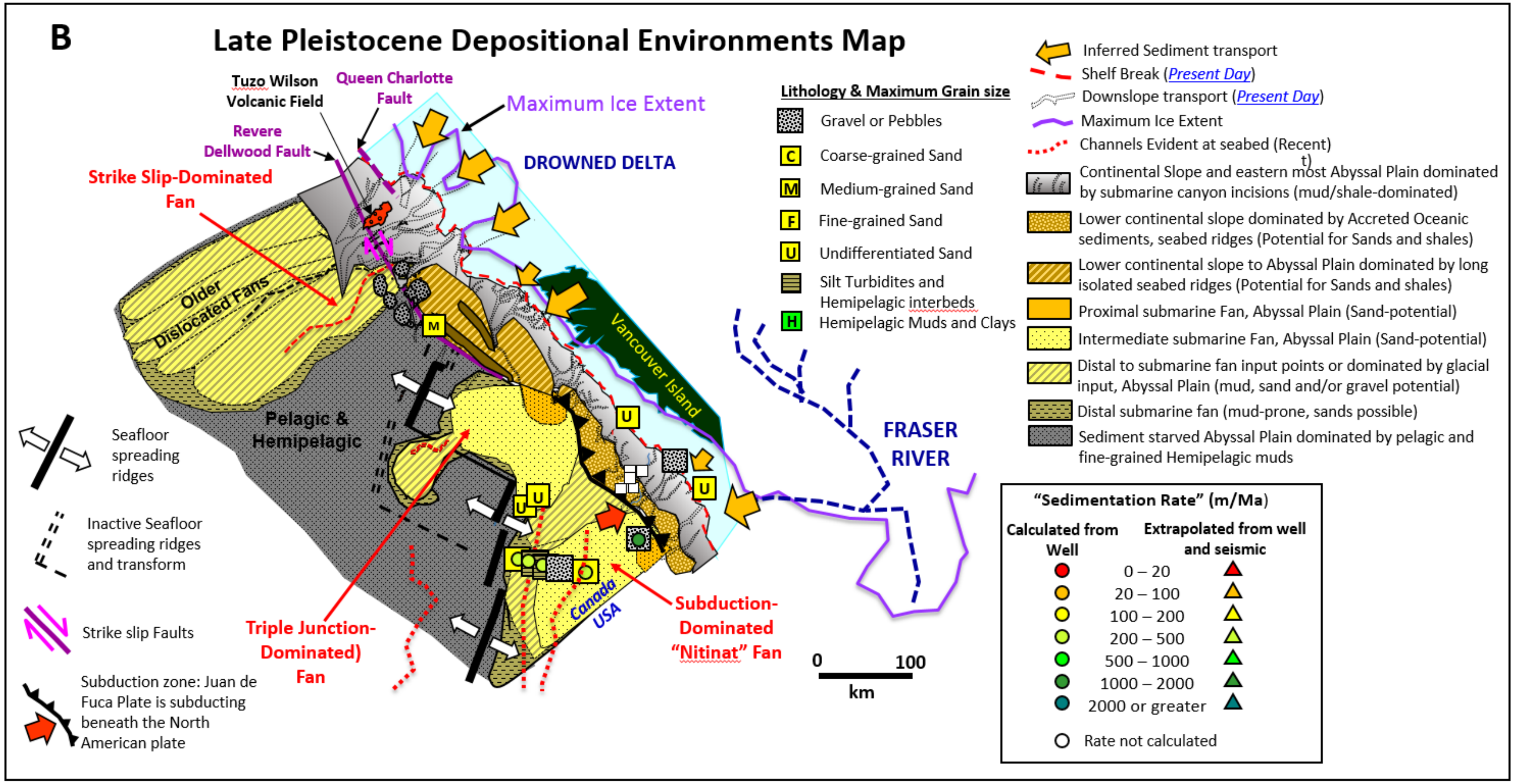

Figure C-5B. Offshore Pacific Late Pleistocene Depositional Environments Model. Model integrates available geophysical and geological data with sedimentary processes to predict geological conditions away from well control. The tectonic reconstruction of Explorer ridge with Respect to North America is approximate. Refer to Figure C-5A and Appendix C.6 for a summary of data that were consulted and provided constraints to these models.

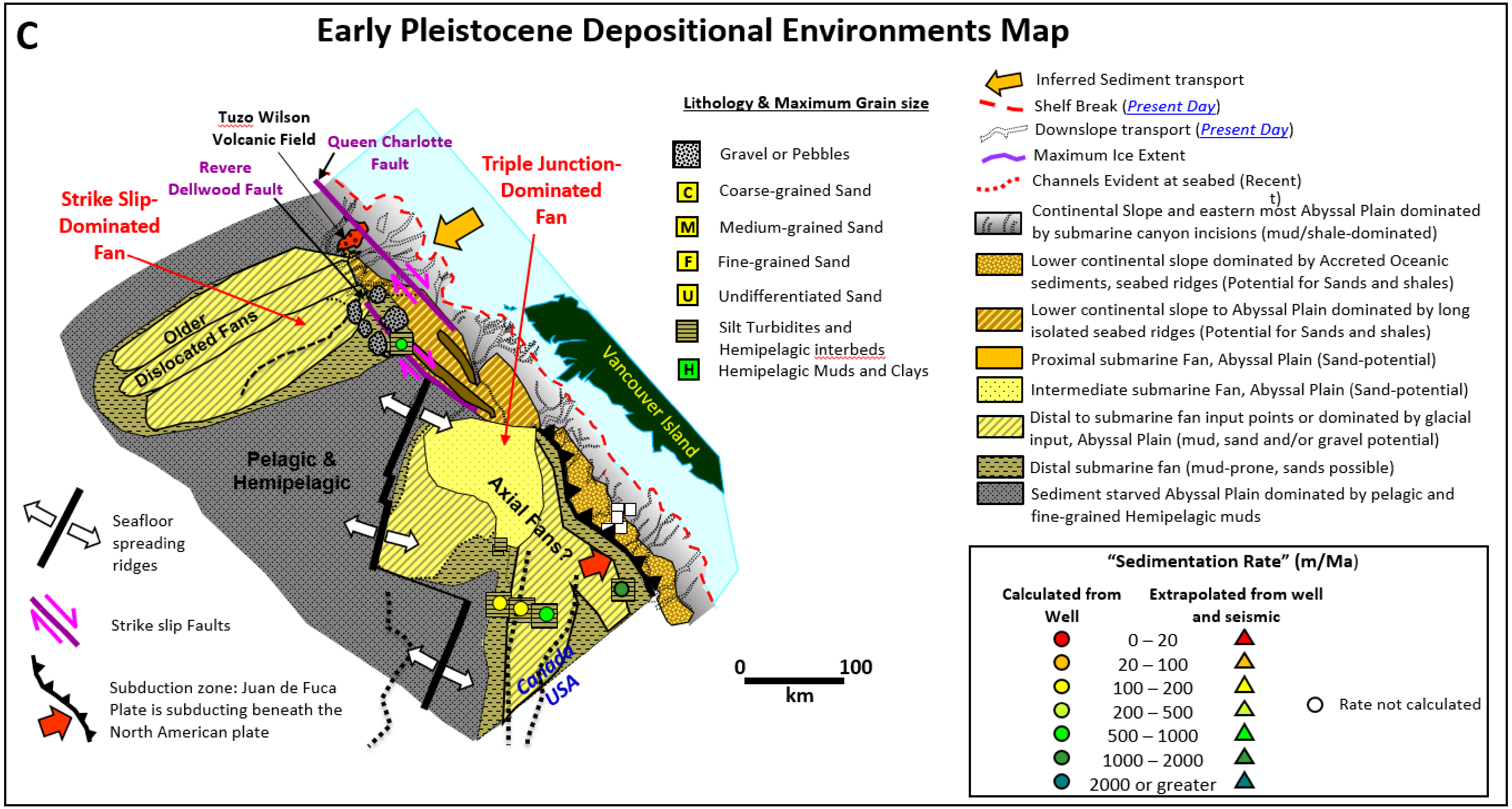

Figure C-5C: Offshore Pacific Early Pleistocene Depositional Environments Model. Pacific offshore Early Pleistocene depositional environment model. Model integrates available geophysical and geological data with sedimentary processes to predict geological conditions away from well control. The tectonic reconstruction of Explorer ridge with respect to North America is approximate. Refer to Appendix C.6 for a summary of data that were consulted and provided constraints to these models.

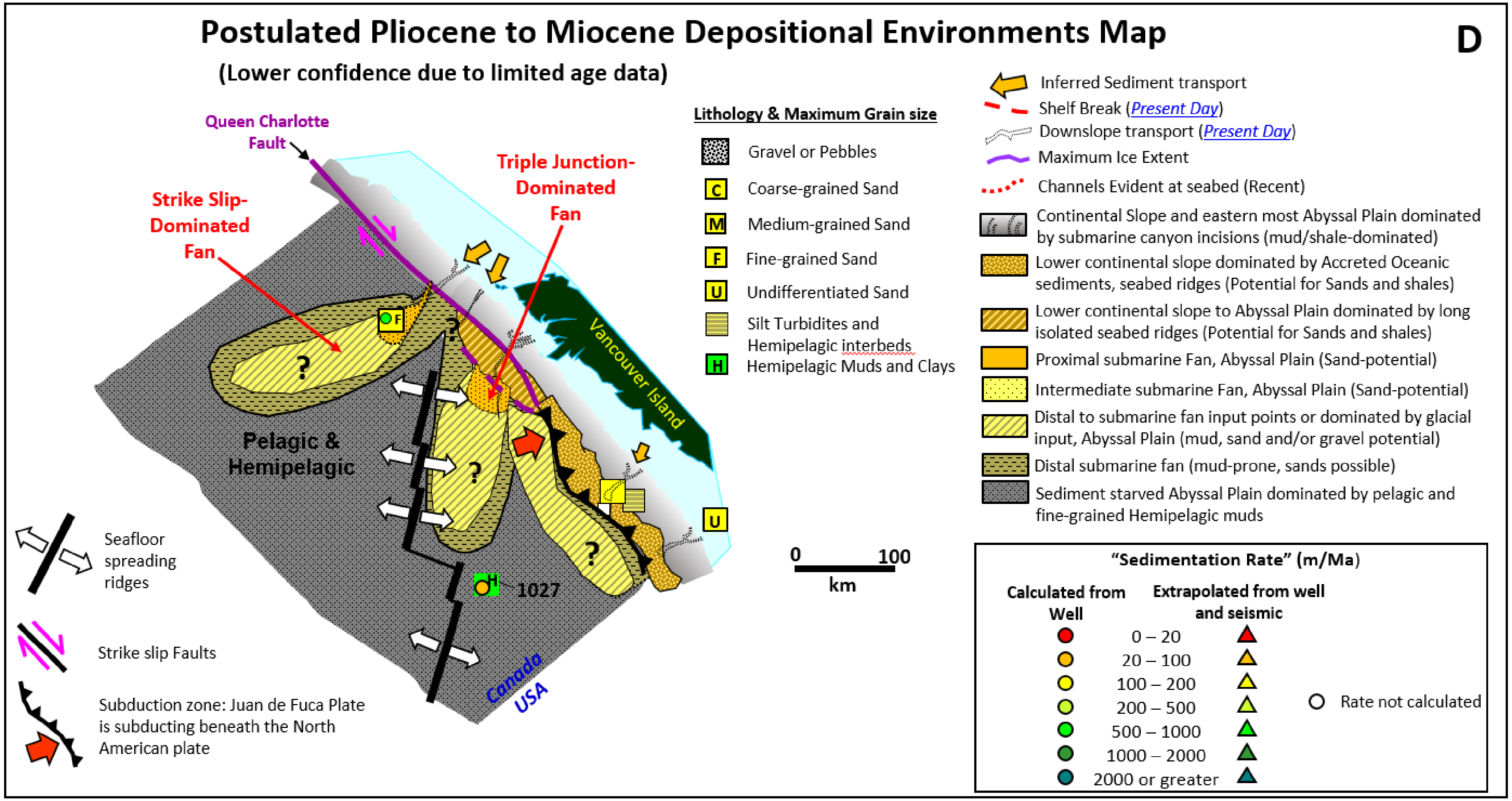

Figure C-5D: Offshore Pacific Pliocene to Miocene Depositional Environments Model. Model integrates available geophysical and geological data with sedimentary processes to predict geological conditions away from well control. The tectonic reconstruction of Explorer ridge with respect to North America is approximate. Refer to Appendix C.6 for a summary of data that were consulted and provided constraints to these models.

sands and sandy turbidites are proven in Leg 168 wells (Sites 1023, 1024, 1025, 1026 and 1027) and Leg 146 (Site 888). At ODP Leg 168 and IODP EXP 1301 sites, maximum grain size ranges from medium-grained sand to gravel and maximum thickness of sand beds is 7m (Underwood et al., 2005; Kiyokawa and Yokoyama, 2009). Individual turbidite beds commonly have erosional bases, topped by normally graded sands that fine upwards to silts and thin hemipelagic clays. Many sites in Leg 168 show an overall coarsening upward trend (sand content increases upward) as is seen in other subduction zones where oceanic plate sediments are carried closer to proximal sediment input sites by the down going plate (e.g. Nankai Trough, Japan, Pickering and Hiscott, 2016). Seismic profiles reveal localized erosional channels and high amplitude reflection packet (HARP) seismic facies that are consistent with proximal sand-prone channels (Figure C-1C). ODP Leg 146 Site 888 encounters one channel sand, but is otherwise dominated by fine-grained fining upwards deposits. The dominantly fine-grained character of sediments at this site may reflect i) a position at the edge of the Nitinat fan, ii) the intersection of channel levee systems in the well, or iii) the deflection of turbidity currents away from this site by seabed ridges further up-dip. It is possible that the subduction trench may have formed a bathymetric low at the seabed at times in the past, as is the case in the southern Cascadia margin. For this reason thicker trench fill sediments may contain confined channel sands and channel levee deposits associated with periods of axial sediment transport.

Submarine Fan near Triple Junction Region, Explorer, Pacific and Juan de Fuca plates (Figures C-5A, B, C, and D):

This fan developed in a complex and tectonically active area on the Explorer, Pacific and Juan de Fuca plates (McManus et al., 1972) and is here interpreted to cover an area of at least 23000 km^2. Multibeam data show that the Revere Channel extends beyond the Sovanco Fracture Zone to deliver sediments to the Pacific Plate (Dziak, 2005). Total sediment thickness is estimated to range from approximately 0 to 600 m on the Pacific Plate, and 200 to more than 2500 m on the Explorer microplate. This triple junction-dominated fan appears to rest on Pliocene to Pleistocene age oceanic crust, so the fan is inferred to be a Pliocene or younger feature (Figures C-4 and C-5D). Older portions of the fan that accumulated northeast of the present day Sovanco Transform fault likely accumulated after reorganzitation of the plate boundary that resulted in the northward movement of the Sovanco Fracture zone that isolated the Explorer seamount spreading ridge segment (Botros and Johnson, 1988. Botros and Johnson (1988) constrain the timing of this reorganization, which involved clockwise rotation of the Sovanco Fracture zone, to approximately 2.5 Ma, and this was followed at approximately 1 Ma by counter clockwise rotation of the Sovanco Fracture zone that likely resulted in some degree of compression and intraplate deformation. It is likely that seabed topography developed in this dynamic setting in response to this intraplate deformation, which may have presented barriers to westward (slope perpendicular) sediment transport, during the middle Pleistocene. Lower fan deposits observed west of the present day Sovanco Transform likely predate this deformation, while upper fan deposits, that formed east of the transform likely did so as a result of confined basin conditions and axial transport of sediments southward along Explorer plate and onto the Juan de Fuca plate.
Modern bathymetry data show some seabed channeling that crosses the Sovanco transform zone, indicating slope perpendicular sediment transport has occurred more recently.

"Queen Charlotte" Fan (Dehlinger et al., 1971) across strike slip faults, Pacific Plate (Figures C-5B, C, and D):

This elongate fan is located in the northern area of the study area on the Pacific Plate and extends west of the Revere-Dellwood Fault (RDF), with an inferred sediment source in the vicinity of the Moresby Trough. Dehlinger and others (1971) referred to this feature as the "Queen Charlotte" Fan in 1971. Shaw and others (2017) refer to the "Queen Charlotte Trough Mouth Fan" in association with Pleistocene glaciation. The fan covers an area of at least 52 000 km^2 and total sediment thickness is estimated to range from 0 to 700 m. Channels, including the South Moresby Gully, are evident at the present day sea bed. Some of these channels have been cross cut and dislocated 40 km or more by the Queen Charlotte Fault (QCF), which resulted in abandonment (Shaw et al., 2017). Dislocation for fan deposits from their up-dip feeder channels has occurred more recently across the Revere-Dellwood fault (RDF).

This “strike-slip-dominated” fan is thin compared to the “triple junction-dominated” and Nitinat fans located further south (Figure C-2). This is because fan growth is occurring laterally (rather than by aggradational or compensational processes seen in fans to the south) as a result of strike-slip displacement where fan deposits on the Pacific Plate have moved progressively northward relative to the sediment inputs located on the opposite side of the RDF and/or QCF (Figures C-5B, C, and D). This movement has likely resulted in successive channel abandonments and the initiation of new channels and new fan deposits outboard of the existing sediment delivery pathways. Similar processes have been reported in the Baranof Fan, located just north of northern Canada/United States jurisdictional boundary in the Gulf of Alaska (Walton et al., 2014). A Pliocene turbidite sand was interpreted in the DSDP Leg 18, Site 177 well, which is located within the Revere-Dellwood Fault shear zone. On the basis of seismic character the sand layer was interpreted to be as much as 56m thick (Hayes, 1973). If age equivalent sands are present west and presumably some distance north of Site 177, it is possible that this fan may contain Pleistocene to Pliocene (or older) age strata. Oceanic crust and sediments located west of DSDP 177 (and west of the Revere Dellwood Fault zone) are Pleistocene and younger in age (Figure C-4). Older Pliocene and Miocene age crust are present further north and west of Site 177. Since basement was not tested at Site 177 it is possible that the age equivalent sands encountered in this well may be present in a more northern part of the fan. On the basis of paleomagnetic data, this fan could be as old as Miocene in its northern regions. No age data or stratigraphic analyses for this fan were identified at the time of this study so until a scientific drilling program is undertaken, the timing of initiation and maximum age of these fan deposits is not known.

C.7 Organic matter

C.7.1 Factors controlling organic carbon presence and preservation

Abundant fine-grained sediments including silt and mud-rich turbidite layers (e.g. Bouma Divisions D and E), hemipelagic muds, and pelagic muds and oozes are present in wells and are anticipated to exist in varying concentrations throughout the study area (e.g: ODP Leg 168, ODP Leg 139). Potential may exist for organic carbon enrichment of fine grained sediments below upwelling cells in ocean water above slope regions in the study area (e.g. Winona Basin, Accretionary Complex and within Trench fill) during times of high biological productivity and well-established oxygen minimum zones (Arthur et al., 1984). Examples from analogous deep water convergent margin settings include offshore California and Peru, where slope sediments near subduction trenches can have very high organic content (e.g. the Miocene Monterey Formation, California’s primary petroleum source rock with up to 17 wt% TOC) (Capone and Hutchens, 2013; Suess et al., 2014; Luckge et al., 1996). Late Quaternary millennial-scale upwelling events are documented by Vancouver Island Margin sediments with up to 3 wt% TOC (Chang et al. (2008).

Terrestrial Type III kerogen may be present in turbidite deposits and marine Type II kerogen may be common in hemipelagic to pelagic deposits. The concentration of hemipelagic and pelagic Type II organic rich muds may be lower in areas of active turbidite fan deposition, and higher in areas that are distal to active sediment supply. Type III organic carbon concentrations might be lower in glacial-derived turbidite deposits if the fraction of coarse clastic material is high, and higher where fed by large deltas during periods of warm and humid climate conditions (Einsele, 2000). Potential also exists for the erosion, transport and re-deposition of organic-rich material from up-dip areas such as occasional to abundant coals, isolated wood fragments and plant debris that are present within Miocene and Lower Pliocene age marine deposits in the Tofino and Queen Charlotte basins (Johns et al., 2015).

Organic carbon preservation potential is expected to be greater in areas where sedimentation rate is sufficiently high and/or in areas where water column stratification has created anoxic or euxinic conditions. Organic matter deposited in oxygenated waters with lower sedimentation rates may experience early degradation, resulting in low organic carbon content due to lack of preservation (Meyers and Shaw, 1996).

Ocean currents also can affect the distribution of organic matter. Surface waters warm during interglacial cycles and can result in significant northward migration of the transitional water biofacies, as documented during the Early-Middle Pliocene (DSDP 18, Site 177 and 173 (Ingle, 1973)). Cooler waters and a southward migration of the biofacies occurred during glacial cycles in the Pleistocene.

C.7.2 Organic matter and sedimentation rates in the Study Area

Available geochemical data (pyrolysis data, biomarker and head space gas analyses) were reviewed to evaluate the potential for organic rich source rocks to be present within the study area (e.g. Total Organic Carbon (TOC) data obtained from ODP Leg 168, IODP Leg 311, Leg 139, Leg 146 and DSDP Leg 18 show consistently low to moderate total organic carbon values (TOC typically ranges from 0.3 to less than 1.5 wt%) in the thin and often abbreviated marginal successions that were tested (Table C-1; Simoneit, 1994; Whiticar et al., 1995). Biomarkers (Simoneit, 1994) and carbon : nitrogen ratios of 10:1 (Whiticar et al., 1995) suggest a mixed marine and terrestrial kerogen type.

Pyrolysis data from tested areas may not be representative of organic carbon potential in all regions of the study area. Well sites drilled in the study area were selected to address a variety of research questions; none were drilled with the objective of encountering economic accumulations of oil and gas. In most offshore areas, dry holes (wells that did not encounter hydrocarbons) represent petroleum systems tests that were unsuccessful. Post drill analyses are typically conducted to evaluate which elements of the petroleum system worked, and which didn’t. Study area wells show consistently low organic richness so the geologic conditions at sample sites (total sediment thickness, completeness of the section and/or evidence of erosion or non-deposition, local temperature conditions, age and depositional environment of section) were considered to understand the uncertainty for source rock presence within the study area. This exercise yielded the following conclusions: thicker sedimentary deposits within the study area, including more deeply buried Lower Pleistocene to Pliocene sections in the Winona Basin and Miocene/Pliocene to early Pleistocene trench fill on the Explorer and Juan de Fuca plates have not been tested, so organic carbon potential in thicker and older basin fill is unknown. Analyses of samples that have been subjected to high heat or that have already generated hydrocarbons will yield depleted values that should not be considered to represent original organic content. Samples that targeted thin deposits near spreading ridges and/or basement highs have lower potential for organic carbon preservation due to high temperatures and low sedimentation rates that likely led to oxidation of organic matter before it could be buried and preserved (Meyers and Shaw, 1996). Erosion of fine-grained deposits by turbidite channels and sediment bypass caused by conditions on the shelf and upper slope or as a result of trench confined axial fans have also contributed to an incomplete stratigraphic record at some test sites.

Potential for conventional thermogenic hydrocarbons and shallow biogenic gas were considered in the study area. Conventional ‘thermogenic’ hydrocarbon potential exists in areas where sufficient organic richness, heat, depth of burial and time are available to generate and expel hydrocarbons. 1D basin models were generated to understand the potential for conventional hydrocarbons in the study area *if* source rocks with sufficient organic richness are present (Appendix D.1). Biogenic gas potential is higher in areas with high sedimentation rates (200 to 1500 m/Ma), fair to good organic richness (e.g. TOCs greater than 0.5 wt%, HI's greater than 100 mg/g TOC) and low temperatures (0 to 40°C and potentially up to 75°C) (Schneider et al., 2016).

Sedimentation rates were compiled from published well analyses, and the sediment thickness map was used to create a crude "minimum average sedimentation rate" map. Organic matter is not likely to be preserved where sedimentation rates are very low (e.g. less than 20 m/Ma). Sedimentation rates observed on the Juan de Fuca Plate range from less than 100 to 500 m/Ma in distal turbidites (Su et al., 2000), and from less than 100 to more than 1000 m/Ma in more proximal fan and trench fill deposits at ODP 146 Site 888 (Whiticar et al., 1995). Sedimentations rates as high as 500 m/Ma are also reported at DSDP Leg 18, Site 177 (Site 177 Shipboard Report, 1971) and sedimentation rates determined by extrapolation from Site 177 along seismic lines in the Winona Basin may have exceeded 1500 m/Ma at times.

Table C-1. Summary of organic matter data for Pacific Offshore

Headspace gas values represent average C1 headspace gas measured in ppm.

Region	ODP Leg and Location	Sediment Characteristics	TOC (wt%)	S1 (mg HC/g)	S2 (mg HC/g)	HI	Data Sources	Headspace gas C1 Average (ppm)
Juan de Fuca Study Area (Middle Valley)	ODP Leg 139	Stacked turbidite sequences with hemipelagic interbeds	0-1.1	No rockeval			Simoneit 1994	52051.86756
Juan de Fuca Study Area (Thinner, marginal sediments)	ODP Leg 168	Stacked turbidite sequences with hemipelagic interbeds	0.29-1.76	none	0.08-3.11	80-220	Rock-eval from Leg 168.	14495.2
Juan de Fuca Study Area (Trench Fill)	ODP Leg 146 Site 888	Stacked turbidite sequences with hemipelagic interbeds		No rockeval				212061
Juan de Fuca - US (Trench Fill - US)	ODP Leg 146 Sites 891-892) (Trench fill)	Stacked turbidite sequences with hemipelagic interbeds		No rockeval				211579
Accretionary Complex	Accretionary Complex	Stacked turbidite sequences with hemipelagic interbeds (deposited in place & older accreted strata)	0.07-1.73	0.01-0.29	0.05-2.61	27-151	Rock-eval from Leg 311	640365.0482

C.7.3 Hydrocarbon indicators

Hydrocarbon indicators have previously been reported in onshore, shelf and slope regions adjacent to the study area; indicators were also identified within the study area as part of this assessment (Figure 4):

1. **Onshore:** Numerous oil, tar, and gas seeps have been identified on Haida Gwaii. Geochemical studies indicate these seeps have migrated from Jurassic and Tertiary sources. Ten exploration wells have been drilled on Haida Gwaii between 1950 and 1984. The Tian Bay well encountered gas flows and oil staining has been noted in Cretaceous, and Tertiary strata in some of the onshore wells (Hannigan et al., 2001).

2. **Shelf and slope:** Between 1967 and 1969 Shell Canada drilled 16 wells on the shelf. The Sockeye B-10 well penetrated 40 m of Miocene sandstone showing live-oil-staining that is suspected to have migrated from the Jurassic Kunga Group rocks (Hannigan et al, 2001). Of 6 wells drilled in the Tofino Basin on the upper slope, shallow gas shows were encountered in Pluto I-87 and Prometheus H-68 (Schuemann et al., (2014) citing Bustin, 1995 and Shouldice 1973). Gas plumes / cold seeps observed during GSC Pacific marine expeditions (2011001PGC, 2011002PGC; Barrie, 2011; Scherwath, et al., 2017a) are mainly confined to the shelf, adjacent to the study area.

3. **Deepwater:** There has been no industry drilling in the deep water. Drilling programs (DSDP/ODP/IODP) in the deep-water region were drilled for scientific reasons on various topics and were not drilled to explore for hydrocarbons (Appendix B.2). Oil shows that include condensed aromatics and olefins were encountered in Middle Valley (ODP Leg 139) wells. These hydrocarbons are interpreted to be the result of local, hydrothermally driven processes due to proximity to high temperature hydrothermal vents (Simoneit, 1994; Rushdi and Simoneit, 2001, Ventura et al., 2012).

Seismic data show that several indicators of a potential working petroleum system are present in the eastern half of the study area (Figure 4A). These indicators include numerous amplitude anomalies, bottom simulating reflections (BSRs), as well as some possible vent features and chimneys (described in Riedel and Rohr, 2012). Elevated amplitudes, or bright spots, mapped in the study area have been differentiated from basalts based on their polarity (bright spots arising from gas are opposite in polarity to the seafloor, while bright spots arising from basalts are the same polarity as the seafloor). These bright spots are present on the Explorer microplate (Rohr, Furlong and Riedel, *in press*) as well as on several lines on the Juan de Fuca Plate (e.g. Figure C-1C). Preliminary amplitude versus offset (AVO) work completed by personnel at GSC-Calgary indicates that bright spots on the Juan de Fuca Plate might show a response expected for gas; this has also been suggested by previous work (i.e. McIver, 1973; Hasselgren and Clowes, 1995). BSRs have been mapped in the Winona Basin (after Riedel and Rohr, 2012) as well as the Accretionary Complex (e.g. Riedel et al., 2010). Within the Accretionary Complex, the presence of gas hydrates has been confirmed by drilling (e.g. Riedel et al., 2010).

APPENDIX D – QUALITATIVE ASSESSMENT DETAIL (PETROLEUM, MINERALS AND OTHER RESOURCES)

D.1 Qualitative Petroleum Potential Assessment:

D.1.1: Petroleum Systems Analysis

1D Basin modelling overview and model locations

1D basin models were generated to evaluate the potential for conventional hydrocarbon generation across the study area. As noted in Appendix C.6, source rock presence and quality within the study area is uncertain. Average measured TOC content is low (less than 1%) for available data from thin and or marginal test sites. Information from analogous deep water basins in subductions zones indicates potential for sediments to contain higher TOC (up to 10% or more) in association with upwelling cells. Consequently it is possible that organic rich sediments may be present in the study area. Additionally, zones with higher preservation of organic matter (higher TOC) are expected where sediments are deposited in anoxic and/or euxinic parts of the basin. The 1D models presented in this section were designed to evaluate petroleum maturation potential (at what burial depth and temperature a postulated source rock would be mature and able to generate and expel hydrocarbons) at selected sites.

Different scenarios were tested to account for variation in sediment thickness, geothermal gradient, time, and localized geologic events such as basalt intrusions. Four representative 1D models include: i) Winona Basin; ii) Accretionary Complex, iii) Juan de Fuca Plate (Middle Valley) and iv) Juan de Fuca Plate (Trench). Model locations targeted thicker sedimentary accumulations in Middle Valley and the Juan de Fuca trench.

Model Inputs and Assumptions

Each 1D model was populated with a simplified stratigraphic column based on assumptions for sediment age, thickness, and lithology. Model inputs are summarized in Table D-1. A range of reasonable thermal conditions for each location (described further in Appendix C.4) were applied to each model to test i) burial history and ii) potential to mature organic matter and generate conventional burial-driven hydrocarbons. A summary of sediment ages, sediment thicknesses, and thermal conditions for the various scenarios tested is provided in Tables D-2A and D-2B. For each model, the sediment column was estimated using current knowledge of the depositional environment (Appendix C.6).

1D Model Results

A total of 27 scenarios have been tested for 1D models at four locations in the study area (Figure 4) to evaluate hydrocarbon generation potential. Results are summarized in Table D-2A and B.
A geologically representative "base case" model was selected for each area (Figure D-1; Table D-2A), and, where possible, model results were considered and extrapolated through the study area to inform the hydrocarbon assessment. The sparsity of control data demanded extensive sensitivity testing that involved multiple iterations of models at each chosen location to reflect the variability in thermal conditions, sedimentary overburden thickness and depositional age. Results indicate that hydrocarbon generation potential on the Juan de Fuca Plate is very limited: the potential to generate oil is only predicted in the thickest parts of the subduction trench and Middle Valley. Potential is greater in the thicker sediments of Winona Basin, where oil and gas generation is predicted. Generation potential in the Accretionary Complex is predicted to occur where thickness exceeds 2.4 km.

Table D-1. Selected base-case inputs for 1D models.

Note: Some of the papers originally only cited heat flow values so they were converted to geothermal gradient using the equation proposed by McKenzie et al. (2005): Q=k*(dT/dz). Q is heat flow; k is thermal conductivity; dT/dZ is geothermal gradient; and W/(m*K) is a standard conductivity unit (Watts per meter Kelvin). The referenced heat flow values (units are mW/m^2) are in parentheses next to their converted geothermal gradient values. A thermal conductivity of the oceanic crust (k=3.183 W/(m*K)) is used in Middle Valley, and the thermal conductivity of clastic sediments (k=2 W/(m*K)) is used for the Accretionary Complex.

Region	Age Crust (Ma) from Paleomagnetic data	Age Sediments (Ma)	Geothermal Gradient C/km			Reference
			base case	high	low	
Winona Basin	No paleomagnetic data or basement tests 5.3 (inferred)	Pliocene (or older?) and younger	75	184	30	Davis and Riddihough, 1992
Accretionary Complex	3 to 10	Miocene and younger	55	n/a	n/a	Grevemeyer and Villanger, 2001
			55 (Q=110)	75 (Q=150)	25 (Q=50)	Hyndman et al., 1990
Juan de Fuca Plate (Middle Valley)	1	Pleistocene and younger	75	10000	80	Simoneit, 1994
				7800 (Q=24559)	40 (Q=133)	Davis and Villinger, 1992
Juan de Fuca Plate (Trench)	0 to 5.3, locally up to 7	Miocene and younger	68	100	25	Whiticar et al., 1995

Table D-2A. Selected base-case results for 1D models.

Region	Geothermal Gradient (°C/km)	Depth to Basement (mbsf)	Water depth (m)	Max Temperature (°C)	Depth to 75 °C (biogenic floor) (mbsf)	Predicted Depth to top of maturity window (represented by %Ro) (mbsf)	Thickness of thermogenic generation zone (m)
Winona Basin	75	6100	1913	458	1000	2200	1400
Middle Valley	75	2000	2505	150	1000	2300	-300*
Accretionary Complex	55	3000	1960	165	1350	2400	600
Juan de Fuca Plate	68	2212	2497	150	1100	2100	112

* At least 2,300 m of sediments is needed to generate hydrocarbon at Middle Valley when geothermal gradient is 75°C/km. The sediment thickness in the area is expected to be less than 2 km so at least 300 m more sediment is needed to reach maturity window. Hydrothermal influence may generate hydrocarbons on a local scale and at shallow depths.

Table D-2B. Table of results for each of the different scenarios tested.

Region	Geothermal Gradient	Depth to Basement (mbsf)	Crust Age (Ma)	Predicted depth to oil window (mbsf)	Thickness of thermogenic generation zone (m)
Winona Basin	25	6100	5.3	no Maturation	n/a
Winona Basin	35	6100	5.3	4500	1600
Winona Basin	50	6100	5.3	3200	2000
Winona Basin	75	6100	5.3	2200	1200
Winona Basin	75	4600	5.3	2200	1200
Winona Basin	100	6100	5.3	1600	1000
Winona Basin	150	6100	5.3	1200	500
Accretionary Complex	25	8040	5.5	1800	2800
Accretionary Complex	35	4040	5.5	2200	400
Accretionary Complex	35	3000	5.5	no Maturation	n/a
Accretionary Complex	35	7000	5.5	2200	3400
Accretionary Complex	35	10000	6.2	2200	2800
Accretionary Complex	55	3000	5.5	2200	600
Accretionary Complex	75	3000	5.5	2200	1300
Juan de Fuca Plate (Middle Valley)	75	2000	1	1800	200
Juan de Fuca Plate (Middle Valley)	75	2000	1	no Maturation	n/a
Juan de Fuca Plate (Middle Valley)	75	1000	1	no Maturation	n/a
Juan de Fuca Plate (Middle Valley)	100	2000	1	1400	600
Juan de Fuca Plate (Middle Valley)	170	2000	1	900	600
Juan de Fuca Plate (Middle Valley)	350	2000	1	500	350
Juan de Fuca Plate (Trench)	25	2500	2.1	no Maturation	n/a
Juan de Fuca Plate (Trench)	45	2500	2.1	no Maturation	n/a
Juan de Fuca Plate (Trench)	68	2500	2.1	2100	400
Juan de Fuca Plate (Trench)	25	2500	5.3	no Maturation	n/a
Juan de Fuca Plate (Trench)	45	2500	5.3	no Maturation	n/a
Juan de Fuca Plate (Trench)	68	2500	5.3	2100	400
Juan de Fuca Plate (Trench)	80	2500	5.3	1700	800

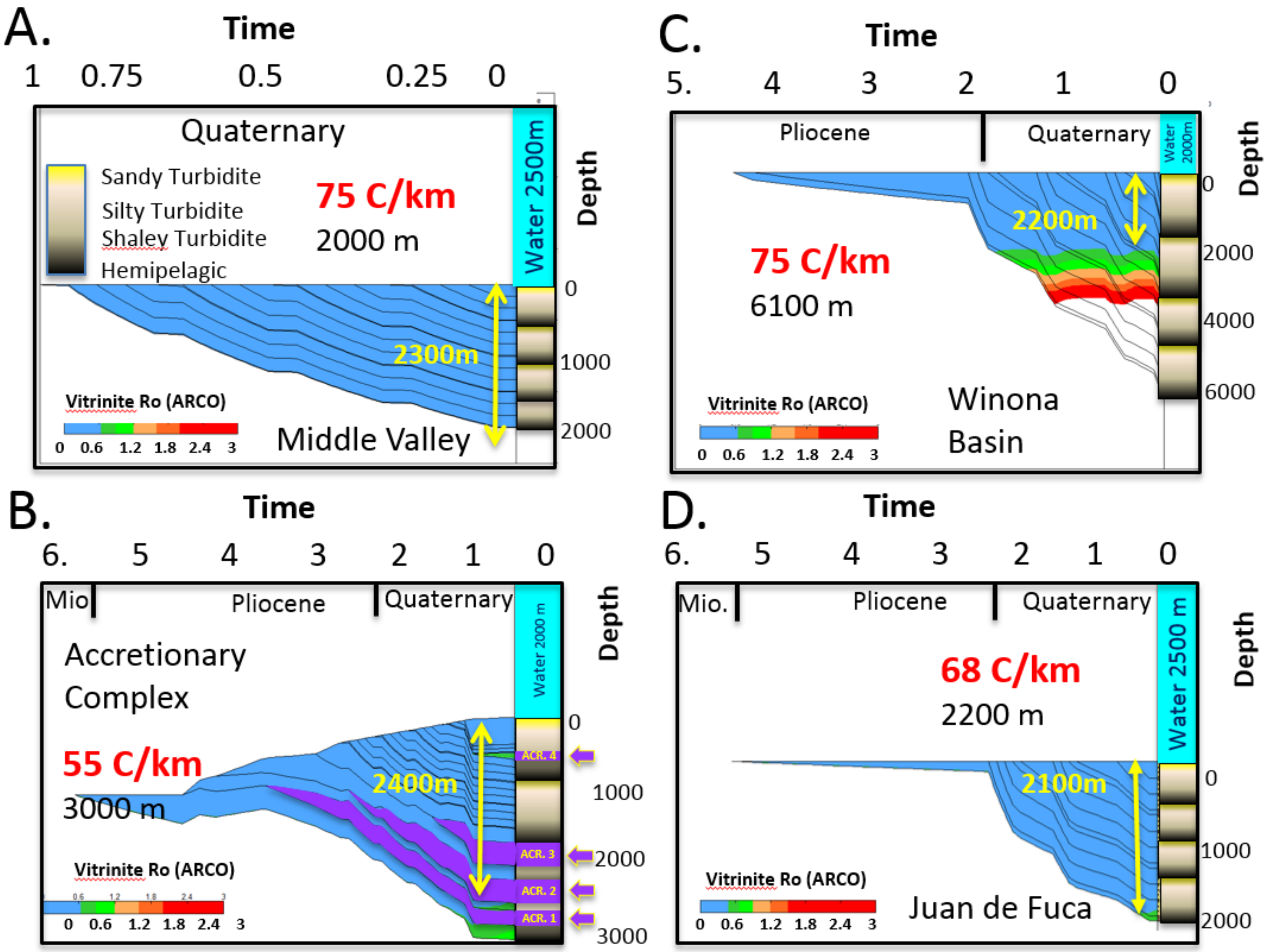

Figure D-1. Base case 1D models for the study area.
(**A**) Juan de Fuca Plate (Middle Valley), (**B**) Accretionary Complex, (**C**) Winona Basin, and (**D**) Juan de Fuca Plate (Trench). NOTE lithology represents a range of turbidite packages ranging from clayey to sandy turbidites. Key: Black numbers (under the geothermal gradient) represents the sediment thickness (depth to basement) used for each model. The double yellow arrow and values beside shows the depth to the top of the predicted oil (maturation) window (in **A** and **B**, sediments are too thin while in **C** and **D**, oil window is reached); Mio. – Miocene; ACR. – accreted sediment packages.

i) Winona Basin:

Following multiple scenarios the 1D model (Table D-2B) in the Winona Basin, a representative geothermal gradient of 75°C/km (Davis and Riddihough, 1982) was applied, resulting in a predicted top of oil generation window at a depth of 2.2 km (Figure D-1C). Multiple basalt intrusions may have locally matured organic matter outside of this oil generation window, but this effect is unlikely to generate any significant quantities of oil (Kulm et al., 1973). The significant thickness of the sedimentary succession suggests that deeper sediments have reached both the oil and gas generation windows (Figure D-1C).

ii) Accretionary Complex:

Multiple scenarios of the 1D model were tested at the Accretionary Complex (Table D-2B). Burial history results suggest that at the study location, at least 2.4 km of sediments are needed to generate oil assuming a geothermal gradient of 55°C / km (Hyndman et al., 1990; Grevemeyer and Villinger, 2001; Figure D-1B). Hyndman and others (1990) reported heat flow values. An assumption of thermal conductivity was needed to convert from heat flow to geothermal gradient and we tested k=3.183 W/m*K (oceanic crust) and 2 W/m*K (clastic sediments. The different thermal conductivities resulted in a wide range of geothermal gradients (Table D-2B).

iii) Juan de Fuca – Middle Valley:

At Middle Valley, multiple scenarios were employed (Table D-2B) and burial history results suggest that a geothermal gradient of 75°C/km is required to generate oil at depths of 2.3 km (Figure D-1A). Multiple basalt intrusions are likely to have caused localized maturation of organic matter, evidenced by the presence of condensed aromatics and olefins in the migrated oil shows. However, this is unlikely to have resulted in significant widespread oil generation. Hydrothermally matured organic matter is well documented in Middle Valley (Simoneit, 1994; Rushdi and Simoneit, 2001, Ventura et al., 2012). The small scale variability in thermal conditions in Middle Valley is well represented by the shallow probe heat flow survey of Davis and Villinger (1992, Figure 15).

iv) Juan de Fuca – Trench:

Multiple scenarios of the 1D model were tested at the Juan de Fuca Trench (Table D-2B). Whiticar and others (1995) estimated a geothermal gradient of 68°C/km at Site 888 (ODP 146). This model shows that at least 2.2 km of sediment is needed to generate oil with this gradient (Figure D-1D).

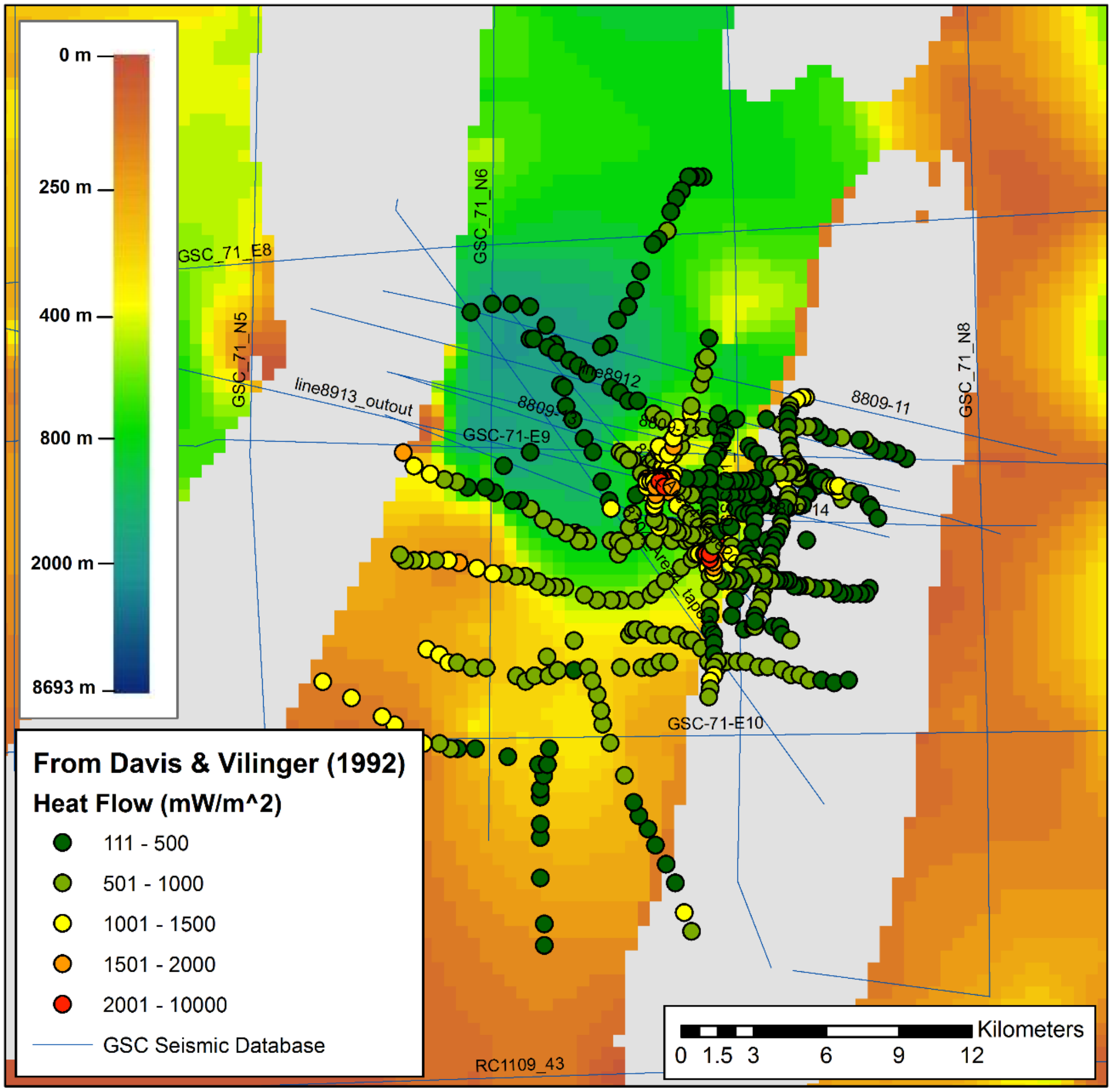

Figure D-2. Juan de Fuca Plate, Middle Valley Heat Flow Map.

Close up of heat flow data from Davis and Villinger (1992) plotted on sediment thickness map.

D.1.2: Petroleum potential in the study area

The results of the petroleum assessment are summarized in the Petroleum Potential Map (Figure 1) and Tables 1A, 1B, and 1C. A qualitative assessment of individual petroleum systems elements was conducted for each of the five regions in the study area (Figure 2) following a four-step approach detailed in Section 4.1 (Main Report). Petroleum system element interpretations and play definitions are based on geological and geophysical work (Appendix C) and informed by 1D basin models (Appendix D). The petroleum assessment considered thermogenic and biogenic systems.

A total of six petroleum plays were considered (Figure 1C):

- Structural Plays:
    - Compressional anticlines and folds,
    - Extensional fault blocks,
    - Strike slip dominated structures and
    - Compression and/or strike slip dominated anticlines and folds)

- Stratigraphic Plays:
    - Turbidite Channel fill
    - Submarine Fan pinch out

Summaries of the geological cumulative chance of success (CCOS) and the technical cumulative chance of success (TCCOS) maps are provided in Figures D-3 and D-4 respectively. The petroleum potential map provided in Figure 1 is a stacked technical cumulative (STCCOS) map, which represents the combined petroleum potential for all plays within the study area.

We conclude that a large part of the study area, including most of the Pacific Plate, has very low potential or no potential for conventional petroleum resources.

Low to moderate conventional petroleum potential is predicted in Winona Basin and the Accretionary Complex (Figure 2).

Low conventional petroleum potential is also predicted for the easternmost areas of the Juan de Fuca plate and Explorer microplate, which contain up to 2.5 km of basin fill with structural and stratigraphic plays.

In addition to the hydrocarbon potential considered above, there is also potential for non-commercial occurrences of hydrothermally generated hydrocarbons (as documented in Middle Valley).

While the Study Area has very limited seismic and well data, this study did not identify any areas with high, predicted potential for significant petroleum resources.

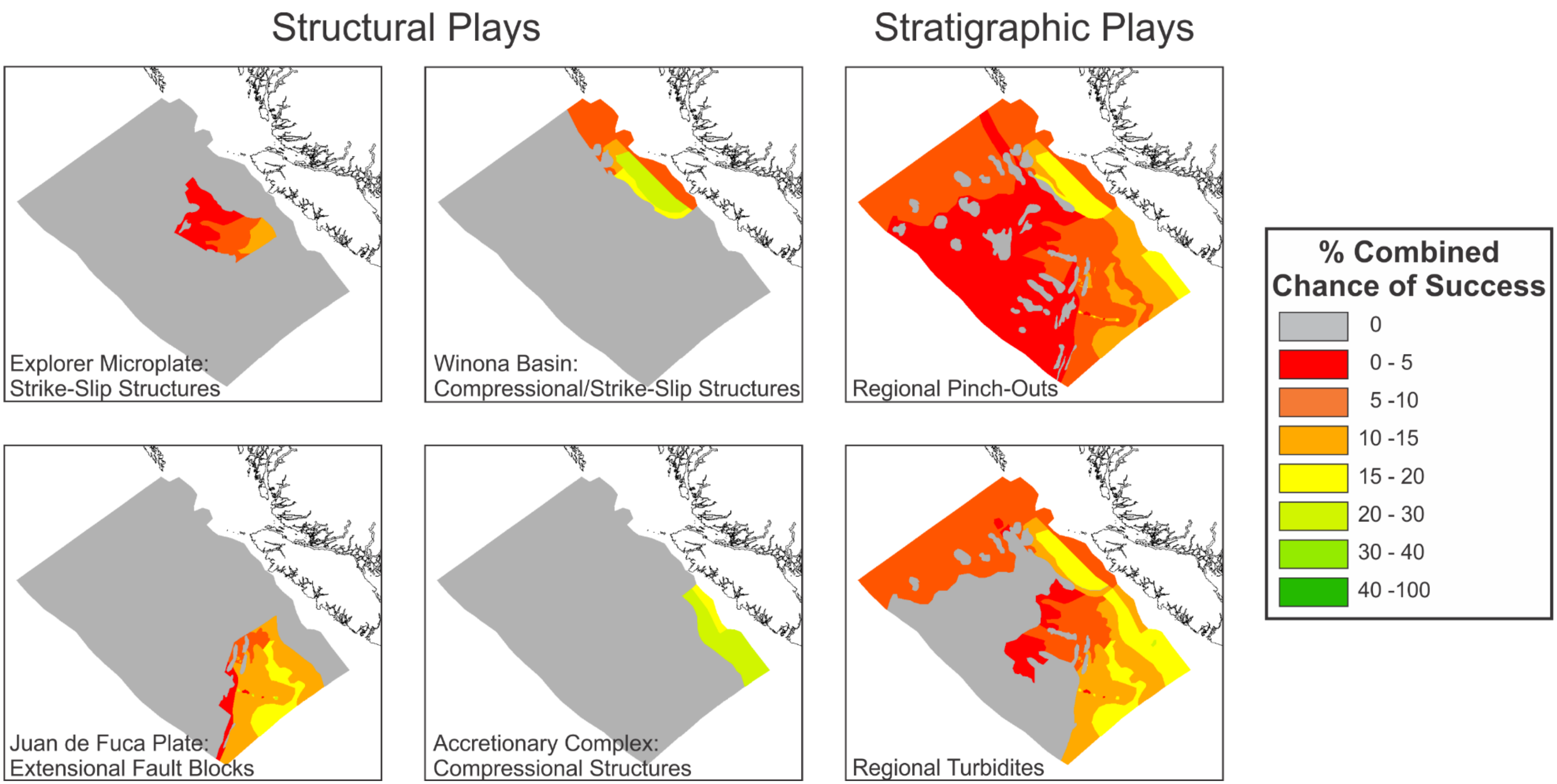

Figure D-3. Geological Combined Chance of Success Maps by Play.

Six plays were assessed (See Table 1C, Main Report). The Winona Basin and Accretionary Complex structural plays. Thermogenic hydrocarbon potential was considered to be greater in the thicker basin fill areas along the eastern edge of the study area (in the Winona Basin and Accretionary Complex regions). Biogenic gas potential was considered to be greater in thinner sedimentary deposits on the Juan de Fuca, Explorer and Pacific plates.

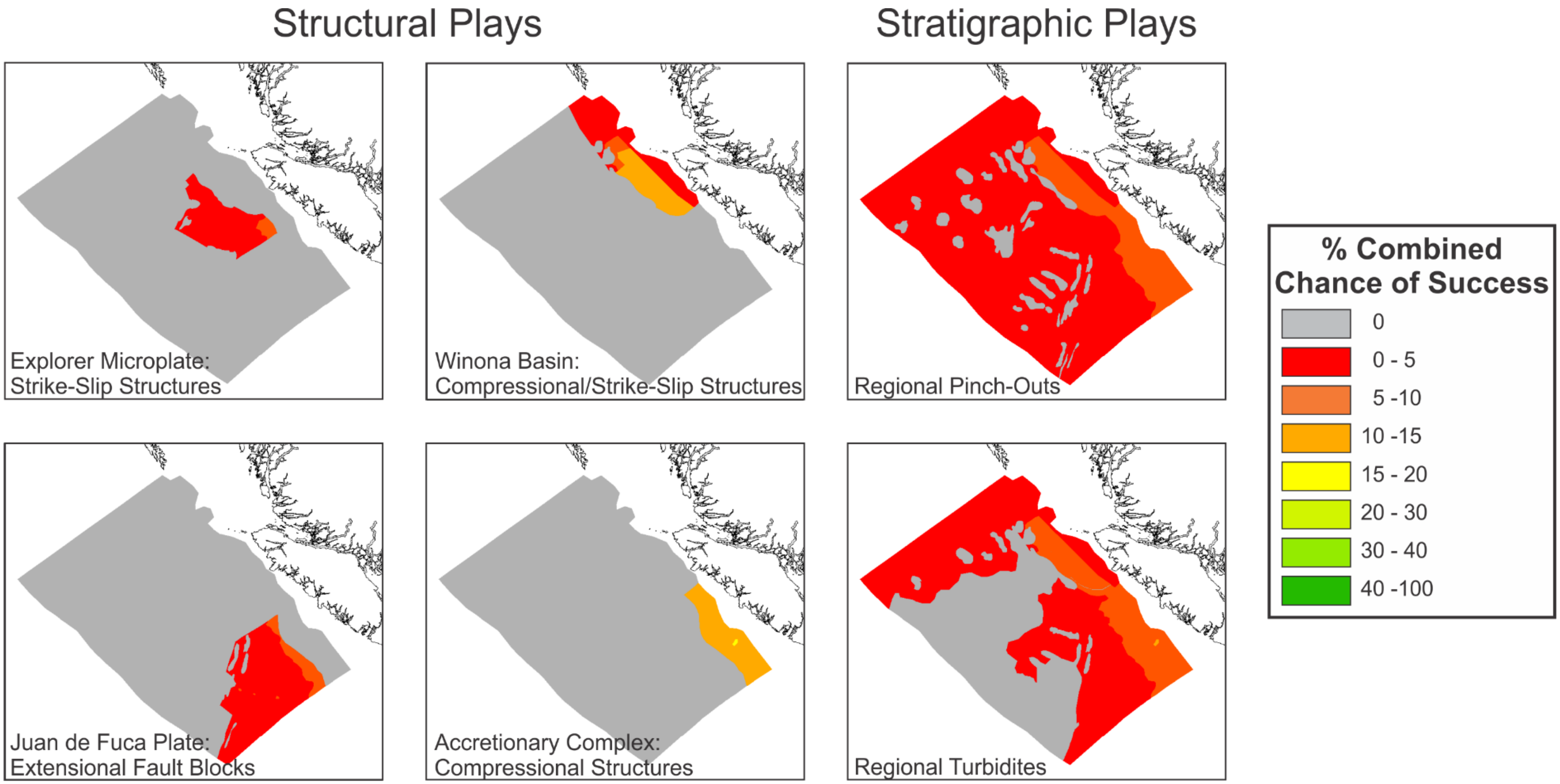

Figure D-4. Technical Combined Chance of Success Maps by Play

Six plays were assessed (See Table 1C, Main Report). Thermogenic hydrocarbon potential was considered to be greater in the thicker basin fill areas along the eastern edge of the study area (in the Winona Basin and Accretionary Complex regions). Biogenic gas potential was considered to be greater in thinner sedimentary deposits on the Juan de Fuca, Explorer and Pacific plates. Global scale factors used to create this map are summarized in Table 1C.

D.2 Unconventional Gas Hydrates Resources

Gas hydrates are ice-like solids that trap light hydrocarbons, typically methane, between frozen water molecules. Gas hydrate is considered an unconventional hydrocarbon primarily due to the fact it's trapping mechanism is geochemical, rather than geo-mechanical. Hydrated gas contains gas molecules in cage structures of ice within sediment pore space. Gas hydrate formation is dependent upon specific temperature and pressure conditions existing in combination with availability of water and gas. Gas hydrate can (i) form and be stable at temperatures above 0°C, and where hydrostatic pressure is greater than that created by 250 m of water or more, and (ii) be detectable at relatively low gas saturations. Consequently, evidence for gas hydrates exist below the sea floor around the globe at any latitude. Gas hydrates form using methane and heavier gases regardless of biogenic, abiogenic or thermogenic origins. They form and dissociate on time scales related to their temperature and pressure controls, so are far more transient than conventional natural gas. Marine gas hydrate is normally hosted within young unconsolidated sediments and tends to be less than 1,000 m below seabed. Other factors that affect gas hydrate formation include: (i) sedimentation rates; (ii) biogenic in situ methane production; (iii) organic carbon content; (iv) influx of methane by advective fluid transport; (v) organic carbon utilization by microbes; (vi) salinity; and (viii) porosity.

Gas hydrate academic and government research, in both terrestrial and marine environments has seen significant scientific advancements over the last twenty years. Numerous textbooks, case studies, and research have been produced regarding its scientific characterization, exploitation as an energy source, and as a global source of environmental carbon. Countries including South Korea and Japan have had national strategic programs to try to develop domestic energy supply from gas hydrate, Today global interest in marine gas hydrate as a viable energy resource has waned significantly, in large part due to breakthrough advancements in the development of less costly and more accessible shale gas plays, and due to technological challenges to reliably and economically produce gas hydrates. Major technological challenges also arise from the propensity of gas hydrate deposits to produce large amounts of both water and sand along with the gas. It is now recognized that the most viable gas hydrate deposits to be exploited are those onshore under permafrost that have a leg of free gas beneath the hydrate. These deposits can be conventionally produced by depressurization that drives continuous gas hydrate dissociation and replenishment of the conventionally-produced free gas leg.

Areas of gas hydrate potential are identified in both the Winona Basin and the Accretionary Complex (Figure 6). Gas hydrates in the Accretionary Complex are sourced by a combination of in situ biogenic methane with minor methane contributions from fluid advection from deeper sources (Riedel et al., 2010). An IODP transect in the area showed that the top of the gas hydrate occurrence zone (GHOZ) deepens landward, most likely due to lower advection rates and lower sedimentation rates closer to the shelf edge (Malinverno et al., 2008). Gas hydrate occurrence is laterally variable because the hydrate has a preference to form in coarser grained sandy or silty facies (Riedel, et al., 2010). In Winona Basin, gas hydrate indicators (bottom simulating reflectors – BSR's) are found up to 40 km outboard of the continental slope confined to folds and ridges (Riedel and Rohr, 2012). Contrary to what was observed in the accretionary complex, gas hydrates in Winona Basin are inferred to be derived from thermogenic methane (Riedel and Rohr, 2012). Gas hydrates produced by biogenic methane are generally pervasive throughout the area. However, in Winona Basin the BSR's are isolated in structural highs suggesting the methane is being sourced by advective fluids from a deeper thermogenic source (Riedel and Rohr, 2012). In 2001, Majorowicz and Osadetz estimated the Canadian Pacific offshore natural gas potential from gas hydrates to be 0.32-2.4 x 10^{13} m^3 (this value includes gas hydrates in the study area and those to the north adjacent to Haida Gwaii).

D.3 Emerging Technology Initiatives

D.3.1 Submarine Geothermal Energy Potential

Seafloor spreading centres have potential to be a significant future source of clean, renewable geothermal energy, due to high temperatures (greater than 300°C) that can be encountered at shallow depths below seafloor (Hiriart, 2010; Atkins and Audunsson, 2013, Snell 2015). This constantly replenishing thermal energy is created and stored in the earth by the radioactive decay of isotopes including potassium, uranium and thorium (Laszlo, 1981; L. Ryback, 2007). Hiriart and others (2010) noted that if only 1% of the known hydrothermal vent sites around the world were exploited, as much as 130 000 MegaWatts (MW) of electricity could be generated, which is about the same amount of geothermal power generated on land using all existing techniques. New technology innovations are needed before marine geothermal energy generation will be possible. Advances are already being made with the design of prototypes of submarine generators that could sit above active hydrothermal vents as well as semi-submersible generators so that drilling and environmental impact may be minimized (Hiriart et al., 2010). Iceland, widely recognized as one of the most sustainable energy systems in the world, derives its geothermal power from an aerially exposed seafloor spreading centre that cuts through its centre. High temperature geothermal resources are also expected in offshore Iceland (Atkins and Audusson, 2013). The first offshore geothermal exploration leases were issued in April, 2017 (Iceland Magazine, 2017) and advances are being made to design technologies to reduce the environmental impact of development.

Offshore exploration methods for marine geothermal potential are presently focused on the identification of hydrothermal vent fields. Atkins and Audunsson (2013) identify candidates in offshore Iceland and rank prospects by comparing location, distance to land, water depth and vent temperatures. In April 2017, the Icelandic National Energy Authority granted North Tech Energy a permit to search for geothermal energy on two exploration areas on the Icelandic continental shelf (Iceland Magazine, 2017). Most seafloor spreading centres are far from land, with the exception of Iceland, but a large swath of active seafloor spreading centres are present in Canadian waters. Hydrothermal vent fields and high temperature conditions are documented at spreading centres in the study area (refer to Figure 4 and Appendix 3.2.4). Figure 6 shows the extent of high temperature areas where geothermal energy and hydrothermal hydrocarbon potential are possible. Active spreading ridges are not expected elsewhere in the Canadian offshore so the only area of high potential for generating large quantities of energy from marine geothermal resources in Canadian waters occurs in the study area. Numerous hot springs are present on land in British Columbia, with geothermal energy resource potential estimated at 3,000 to 5,000 MegaWatts (EnergyBC, 2017).

D.3.2 Carbon Capture and Sequestration

CCS could contribute significantly to the stabilization of greenhouse gas concentrations in the atmosphere over the next several decades (Goldberg et al., 2008 citing: Working Group III of the Intergovernmental Panel on Climate Change (IPCC) (2005)). Ocean Networks Canada (ONC) and Lamont Doherty Earth Observatory (LDEO) are working together on a project to understand the feasibility for Carbon Capture and Sequestration (CCS) at the Cascadia node of the NEPTUNE cabled observatory. The porous basalt of the oceanic crust of the Juan de Fuca and Pacific plates is a potential storage space for captured atmospheric carbon. An effective storage space must have sufficient reservoir capacity with enough stability to prevent CO_2 leakage. Mechanisms for trapping CO_2 in this region likely include: (i) mechanisms common to CCS reservoirs on land and offshore (ionic, capillary and physical trapping (where low permeability layers prevent the CO_2 gas from seeping to the surface), (ii) mechanisms unique to basalt crust (mineralization, where CO_2 reacts with the Mg and Ca ions in the basalt to form stable carbonate minerals) and (iii) mechanisms unique to subseafloor environments (hydrate trapping, where CO_2 hydrates form) (pers. comm. Goldberg, 2018; Goldberg and Slagle, 2009). Gravitational traps are not expected to be likely in this region (Marieni et al., 2013). Geochemical trapping is the preferred mechanism of CCS in this area as it provides a stable long-term storage solution for CO_2 gas.

Goldberg and Slagle (2009) outlined the geological conditions for oceanic crust to be used as a CCS reservoir in the marine environment. Basaltic oceanic crust is a particularly effective CCS reservoir because permanent geochemical trapping of carbon is achieved when carbon dioxide gas (CO_2) reacts with ions in the basalt and forms a stable solid carbonate (this process differs from CCS reservoirs in the Western Canadian Sedimentary Basin where the CO_2 that is sequestered remains a gas, which requires long term monitoring). A potential marine CCS reservoir has oceanic crust that is 15 Ma or younger, a sediment cover at least 200 m thick; and should be in water depths greater than 800 m, located at least 20 km from any recharge/discharge areas (e.g. spreading ridges and seamounts) and should not be in areas of enhanced seismicity. A potential CCS reservoir should also have sufficient porosity for sequestration, should not have pore spaces filled by oil or gas and the deep sea sediments that cover the basaltic reservoirs should form low permeability barriers that impede vertical fluid migration. Assessment of seabed and shallow sediment porosities and permeabilities was beyond the scope of this assessment due to limited data and expected local scale variability in mixed turbidite and pelagic sediments in the study area. Underwood and others (2005) report that basal hemipelagic layers encountered in ODP Leg 168 wells become effective hydrologic seals with seepage rates of approximately 1 mm/yr once the sediment-basalt interface is buried by 100 to 150 m of strata. Areas likely to contain potential CCS reservoirs are depicted in Figure 6.

D.4 Mineral Resources

Although the primary mandate of the MCT initiative is to assess conventional petroleum potential, early in the research process it was noted that the Pacific offshore may contain significant base metal-mineral resources. Areas with potential to contain mineral resources include spreading ridges, seamounts, and the seafloor at depths >3500 m (Figure 7). These areas are potential hosts for volcanogenic massive sulphides (VMS), Ferromanganese crusts (Mn, Fe Crusts), and manganese nodules (Mn Nodules) (Hannington et al., 2017).

D.4.1 VMS deposits

VMS deposits form when hot fluids from seafloor volcanic vents chemically react with seawater (Tornos et al., 2015). This change in chemistry precipitates a variety of precious and base metals (as minerals) including copper, zinc, lead, gold, and silver. Subsea mining of VMS deposits is a developing field. In September, 2017, Japan announced the successful completion of the world's first pilot test for the excavation and retrieval of seafloor polymetallic sulphides from under the sea, at a water depth of 1,600 m near Okinawa Prefecture (RSC Mining and Mineral Exploration website, 2017; SubSeaWorldNews, 2017). The Solwara 1 VMS mine in offshore of Papua New Guinea is reaching the development stage (Lipton 2012). Active vent fields (and associated VMS deposits) have been mapped in the Pacific offshore, with the Endeavour vent field representing a primary study area (Figure 7; Jamieson et al., 2014). Early estimates of mineral tonnage (~45 000 tonnes) at Endeavour was focused around the active vents, however new assessment techniques and exploration into inactive vent fields has increased estimated tonnage to 1.5 million tonnes (Jamieson et al., 2014). Active spreading ridges extend southward into US waters, and westward past the Economic Exclusive zone, into international waters, but no other active spreading ridges are known in the Canadian offshore so it is likely that the only area of high potential for VMS deposits in Canadian waters occurs in the study area.

D.4.2 Ferromanganese Crusts

Ferromanganese (Mn, Fe crusts, Figure 7) slowly precipitate from cold bottom water and are often enriched in Rare Earth Elements (REE's, Hein and Peterson, 2013). High technology devices such as computers, cell phones, and solar panels are dependant on REE's. The Tropic Seamount (located more than 500 km from the Canary Islands) may contain 2.67 tonnes of the rare earth element tellurium (~8% of the world's supply of tellurium; Jamasmie, 2017). Ferromanganese crusts can form in depths of 400 to 7000 m, but the zone of primary enrichment occurs between 800 to 2,500 m depth. Limited information is available for rind thickness (4 to 20 mm from NOAA database from seabed dredge samples in and adjacent to the study area) and mineral grade/tonnage/concentration for these samples is unknown. Conrad et al. (2016) analyzed ferromanganese crusts in the analogous offshore California continental margin, and found crust growth rates ranging from 1 mm to 21.9 mm/Ma, with typical growth rates of 4.7 mm/Ma. Rare earth element concentrations for these young seamounts (<11 Ma) are only slightly lower than those observed for the much older (up to 80 Ma) Pacific Prime Fe-Mn Crust Zone (PCZ) crust (an area in the Central Pacific that is recognized as being of the greatest economic interest in the world for mining mineral-rich crusts (Kelly and Amon, 2017)). Numerous seamounts that are likely to contain Ferromanganese crusts are present within the study area, and a smaller number are present to the north of the study area, including the SGaan Kinghlas - Bowie Seamount MPA.

D.4.3 Manganese Nodules

Manganese nodules (Figure 7) form at water depths between 3,500 and 6,000 m through the interaction of thermal fluids and seawater in an oxygenated abyssal plain environment (Hein and Peterson, 2013). These nodules contain Ni, Cu, Li, and REE's. Although the REE's are less concentrated in nodules than in crusts, manganese nodules are easier to extract (Hein and Peterson, 2013). The northwest corner of the Pacific study area has water depths >3,500 m and low sedimentation, over an area of approximately 9,200 km^2. For these reasons, it was considered the only high potential area for Mn nodules. A much larger area (~49 000 km^2) likely to contain manganese nodules is identified north of the study area.

APPENDIX E – REFERENCED AND REVIEWED DOCUMENTS

Adams, J., 1990. Paleoseismicity of the Cascadia subduction zone: Evidence from turbidites off the Oregon-Washington margin; Tectonics, Vol. 9, Issue 4 (August), p. 569-83, https://doi.org/10.1029/TC009i004p00569

Akiba, F., Inoue, Y., Saito-Kato, M., and Pohlman, J., 2009. Data report: diatom and foraminiferal assemblages in Pleistocene turbidite sediments from the Cascadia margin (IODP Expedition 311), northeast Pacific; *in* Riedel, M., Collett, T.S., Malone, M.J., and the Expedition 311 Scientists, Proc. IODP**,** 311: Washington, D.C. (Integrated Ocean Drilling Program Management International, Inc.). https://doi.org/10.2204/iodp.proc.311.211.2009

Amante, C. and Eakins, B.W., 2009. ETOPO1 1 Arc-Minute Global Relief Model: Procedures, Data Sources and Analysis; NOAA Technical Memorandum NESDIS, NGDC-24; National Geophysical Data Center, NOAA, 19 p., https://doi.org/10.7289/V5C8276M

Arnott, B., Ross, G., and Ozadetz, K., 2016. The nature and origin of organic-rich (source) strata in deepwater rocks of the Neoproterozoic Windermere Supergroup; abstract, in AAPG annual convention and exhibition, Calgary, Canada.

Arthur, M.A., Dean, W. E., and Stow, D.A.V., 1984. Models for the deposition of Mesozoic-Cenozoic fine-grained organic-carbon-rich sediment in the deep sea; The Geological Society of London, Special Publications, Vol.15, No. 1, p. 527-560. https://doi.org/10.1144/GSL.SP.1984.015.01.34

Atkins, D. and Audunsson, H., 2013. Exploration techniques for locating offshore geothermal energy near Iceland; Proceedings, 38th Workshop on Geothermal Reservoir Engineering, Stanford University, Stanford, California. February 11-13, 2013. SGP-TR-198

Atwater, B.F., Carson, B., Griggs, G.B., Johnson, H.P. and Salmi, M.S., 2014. Rethinking turbidite paleoseismology along the Cascadia subduction zone, Geology, Vol. 42, No. 9, p. 827-830, https://doi.org/10.1130/G35902.1

Atwater, T. and Menard, H.W., 1970. Magnetic lineations in the Northeast Pacific; Earth and Planetary Science Letters, Vol. 7, Issue 5 (February), p. 445-450, https://doi.org/10.1016/0012-821X(70)90089-0

Audet, P., Bostock, M. G., Mercier, J.P., Cassidy, J. F., 2008. Morphology of the Explorer – Juan de Fuca slab edge in northern Cascadia: Imaging plate capture at a ridge-trench-transform triple junction; Geology; Vol. 36, No. 11 (November), p. 895-898, https://doi.org/10.1130/G25356A.1

Barr. S.M. and Chase, R.L., 1974. Geology of the northern end of Juan de Fuca Ridge and sea-floor spreading; Canadian Journal of Earth Sciences, Vol. 11, No. 10, p. 1384-1 406. https://doi.org/10.1139/e74-134

Barrie, J.V., 2011. Hydrocarbon Gas Seep Sightings – Marine Expeditions 2011001PGC and 2011002PGC; Expedition Database (ED), Natural Resources Canada, <http://ed.gdr.nrcan.gc.ca/index_e.php> [accessed May 28, 2018]

Barrie, J.V. and Conway, K.W., 2002. Rapid sea level changes and coastal evolution on the Pacific margin of Canada; Sedimentary Geology, Vol. 150, p. 171-183.

Barrie, J.V., and Conway, K.W., 2010. Paleogeographic reconstruction of Hecate Strait British Columbia: changing sea levels and sedimentary processes reshape a glaciated shelf; *in* Li, M.Z., Sherwood, C.R., Hill, P.R (Eds.), Sediments, Morphology and Sedimentary Processes on Continental Shelves; International Association of Sedimentology, Special Publication.

Barrie, J.V., Conway, K.W. and Harris, P.T., 2013. The Queen Charlotte Fault, British Columbia: Seafloor anatomy of a transform fault and its influence on sediment processes; Geo-Marine Letters, Vol. 33, Issue 4 (August), p. 311–318, https://doi.org/10.1007/s00367-013-0333-3

Barrie, J.V., Hetherington, R., and Macleod, R., 2014. Pacific margin, Canada shelf physiography: a complex history of glaciation, tectonism, oceanography and sea-level change, Chapter 22 From: Chiocci, F. L. and Chivas, A. R. (eds) 2014. Continental Shelves of the World: Their Evolution during the Last Glacio-Eustatic Cycle. Geological Society, London, Memoirs, Vol. 41, p. 305–313. http://dx.doi.org/10.1144/M41.22

Becker, K. and Davis, E.E., 2003, New evidence for age variation and scale effects of permeabilities of young oceanic crust from borehole thermal and pressure measurements: Earth and Planetary Science Letters, Vol. 210, (3-4), p. 499-508. https://doi.org/10.1016/S0012-821X(03)00160-2

Becker, K. and Davis, E.E., 2005. A review of CORK designs and operations during the Ocean Drilling Program. In Fisher, A.T., Urabe, T., Klaus, A., and the Expedition 301 Scientists, Proc. IODP, 301: College Station, TX (Integrated Ocean Drilling Program Management International, Inc.). https://doi:10.2204/iodp.proc.301.104.2005

Becker, K. and Fisher, A.T., 2000. Permeability of upper oceanic basement on the eastern flank of the Juan de Fuca Ridge determined with drill-string packer experiments; Journal of Geophysical Research, Vol. 105, Issue B1, p. 897–912. https://doi.org/10.1029/1999JB900250

Best, M.M.R., Barnes C.R., Bornhold, B.D., and Juniper, S.K., 2015. Integrating continuous observatory data from the coast to the abyss: Assembling a multidisciplinary view of the ocean in four dimensions; *in* Seafloor Observatories; Springer Praxis Books, Springer, Berlin, Heidelberg, p. 5-21, https://doi.org/10.1007/978-3-642-11374-1_2

Botros, H. and Johnson, P., 1988. Tectonic evolution of the Explorer-Northern Juan de Fuca Region from 8 Ma to the present. Journal of Geophysical. Research: Solid Earth 93:B9, 10421-10437. https://doi.org/10.1029/JB093iB09p10421

Bustin, R.M. (1997). Petroleum source rocks, organic maturation and thermal history of the Queen Charlotte basin, British Columbia; Bulletin of Canadian Petroleum Geology, Vol. 45 (3), p. 255–278.

Canales, J.P., Detrick, R.S., Carbotte, S.M., Kent, G.M., Diebold, J.B., Harding, A., Babcock, J., Nedimovic, M., and van Ark, E., 2005. Upper crustal structure and axial topography at intermediate-spreading ridges: Seismic constraints from the southern Juan de Fuca Ridge; Journal of Geophysical Research, Vol. 110, B12104 (December), https://doi.org/10.1029/2005JB003630

Capone, D.G. and Hutchins, D.A., 2013. Microbial biogeochemistry of coastal upwelling regimes in a changing ocean. Nature Geoscience, Vol. 6 (September), p. 711-717. https://doi.org/10.1038/ngeo1916

Carbotte, S.M., Arko, R., Chayes, D.N., Haxby, W., Lehnert, K., O'Hara, S., Ryan, W.B.F., Weissel, R.A., Shipley, T., Gahagan, L., Johnson, K., and Shank T., 2004. New Integrated Data Management System for Ridge2000 and MARGINS Research; Eos, Vol. 85, no 51 (December), p. 553-560, https://doi.org/10.1029/2004EO510002

Carbotte S.M., Detrick, R.S., Harding, A., Canales, J.P., Babcock, J., Kent, G., Van Ark, E., Nedimovic, M., and Diebold, J., 2006. Rift topography linked to magmatism at the intermediate spreading Juan de Fuca Ridge; Geology; Vol. 34, No. 3 (March): p. 209-212. https://doi.org/10.1130/G21969.1

Carbotte, S.M., Nedimovic, M.R., Canales, J.P., Kent, G.M., Harding, A.J., and Marjanovic, M., 2008. Variable crustal structure along the Juan de Fuca Ridge: Influence of on-axis hot spots and absolute plate motions; Geochemistry, Geophysics, Geosystems, Vol. 9, Issue 8, p. Q08001, https://doi.org/10.1029/2007GC001922

Carson, B., 1971, Stratigraphy and Depositional History of Quaternary Sediments in northern Cascadia Basin and Juan De Fuca Abyssal Plain, Northeast Pacific Ocean; Ph.D. Dissertation, University of Washington, Seattle, Washington, 249 p.

Carson, B., 1973. Acoustic stratigraphy, structure and history of Quaternary deposition in Cascadia Basin; Deep-Sea Research, Vol. 20, p. 387-396.

Carson, B. and McManus, D.A., 1971. Analysis of turbidite correlation in Cascadia Basin, northeast Pacifc Ocean; Deep-Sea Research, Vol. 18, p. 593-604.

Carson, P.R. and Nelson, C.H., 1987. Marine geology and resource potential of Cascadia Basin; *in* Scholl, D.W., et al., eds., Geology and Resource potential of the continental margin of western North America and adjacent ocean basin – Beaufort Sea to Baja California: Houston, Texas, Circum-Pacific Council for Energy and Mineral resources Earth Science Series, p. 523-535.

Cassidy, J.F., Ellis, R.M., Karavas, C., and Rogers, G.C., 1998. The northern limit of the subducted Juan de Fuca plate system, Journal of Geophysical Research, Vol. 103, Issue B11 (November), p. 26949-26961, https://doi.org/10.1029/98JB02140

Cassidy, J.F., Rogers, G.C., Lamontagne, M., Halchuk, S., and Adams, G., 2010. Canada's earthquakes: 'The good, the bad, and the ugly'. Geoscience Canada, Vol. 37, No. 1 (March), p.1-16, <https://journals.lib.unb.ca/index.php/GC/article/view/15300> [accessed May 28, 2018].

Chang, A.S., Pedersen, T.F. and Hendy, I.L., 2008. Late quaternary paleoproductivity history on the Vancouver Island margin, western Canada: A multiproxy geochemical study, Canadian Journal of Earth Sciences, Vol. 45, No. 11 (November), p. 1283-1297, https://doi.org/10.1139/E08-038

Chapman, R., Pohlman, J., Coffin, R., Chanton, J., and Lapham, L., 2004. Thermogenic gas hydrates in the northern Cascadia margin; Eos, Transactions American Geophysical Union, Vol. 85, No. 38 (September), p. 361-365, https://doi.org/10.1029/2004EO380001

Clague, J.J., 1989, Late Quaternary Sea Level Change and Crustal Deformation, southwestern British Columbia. Current Research Part E, Cordillera and Pacific Margin/Recherches En Cours Partie E, Cordillère Et Marge Du Pacifique; by Geological Survey of Canada; Paper No. 89-1E, 1989 p. 233-236, https://doi.org/10.4095/127492

Clague, D.A., Caress, D.W., Thomas, H., Thompson, D., Calarco, M., Holden, J., and Butterfield, D., 2008. Abundance and distribution of hydrothermal chimneys and mounds on the Endeavour Ridge determined by 1-m resolution AUV multibeam mapping surveys. Eos, Transactions, American Geophysical Union 89(53): Fall Meeting Supplement Abstract V41B-2079.

Clague, J., Harper, J.R., Hebda, R.J. and Howes, D.E., 1982. Late Quaternary sea levels and crustal movements, coastal British Columbia, Canadian Journal of Earth Scientists., Vol. 19, No. 3 (March), p. 597–618, https://doi.org/10.1139/e82-048

Clowes, R., Baird, D.J., and Dehler, S.A., 1997. Crustal structure of the Cascadia subduction zone, southwestern British Columbia, from potential field and seismic studies. Canadian Journal of Earth Sciences. Vol. 34, No. 3 (April), p. 317-335. https://doi.org/10.1139/e17-028

Conrad, T., Hein, J.R., Paytan, A., and Clague, D.A., 2016. Formation of Fe-Mn crusts within a continental margin environment, Ore Geology Reviews, *in press*.

Coogan, L.A. and Dosso, S., 2012. An internally consistent, probabilistic, determination of ridge-axis hydrothermal fluxes from basalt-hosted systems; Earth and Planetary Science Letters, Vol. 323-4, p. 92-101, https://doi.org/10.1016/j.epsl.2012.01.017

Cousens, B.L., Allan, J.F., Leybourne, M.I., Chase, R., and Van Wagoner, N., 1995. Mixing of magmas from enriched and depleted mantle sources in the northeast pacific: West valley segment, Juan de Fuca ridge; Contributions to Mineralogy and Petrology, Vol. 120, No. 3-4, p. 337-57.

Crawford, W.R. and Thomson, R.E., 1991. Physical oceanography of the Western Canadian continental shelf; Continental Shelf Research, Vol.11, Issues 8-10 (August-October), p. 669-683, https://doi.org/10.1016/0278-4343(91)90073-F

Davis, E. E. and Becker, K., 2002. Observations of natural state fluid pressures and temperatures in young oceanic crust and inferences regarding hydrothermal circulation; Earth and Planetary Science Letters, Vol. 204, Issues 1-2(November), p. 231-248, https://doi.org/10.1016/S0012-821X(02)00982-2

Davis, E.E. and Clowes, R.M., 1986. High velocities and seismic anisotropy in Pleistocene turbidites off Western Canada; Geophysical Journal International, Vol. 84, No. 2 (February), p. 381-99. https://doi.org/10.1111/j.1365-246X.1986.tb04361.x

Davis E.E. and Currie, R.G.,1992. Geophysical observations of the northern Juan de Fuca Ridge system: lessons in seafloor spreading. Canadian Journal of Earth Sciences, 1993, Vol. 30, No. 2 (February), p. 278-300, https://doi.org/10.1139/e93-023

Davis, E.E., Fisher, A., and Firth, J., 1997. Hydrogeology of the upper oceanic crust: JOIDES Journal, Vol. 23, p. 6-X3.

Davis, E. E., Heesemann, M., Lambert, A., and He, J., 2017. Seafloor tilt induced by ocean tidal loading inferred from broadband seismometer data from the Cascadia subduction zone and Juan de Fuca Ridge; Earth and Planetary Science Letters, Vol. 463, p. 243-252.

Davis, E. E., Horel, G.C., MacDonald, R.D., Villinger, H., Bennett, R.H., and Li, H., 1991, Pore pressures and permeabilities measured in marine sediments with a tethered probe. Journal of Geophysical Research, Vol. 96, p. 5975-5984.

Davis, E. E. and Hyndman, R.D., 1989. Accretion and recent deformation of sediments along the northern Cascadia subduction zone. Geological Society of America Bulletin, Vol. 101, No. 11 (November), p. 1465-1480, https://doi.org/10.1130/0016-7606(1989)101<1465:AARDOS>2.3.CO;2

Davis, E. E. and Lister, C.R.B., 1977. Tectonic Structures on the Juan de Fuca Ridge, Geol. SOC. Amer., Bull., Vol. 88, pp. 346-3133.

Davis, E. E. and Riddihough, R.P., 1982. The Winona Basin: Structure and tectonics, Canadian Journal of Earth Sciences, Vol. 19, No. 4 (April), p. 767–788, https://doi.org/10.1139/e82-065

Davis, E.E. and Seemann, D.A., 1981. A compilation of seismic reflection profiles across the continental margin of western Canada. Geological Survey of Canada, Open File Report 751, 1981, https://doi.org/10.4095/129686

Davis, E.E. and Villinger, H., 1992. Tectonic and thermal structure of the Middle Valley sedimented rift, northern Juan de Fuca Ridge, in Davis, E.E., Mottl, M.J., and Fisher, A.T., Proceedings of the Ocean Drilling Program, Initial Reports, Vol. 139, p. 9-42.

Davis, E.E., Chapman, D.D. and Villinger, H., 1989. Heat-flow variations correlated with buried basement topography on the Juna de Fuca Ridge flank. Nature 342, No. 6249 (November), p.533-537.

Davis, E.E., Hyndman, R.D. and Villinger, H.W., 1990. Rates of Fluid Expulsion across the Northem Cascadia Accretionary Prism: Constraints from New Heat Flow and Multichannel Seismic Reflection Data. Journal of Geophysical Research, Vol. 95, No. B6, p. 8869-8889.

Davis, E.E., Mottl, M., and Fisher, A.T., 1991, Ocean Drilling Program, Leg 139 preliminary report; Middle Valley, Juan de Fuca Ridge: Preliminary Report – Texas A&M University, Ocean Drilling Program, Vol. 39, p. 1-55.

Deep Sea Drilling Project, 1989. Archive of Core and Site/Hole Data and Photographs from the Deep Sea Drilling Project (DSDP); NOAA National Centers for Environmental Information, https://doi.org/10.7289/V54M92G2

Dehler, S.A. and Clowes, R.M., 1992. Integrated geophysical modelling of terranes and other structural features along the western Canadian margin; Canadian Journal of Earth Sciences, Vol. 29, No. 7 (July), p. 1492-1508, https://doi.org/10.1139/e92-119

Dehler, S.A., Keen, C.E. and Rohr, K.M.M. 1997. Tectonic and thermal evolution of Queen Charlotte Basin: Lithospheric deformation and subsidence models. Basin Research, Vol. 9, p. 243–261.

Delaney, J.R., McDuff, R.E., and Lupton, J.E., 1984. Hydrothermal fluid temperatures of 400°C on the Endeavour Segment, northern Juan de Fuca Ridge. Eos, Transactions, American Geophysical Union Vol. 65 (45): Fall Meeting Supplement 973.

Delaney, J.R., Robigou, V. and McDuff, R., 1992. Geology of a vigorous hydrothermal system on the Endeavour Segment, Juan de Fuca Ridge. Journal of Geophysical Research Vol. 97:19, p.663-682 https://doi.org/10.1029/92JB00174.

Dietrich, J.R., 1995. Petroleum resource potential of the Queen Charlotte Basin and environs, west coast Canada. Bulletin of Canadian Petroleum Geology, Vol. 43, No. 1, p. 20-34.

Dietrich, J.R., Higgs, R., Rohr, K.M., and White, J.M., 1993. The Tertiary Queen Charlotte Basin: a strike-slip basin on the western Canadian continental margin; in Tectonic Controls and Signatures in Sedimentary Successions, L. Frostick and R. Steel (eds.); Special Publication Number 20, International Association of Sedimentologists, p. 161-169.

Dietrich, J.R., Morrell, G.R., and Fortier, M.C., 1992. Petroleum resource potential in the proposed area of Gwaii Haanas/ South Moresby National Park, British Columbia. Geological Survey of Canada, Open File 2557, 16 p., https://doi.org/10.4095/133483

Dillion, W., Grow, J., and Paull, C.K., 1980. Unconventional gas hydrate seals may trap gas off southeast US. [North Carolina, South Carolina]; Oil and Gas Journal, Vol. 78, no. 1 (January), p. 124-130.

Earth Institute Columbia University (July 14, 2008). Undersea volcanic rocks may offer vast repository for greenhouse gas. Retrieved from <http://www.earth.columbia.edu/articles/view/2204>

Einsele, G., 2000. Sedimentary Basins. Evolution, Facies, and Sediment Budget (Chapter 10), 2nd ed. 792 p.

Energy BC (December 14, 2017). High Temperature Geothermal in British Columbia. Retrieved from: <http://www.energybc.ca/hightempgeo.html#section3> [accessed May 28, 2018]

Ewing, J., Ewing, M., Aitken, T. and Ludwig, W. J., 1968. North Pacific sediment layers measured by seismic profiling, The Crust and Upper Mantle of the Pacific Area, Geophys. Monogr. Ser., 12L. Knopoff, C. L. Drake, P. J. Hart, p. 147–173, AGU, Washington, D.C.

Expedition 311 Scientists, 2006a. Expedition 311 summary; *in* Riedel, M., Collett, T.S., Malone, M.J., and the Expedition 311 Scientists, Proc. IODP, 311: Washington, DC (Integrated Ocean Drilling Program Management International, Inc.). doi:10.2204/iodp.proc.311.101.2006

Expedition 311 Scientists, 2006b. Site U1325; *in* Riedel, M., Collett, T.S., Malone, M.J., and the Expedition 311 Scientists, Proc. IODP, 311: Washington, DC (Integrated Ocean Drilling Program Management International, Inc.). doi:10.2204/iodp.proc.311.103.2006

Expedition 311 Scientists, 2006c. Site U1326; *in* Riedel, M., Collett, T.S., Malone, M.J., and the Expedition 311 Scientists, Proc. IODP, 311: Washington, DC (Integrated Ocean Drilling Program Management International, Inc.). doi:10.2204/iodp.proc.311.104.2006

Expedition 311 Scientists, 2006d. Site U1327; *in* Riedel, M., Collett, T.S., Malone, M.J., and the Expedition 311 Scientists, Proc. IODP, 311: Washington, DC (Integrated Ocean Drilling Program Management International, Inc.). doi:10.2204/iodp.proc.311.105.2006

Expedition 311 Scientists, 2006e. Site U1328; *in* Riedel, M., Collett, T.S., Malone, M.J., and the Expedition 311 Scientists, Proc. IODP, 311: Washington, DC (Integrated Ocean Drilling Program Management International, Inc.). doi:10.2204/iodp.proc.311.106.2006

Expedition 311 Scientists, 2006f. Site U1329; *in* Riedel, M., Collett, T.S., Malone, M.J., and the Expedition 311 Scientists, Proc. IODP, 311: Washington, DC (Integrated Ocean Drilling Program Management International, Inc.). doi:10.2204/iodp.proc.311.107.2006

Fink, C.R. and Spence, G.D., 1999. Hydrate distribution off Vancouver Island from multi-frequency single-channel seismic reflection data; Journal of Geophysical Research, Vol. 104, Issue B2 (February), p. 2909-2922, https://doi.org/10.1029/98JB02641

Fisher, A.T., 2005. Marine Hydrogeology: recent accomplishments and future opportunities; Journal of Hydrogeology Vol. 39, Issue 1 (March), p. 69-97, https://doi.org/10.1007/s10040-004-0400-y

Fisher, A.T., Davis, E.E., and Escutia, C. (Eds.), 2000. Proceedings of the Ocean Drilling Program, Scientific Results, Vol. 168: College Station, TX (Ocean Drilling Program), https://doi.org/10.2973/odp.proc.sr.168.2000

Fowler, M.G., Snowdon, L.R., and Brooks, P.W., 1987. Hydrous pyrolysis and biomarker characterization of bitumens in Queen Charlotte Island basalts; *in* L. Matavelli and L. Novelli (Eds.); 13th International Meeting on Organic Geochemistry (p. 137), Venice, Italy.

Fowler, M.G., Snowdon, L.R., Brooks, P.W., and Hamilton, T.S., 1988. Biomarker characterization and hydrous pyrolysis of bitumens from Tertiary volcanics, Queen Charlotte Islands, British Columbia, Canada. In L. Mattavelli and L. Novelli (Eds.), Advances in Organic Geochemistry 1987 Vol. 2, p. 715–726. Oxford: Pergamon Press.

Gablina, I.F., Dobretsova, I.G., Beltenev, V.E., Lyutkevich, A.D., Narkevskii, E.V., and Gustalis, A.N., 2011. Peculiarities of present-day sulfide mineralization at 19º15' – 20º08' N, Mid-Atlantic Ridge, Doklady Earth Sciences, Vol.. 442 (Part 2), p. 163-167.

Ganguly, N., Spence, G.D., Chapman, N.R., and Hyndman, R.D., 2000. Heat flow variations from bottom simulating reflectors on the Cascadia margin; Marine Geology, Vol.164, Issues 1-2 (February), p. 53-68, https://doi.org/10.1016/S0025-3227(99)00126-7

Gardner, J.V. Cacchione, D.A., Drake, D.E., Edwards, B.D. Field, M.E., Hampton, M.A., Karl, H.A., Kenyon, N.H., Masson, D.G., McCulloch, D.S., and Grim, M.S, 1993. Map showing sediment isopachs in the deep sea basins of the Pacific Continental Margin, Strait of Juan de Fuca to Cape Mendodino; U. S. Geological Survey (USGS), Miscellaneous Investigations Series Map 1-2091-A (1 Sheet), Scale 1:1 000 000, https://pubs.usgs.gov/imap/2090/a/

Geological Survey of Canada, 2014. Geoscience Data Repository for Geophysical Data, Gravity, Point Data, Natural Resources Canada, http://gdr.agg.nrcan.gc.ca/gdrdap/dap/search-eng.php

Goldberg, D.S., Lackner, K.S., Han, P., Slagle, A.L., and Wang, T., 2013. Co-Location of Air Capture, Subseafloor CO_2 Sequestration, and Energy Production on the Kerguelen Plateau; Environmental Science & Technology, Vol. 47 (13), p. 7521-7529, https://doi.org/10.1021/es401531y

Goldberg, D. and Slagle A.L., 2009. A global assessment of deep sea basalt sites for carbon sequestration; Energy Procedia 1, p. 3675-3682. https://doi.org/10.1016/j.egypro.2009.02.165

Goldfinger, C., Dziak, R.P., and Fox, C., 2002. Offshore structure of the Juan de Fuca Plate from marine seismic and sonar studies. In The Cascadia subduction zone and related subduction systems - seismic structure, intraslab earthquakes and processes, and earthquake hazards; by Kirby, S (ed.); Wang, K (ed.); Dunlop, S (ed.); Geological Survey of Canada, Open File 4350, 2002 p. 13-16, https://doi.org/10.4095/222489

Goldfinger, C., Nelson, C.H., Morey, A.E., Johnson, J.R., Patton, J., Karabanov, E., Gutierrez-Pastor, J., Eriksson, A.T., Gracia, E., Dunhill, G., Enkin, R.J., Dallimore, A., and Vallier, T., 2012. Turbidite event history – Methods and implications for Holocene paleoseismicity of the Cascadia Subduction Zone; U.S. Geological Survey, Professional Paper 1661-F, 170 p., 64 figures, available at https://pubs.usgs.gov/pp/pp1661f/pp1661f_text.pdf

Grasby, S.E., Allen, D.M., Bell, S., Chen, Z., Ferguson, G., Jessop, A., Kelman, M., Ko, M., Majorowicz, J., Moore, M., Raymond, J., and Therrien, R., 2012. Geothermal energy resource potential of Canada; Geological Survey of Canada, Open File 6914, 1-322 p., https://doi.org/10.4095/291488

Grevemeyer, I. and Villinger, H., 2001. Gas hydrate stability and the assessment of heat flow through continental margins. Geophysical Journal International, Vol. 145, Issue 3 (June), p. 647–660, https://doi.org/10.1046/j.0956-540x.2001.01404.x

Griggs, G.B. and Kulm, L.D., 1970. Sedimentation in Cascadia deep-sea channel; Geological Society of America Bulletin, Vol. 81, No.5 (May), p.1361-1384, https://doi.org/10.1130/0016-7606(1970)81[1361:SICDC]2.0.CO;2

Hampton, M.A. and Karl, H.A., and Kenyon, N.H., 1989, Sea-floor drainage features of Cascadia Basin and the adjacent continental slope, Northeast Pacific Ocean: Marine Geology, Vol. 87, No. 2-4, p. 249-272. https://cmgds.marine.usgs.gov/fan_info.php?fan=F484WO

Hamilton, T.S. and Cameron, B.E.B., 1989. Hydrocarbon occurrences on the western margin of the Queen Charlotte basin. Bulletin of Canadian Petroleum Geology, Vol. 37 (4), p. 443–466.

Han, S., Carbotte, S.M., Canales, J.P., Nedimović, M.R., Carton, H., Gibson, J.C., and Horning, G. W., 2016. Seismic reflection imaging of the Juan de Fuca plate from ridge to trench: New constraints on the distribution of faulting and evolution of the crust prior to subduction; Journal of Geophysical Research Solid Earth, Vol. 121, Issue 3 (March), p. 1849-1872, https://doi.org/10.1002/2015JB012416

Hannigan, P.K. and Dietrich, J.R., 2011. Petroleum resource potential of the Hecate Strait/Queen Charlotte Sound Glass Sponge Reef areas of interest, Pacific margin of Canada; Geological Survey of Canada, Open File 6860, 53 p., https://doi.org/10.4095/291497

Hannigan, P.K.; Dietrich, J.R; Lee, P.J. and Osadetz, K.G., 1998. Petroleum resource potential of sedimentary basins on the Pacific margin of Canada; Geological Survey of Canada, Open File 3629, 85 p., https://doi.org/10.4095/209925

Hannigan, P.K., Dietrich, J.R., Lee, P.J., and Osadetz, K.G., 2001. Petroleum resource potential of sedimentary basins on the Pacific margin of Canada; Geological Survey of Canada, Bulletin 564, 72 p., https://doi.org/10.4095/212649

Hannigan, P.K., Dietrich, J.R. and Osadetz, K.G., 2005. Petroleum resource potential of the proposed Scott Islands Marine Wildlife area, Pacific margin of Canada, Geological Survey of Canada, Open File 4829, 53 p., https://doi.org/10.4095/220354

Hannington, M., Petersen, S., and Krätschell, A., 2017. Subsea mining moves closer to shore; Nature Geoscience, Vol. 10, p. 158-159, https://doi.org/10.1038/ngeo2897

Haq, B.U., Hardenbol, J., and Vail, P.R., 1987. Chronology of fluctuating sea levels since the Triassic; Science, Vol. 235, p. 1156-1167.

Hashimoto, Y. and Minamizawa, S., 2009. Data report: quantitative analysis of grain size distribution for coarse sediments in an accretionary prism: an example from the Cascadia accretionary prism; *in* Riedel, M., Collett, T.S., Malone, M.J., and the Expedition 311 Scientists, Proc. IODP, 311: Washington, D.C. (Integrated Ocean Drilling Program Management International, Inc.), https://doi.org/10.2204/iodp.proc.311.205.2009

Hasselgren, E. and Clowes, R., 1995. Crustal structure of northern Juan de Fuca plate from multichannel reflection data; Journal of Geophysical Research, Vol. 100, No. B4 (April), p. 6469-6486.

Hayes, J.B., 1973. DSDP Leg 18, Site 177. 29. Petrology of Indurated Sandstones, Leg 18, Deep Sea Drilling Project); https://doi.org/10.2973/dsdp.proc.18.129.1973

Hayward, N. and Calvert, A.J., 2007. Seismic reflection and tomographic velocity model constraints on the evolution of the Tofino forearc Basin, British Columbia; Geophysical Journal International, Vol. 168, Issue 2 (February), p. 634-646 https://doi.org/10.1111/j.1365-246X.2006.03209.x

He, Z., Crews, S., and Corrigan, J., 2007. Rifting and heat flow: Why the McKenzie model is only part of the story; abstract, in AAPG Hedberg Conference, The Hague, the Netherlands, p. 16. Article #90066©2007

Hein, J.R. and Petersen, S., 2013. The geology of Cobalt-rich Ferromanganese Crusts. In: Secretariat of the Pacific Community (2103) Deep Sea Minerals: Cobalt rich Ferromanganese Crusts, a physical, biological, environmental, and technical review. Vol. 1C, p. 7-14.

Hein, J.R. and Petersen, S., 2013. The geology of Manganese Nodules. In: Secretariat of the Pacific Community (2103) Deep Sea Minerals Manganese Nodules, a physical, biological, environmental, and technical review. 1B p. 7-18.

Hiriart, G. and Prol-Ledesma, R.M., Alcocer, S. and Espíndola, S., 2010. Submarine Geothermics; Hydrothermal Vents and Electricity Generation. Proceedings World Geothermal Congress 2010, Bali, Indonesia, 25-29 April, 2010. Available at: <http://www.geothermal-energy.org/pdf/IGAstandard/WGC/2010/3704.pdf> [accessed May 28, 2018]

Horning, G., Canales, J.P., Carbotte, S.M., Han, S., Carton, H., Nedimović, M.R. and van Keken, P.E., 2016. A 2-D tomographic model of the Juan de Fuca plate from accretion at axial seamount to subduction at the Cascadia margin from an active source ocean bottom seismometer surve;, Journal of Geophysical Research Solid Earth, Vol. 121, Issue 8 (August), p. 5859–5879, https://doi.org/10.1002/2016JB013228

Hyndman, R.D., 1992. “Ice” beneath the deep sea: Studies of methane hydrate layers beneath the continental slope off Vancouver Island; Geoscience Canada, Vol. 19, No. 1, p. 21-26.

Hyndman, R., 1995. The Lithoprobe corridor across the Vancouver Island continental margin: The structural and tectonic consequences of subduction. Canadian Journal of Earth Sciences, Vol. 32, No. 10 (November), p. 1777-1802. https://doi.org/10.1139/e95-138

Hyndman, R D. and Wang, K., 1993. Thermal constraints on the zone of major thrust earthquake failure: The Cascadia subduction zone; Journal of Geophysical Research: Solid Earth, Vol. 98, No. B2, p. 2039-60. https://doi.org/10.1029/92JB02279

Hyndman, R.D. and Weichert, D.H. 1983. Seismicity and rates of relative motion on the plate boundaries of Western North America; The Royal Astronomical Society, Geophysical Journal International, Vol. 72, Issue 1 (January), p. 52-82, https://doi.org/10.1111/j.1365-246X.1983.tb02804.x

Hyndman, R.D., Riddihough, R.P., and Herzer, R., 1979. The Nootka Fault Zone – a new plate boundary off Western Canada; The Royal Astronomical Society, Geophysical Journal International, Vol. 58, Issue 3 (September), p. 667-683, https://doi.org/10.1111/j.1365-246X.1979.tb04801.x

Hyndman, R.D., Wang, K., Yuan, T., and Spence, G.D., 1993. Tectonic sediment thickening, fluid expulsion, and the thermal regime of subduction zone accretionary prisms: The Cascadia margin off Vancouver Island. Journal of Geophysical Research, Vol. 98, No. B12, p. 21,865-21,876, DECEMBER 10, 1993. https://doi.org/10.1029/93JB02391

Hyndman, R.D., Yorath, C.J., Clowes, R.M., and Davis, E.E., 1990. The northern Cascadia subduction zone at Vancouver Island: Seismic structure and tectonic history, Canadian Journal of Earth Sciences, Vol. 27, No. 3, p. 313-329. https://doi.org/10.1139/e90-030

Iceland Magazine (April 24, 2017). An unexplored source of Green Energy: submarine geothermal power to be harnessed offshore. Retrieved from: http://icelandmag.visir.is/article/unexplored-source-green-energy-submarine-geothermal-power-be-harnessed-shore

Ingle, J.C. Jr., 1973. Neogene Foraminifera from the northeastern Pacific Ocean, Leg 18, Deep Sea Drilling Project. Initial Reports of the Deep Sea Drilling Project, 18 (1973), p. 517-567.

Integrated Ocean Drilling Program, 2010. Archive of Core and Site/Hole Data and Photographs from the Integrated Ocean Drilling Program (IODP). NOAA National Centers for Environmental Information, https://doi.org/10.7289/V58913SM

Jamasmie, C. (April 13, 2017). British scientists find sub-sea minerals treasure trove. Retrieved from: http://www.mining.com/british-scientists-find-sub-sea-minerals-treasure-trove

James, T.S., Clague, J.J., Wang, K., and Hutchinson, I., 2000. Postglacial rebound at the northern Cascadia subduction zone. Quaternary Science Reviews, Vol. 19, p. 1527-1541.

Jamieson J.W., Clague D.A., and Hannington M.D., 2014. Hydrothermal sulfide accumulation along the Endeavour Segment, Juan de Fuca Ridge; Earth and Planetary Science Letters, Vol. 395, p. 136-148, https://doi.org/10.1016/j.epsl.2014.03.035

Jefferson, C.W., Schmitt, H.R., 1992. Assessment of Mineral Resource Potential, Phase I, in the Proposed area of Gwaii Haanas / South Moresby National Marine Park Reserve; Geological Survey of Canada, Open File 2480, 44 p., https://doi.org/10.4095/133236

Johns, M.J., Trotter, J.A., Barnes, C.R., and Narayan, Y.R., 2012. Biostratigraphic, strontium isotopic and geologic constraints on the landward movement and fragmentation of terranes with the Tofino Basin, British Columbia; Canadian Journal of Earth Sciences, Vol. 49, No. 7 (July), p. 819–856, https://doi.org/doi:10.1139/E2012-032

Johns, M.J., Trotter, J.A., Bonnett, J.M., and Barnes, C.R., 2015. Neogene strontium isotope stratigraphy, foraminifer biostratigraphy, and lithostratigraphy from offshore wells, Queen Charlotte Basin, British Columbia, Canada; Canadian Journal of Earth Sciences, Vol. 52, No. 9 (September), p. 795-822, https://dx.doi.org/10.1139/cjes-2014-0159

Kao, H., Shan, S.-J., Dragert, H. and Rogers, G., 2009, Northern Cascadia episodic tremor and slip: A decade of tremor observations from 1997 to 2007, Journal of Geophysical Research Solid Earth, Vol. 114, Issue B11 (November), B00A12, https://doi.org/10.1029/2008JB006046

Kelly, C. and Amon, D., (December 8th, 2017). Deep-sea Mining Interests and Activities in the Western Pacific. Retrieved from: http://oceanexplorer.noaa.gov/okeanos/explorations/ex1605/background/mining/welcome.html

Kelley, D.S., Carbotte, S.M., Caress, D.W., Clague, D.A., Delaney, J.R., Gill, J.B., Hadaway, H., Holden, J.F., Hooft, E.E.E., Kellogg, J.P., Lilley, M.D., Stoermer, M., Toomey, D., Weekly, R., and Wilcock, W.S.D., 2012. Endeavour Segment of the Juan de Fuca Ridge: One of the most remarkable places on Earth; Oceanography Vol. 25 (1), p. 44–61. https://doi.org/10.5670/oceanog.2012.03.

Kendall, K. and Deptuck, M.E., 2012. Lower Cretaceous shelf-edge trajectories, shelf indenting canyons and the potential transfer of coarser clastics into deeper water, Sable sub-basin, offshore Nova Scotia, CNSOPB Geoscience Open File Poster 2012-002PF, 2 panels.

Kiyokawa, S. and Yokoyama, K., 2009. Provenance of turbidite sands from IODP EXP 1301 in the northwestern Cascadia Basin, western North America; Marine Geology, Vol. 260, Issues 1-4 (May), p. 19-29. https://doi.org/10.1016/j.margeo.2009.01.003

Klett, T.R., Gautier, D.L., and Ahlbrandt, T.S., 2007. An Evaluation of the USGS World Petroleum Assessment 2000 - Supporting Data: U.S. Geological Survey Open-File Report 2007–1021, 5 p.

Knudson, K.P. and Hendy, I.L., 2009. Climatic influences on sediment deposition and turbidite frequency in the Nitinat Fan, British Columbia; Marine Geology, Vol. 262, Issues 1-4 (July), p. 29-38, https://doi.org/10.1016/j.margeo.2009.03.002

Kulm, L.V.D., Von Huene, R., Ingle, J.C., Jr., Kling, S.A., Musich, L.F., Piper, D.J.W., Pratt, R.M., Schrader, H.-J., Weser, O.E. and Wise, S.W., Jr., 1973. Site 177. Initial Reports of the Deep Sea Drilling Project 18: p. 233-285.

Lambeck, K., Esat, T.M, and Potter, E.-K., 2002. Links between climate and sea levels for the past three million years; *in* Nature, Vol. 419, 12 September, 2002, https://doi.org/10.1038/nature01089

Lamont-Doherty Earth Observatory (LDEO) News (January 4, 2010). Scientists target East Coast rocks for CO_2 storage. Retrieved from: <http://www.ldeo.columbia.edu/news-events/scientists-target-east-coast-rocks-co2-storage> [accessed May 28, 2018].

Lamont-Doherty Earth Observatory (LDEO) News (June 9, 2016). In a first, Iceland power plant turns carbon emissions to stone. Retrieved from: http://www.ldeo.columbia.edu/news-events/first-iceland-power-plant-turns-carbon-emissions-stone

László, E., 1981. Geothermal Energy: An Old Ally; Ambio, Vol.10, No. 5, p. 248–249.

Li, Y. and Oldenburg, D.W., 1998. "3D inversion of gravity data", Geophysics, Vol. 63: p. 109-119.

Lin, T.J., et al., 2016. Linkages between mineralogy, fluid chemistry, and microbial communities within hydrothermal chimneys from the Endeavour Segment, Juan de Fuca Ridge, Geochemistry, Geophysics, Geosystems, G^3, Vol. 17, Issue 2, p. 300–323, https://doi.org/10.1002/2015GC006091

Lindquist, S.J., 1999. Petroleum systems of the Po Basin province of northern Italy and the northern Adriatic Sea: Porto Garibaldi (biogenic), Meride/Riva di Solto (thermal), and Marnoso Arenacea (thermal); U.S. Department of the Interior, Denver Open File Report 99-50-D, U.S. Geological Survey, Washington, D.C.

Lipton, I., 2012. Mineral Resource Estimate: Solwara Project, BismarckSea, PNG. Technical Report compiled under NI43-101; Golder Associates, for Nautilus Minerals Nuigini Inc., 218 p.

Lisiecki, L.E. and Raymo, M.E., 2005. A Plio-Pleistocene stack of 57 globally distributed benthic D18O records. Paleoceanography, Vol. 20, PA1003, 17 p. https://doi.org/10.1029/2004PA001071

Lister, C.J., King, H.M., Atkinson, E.A., and Nairn, R., 2018. A probability-based method to generate qualitative petroleum potential maps: adapted for and illustrated using ArcGIS®, Geological Survey of Canada, Open File 8404, *in press*.

Luckge, A., Boussafir, M., Lallier-Verges, E., and Littke, R., 1996. Comparative study of organic matter preservation in immature sediments along the continental margins of Peru and Oman. Part 1: Results of petrographical and bulk geochemical data; OrganicGeochemistry, Vol. 24, Issue 4 (April), p. 437-451, https://doi.org/10.1016/0146-6380(96)00045-9

Lyatsky, H., 2006. Frontier next door: geology and hydrocarbon assessment of sedimentary basins offshore western Canada, Canadian Society of Exploration Geophysicists Recorder, Vol. 31, No. 4 (April), p. 66-75,<https://csegrecorder.com/articles/view/frontier-next-door-geology-and-hydrocarbon-assessment-of-sedimentary-basins> [accessed May 28, 2018]

Lyatsky, H.V. and Haggart, J.W., 1993. Petroleum exploration model for the Queen Charlotte Basin area, offshore British Columbia. Canadian Journal of Earth Sciences, Vol. 30, p. 918–927.

Macauley, G., 1983. Source rock-oil shale potential of the Jurassic Kunga Formation, Queen Charlotte Islands; Geological Survey of Canada, Open File Report 921, 52 p. (1 Sheet), https://doi.org/10.4095/129619

Majorowicz, J. and K. Osadetz, 2001. Gas hydrate distribution and volume in Canada; AAPG Bulletin, Vol. 85, No. 7 (July 2001), p. 1211-1230, https://doi.org/10.1306/8626CA9B-173B-11D7-8645000102C1865D

Malinverno, A., Kastner, M., Torres, M.E., and Wortmann, U.G., 2008. Gas hydrate occurrence from pore water chlorinity and downhole logs in a transect across the northern Cascadia margin (Integrated Ocean Drilling Program Expedition 311), Journal of Geophysical Research, 113, B08103, https://doi.org/10.1029/2008JB005702

Mao, S., L. Buxton, Eglinton, J. Whelan, and L. Liu, 1994. Thermal evolution of sediments from Leg 139, Middle Valley, Juan de Fuca Ridge: an organic petrological study. Vol. 139, p. 495-508. https://dx.doi.org/10.2973/odp.proc.sr.139.209.1994

McIver, R.D., 1973. Hydrocarbon gases from canned core samples, Sites 174A, 176, and 180; *in* Kulm, L.D., von Huene, R., et al., Initial Reports of the Deep Sea Drilling Project, Volume 18: Washington (U.S. Government Printing Office), p. 1013.

McManus, D.A., Holmes, M.L., Carson, B., and Barr, S.M., 1972. Late Quaternary tectonics, northern end of Juan de Fuca Ridge; Marine Geology, Vol. 12, p. 141–164.

Meyers, P.A. and Shaw, T.J., 1996. Organic matter accumulation, sulphate reduction and methanogenisis in Pliocene-Pleistocene turbidites on the Iberia Abyssal plain. Whitmarsh, R.B., Sawyer, D.S., Klaus, A., and Masson, D.G. (Eds.), 1996 Proceedings of the Ocean Drilling Program, Scientific Results, Iberia abyssal plain; covering Leg 149 of the cruises of the Drilling Vessel JOIDES Resolution; Balboa Harbor, Panama, to Lisbon, Portugal; sites 897-901, 10 March-25 May 1993. Vol. 149. https://doi.org/10.2973/odp.proc.sr.149.239.1996

Milne, W.G. and Smith, W.E.T., 1966. "Canadian Earthquakes" - Seismological Series, Dominion Observatory, 1960; 1960-2, 1-23, 1961; 1961; 1961-4, 1-24, 1962; 1962; 1962-2, 1-22, 1963; 1963; 1963-4, 1-30, 1966.

Monger, J.W.H., Souther, J.G. and Gabrielse, H., 1972. Evolution of the Canadian Cordillera: a plate tectonic model; American Journal of Science. Vol. 272, p. 577-602.

Moran, K., 2013. Canada's Cabled Ocean Networks Humming Along; EOS, Vol. 94. Issue 2 (January), p. 17-19, https://doi.org/10.1002/2013EO020002

Mulder, T. and Syvitski, J.P., 1995. Turbidity currents generated at river mouths during exceptional discharges to the world oceans; The Journal of Geology, Vol. 103, No. 3, p. 285-99.

Narayan, Y.R., Barnes, C.R., and Johns, M.J. 2005. Taxonomy and biostratigraphy of Cenozoic foraminifers from Shell Canada wells, Tofino Basin, offshore Vancouver Island, British Columbia Canada; Micropaleontology, Vol. 51, No. 2 p.101-167, https://doi.org/10.2113/51.2.101

NOAA National Centers for Environmental Information (October 3, 2017a). Glacial-Interglacial Cycles. Retrieved from: <https://www.ncdc.noaa.gov/abrupt-climate-change/Glacial-Interglacial%20Cycles> [accessed May 28, 2018]

NOAA National Centers for Environmental Information (October 3, 2017b). Heinrich and Dansgaard-Oeschger Events. Retrieved from: <https://www.ncdc.noaa.gov/abrupt-climate-change/Heinrich%20and%20Dansgaard%E2%80%93Oeschger%20Events> [accessed May 28, 2018]

Nedimović, M.R., Bohnenstiehl, D.R., Carbotte, S M., Canales, J.P., and Dziak, R.P., 2009. Faulting and hydration of the Juan de Fuca plate system. Earth and Planetary Science Letters, Vol. 284, Issue 1-2, p. 94-102. https://doi.org/10.1016/j.epsl.2009.04.013

Nelson, A.R., Atwater, B.F., Bobrowsky, P.T., Bradley, L.A., Clague, J.J., Carver,.G.A., Darienzo, M.E., Grant, W C., Krueger, H.W., Sparks, R., Stafford T W., Jr., and Stuiver, M., 1995. Radiocarbon evidence for extensive plate-boundary rupture 300 years ago at the Cascadia subduction zone. Nature, Vol. 378, p. 371-374.

Nelson, C.H., Goldfinger, C., Johnson, J.E., and Dunhill, G., 2000. Variation of modern turbidite systems along the subduction zone margin of Cascadia basin and implications for turbidite reservoir beds; in Deep-Water Reservoirs of the World: GCSSEPM Foundation 20th Annual Research Conference, December 3-6, 2000. p. 714-738.

NRCAN, 2017a. Endeavor Hydrothermal Vents MPA. Retrieved from: http://www.dfo-mpo.gc.ca/oceans/mpa-zpm/endeavour-eng.html

NRCAN, 2017b. Seismic Zones in Western Canada. Retrieved from: http://www.earthquakescanada.nrcan.gc.ca//zones/westcan-en.php

Parrish, R.R., 1983. Cenozoic thermal evolution and tectonics of the Coast Mountains of British Columbia: 1. Fission track dating, apparent uplift rates, and patterns of uplift. Tectonics, Vol. 2, No. 6, p. 601-631.

Pickering, K.T. and Hiscott, R.N., 2016. Deep marine systems: processes, deposits, environments, tectonics and sedimentation, 1st Edition, Wiley & American Geophysical Union, 672 p.

Pohlman, J.W., Caneul, E.A., Chapman, N.R., Spence, G.D., Whiticar, M., and Coffin, R.B., 2005. The origin of thermogenic gas hydrates on the northern Cascadia Margin as inferred from Isotopic ($^{13}C/^{12}C$ and D/H) and molecular composition of hydrate and vent gas; Organic Geochemistry, Vol. 36, Issue 5 (May), p. 703-716, https://doi.org/10.1016/j.orggeochem.2005.01.011

Pohlman, J.W., Kaneko, M., Heuer, V.B., Coffin, R.B., and Whiticar, M., 2009. Methane sources and production in the northern Cascadia margin gas hydrate system. Earth and Planetary Science Letters, Vol. 287, Issues 3–4 (October), p. 504–512, https://doi.org/10.1016/j.epsl.2009.08.037

Posamentier, H.W. and Erskine R.D., 1991. Seismic Expression and Recognition Criteria of Ancient Submarine Fans. In: Weimer P., Link M.H. (eds.) Seismic Facies and Sedimentary Processes of Submarine Fans and Turbidite Systems. Frontiers in Sedimentary Geology. Springer, New York, N.Y.

Raff, A.D. and Mason, R.G., 1961. Magnetic survey off the west coast of North America, 40°N. Latitude to 52°N. Latitude; Geological Society of America, Bulletin, Vol. 72, p. 1267-1270.

Riddihough, R., 1984. Recent movements of the Juan de Fuca Plate System; Journal of Geophysical Research, Vol. 89, Issue B8 (August), p. 6980–6994, https://doi.org/10.1029/JB089iB08p06980

Riedel, M., Collett, T., Malone, M., Akiba, F., Blanc-Valleron, M., Ellis, M., Guerin, G., Hashimoto, Y., Heuer, V., Higasi, Y., Holland, M., Jackson, P., Kaneko, M., Kastner, M., Kim, J.-H., Kitajima, H., Long, P, Malinverno, A., Myers, G., Palekar, L., Pohlman, J., Schultheiss, P., Teichert, B., Torres, M., Tréhu, A., Wang, J., Wortmann, U., and Yoshioka, H., 2006. Gas hydrate transect across northern Cascadia margin. Eos, Trans. Am. Geophys. Union, Vol. 87(33):325. https://doi.org/10.1029/2006EO330002

Riedel, M., Collett, T., Malone, M.J., and IODP Expedition 311 Scientists, 2009. Gas hydrate drilling transect across northern Cascadia margin – IODP Expedition 311; The Geological. Society of London, Special Publications, Vol. 319, No. 1, p.11–19. http://dx.doi.org/10.1144/SP319.2

Riedel, M., Conway, K.W., Côté, M.M., Middleton, G., Neelands, P.J., Obana, K., Saijo, T., Stacey, C.D., Takahashi, T., Terada, I., and Ulmi, M., 2014. Report of Cruise 2014006PGC, SeaJade-II: Seafloor Earthquake Array Japan-Canada Cascadia Experiment, OBS recovery. Geological Survey of Canada, Open File 7715, 27 p. https://doi.org/10.4095/295548

Riedel, M., Côté, M.M., Manning, D., Middleton, G., Murphy, R, Neelands, P.J., Kodaira, S., Terada, I., Yamamoto, Y., and Saijo, T., 2014. Report of Cruise 2013008PGC, SeaJade-II: Seafloor Earthquake Array Japan-Canada Cascadia Experiment OBS deployment and piston coring of slope failures. Geological Survey of Canada, Open File 7716, 65 p. https://doi.org/10.4095/295552

Riedel, M. and Rohr, K. M.M., 2012. Gas hydrate within the Winona Basin, offshore Western Canada; Marine and Petroleum Geology, Vol. 30, Issue 1 (February), p. 66-80, https://doi.org/10.1016/j.marpetgeo.2011.10.009

Rohr, K.M.M., 2015. Plate Boundary Adjustments of the Southernmost Queen Charlotte Fault. Bulletin of the Seismological Society of America. Vol. 105 (2B): p. 1076–1089, https://doi.org/10.1785/0120140162

Rohr, K.M.M. and Dietrich, J., 1990. Deep seismic survey of Queen Charlotte Basin. Geological Survey of Canada, Open File 2258, 1990, 7 sheets, https://doi.org/10.4095/130912

Rohr, K.M.M. and Dietrich, J.R., 1992. Strike-slip tectonics and development of the Tertiary Queen Charlotte Basin, offshore western Canada: evidence from seismic reflection data. Basin Research, Vol. 4, p. 1-19.

Rohr, K.M.M. and Furlong, K.P., 1995. Ephemeral plate tectonics at the Queen Charlotte triple junction. Geology; November 1995; Vol. 23; No. 11; p.1035-1038.

Rohr, K. M.M. and Gröschel-Becker, H., 1994. Correlation of well logs, physical properties, and surface seismic reflection data, Middle Valley, Juan de Fuca Ridge. In Mottl, M.J., Davis, E.E., Fisher, A.T., and Slack, J.F. (Eds.), Proc. ODP, Sci. Results, 139: College Station, TX (Ocean Drilling Program), p. 585-596, doi:10.2973/odp.proc.sr.139.257.1994

Rohr, K.M.M. and Schmidt, U., 1994. Seismic structure of Middle Valley near Sites 855–858, Leg 139, Juan de Fuca Ridge. In Mottl, M.J., Davis, E.E., Fisher, A.T., and Slack, J.F. (Eds.), Proc. ODP, Sci. Results, 139: College Station, TX (Ocean Drilling Program), 3-17. doi:10.2973/odp.proc.sr.139.204.1994

Rohr, K.M.M. and Tryon, A.J., 2010. Pacific-North America plate boundary reorganization in response to a change in relative plate motion: Offshore Canada; Geochemistry, Geophysics, Geosystems G^3, Vol. 11, Issue 6 (June), Q06007, https://doi.org/10.1029/2009GC003019

Rohr, K.M.M., Furlong, K.P., and Riedel, M., *in press*. Serpentinization, methane and intitation of strike slip faults: the Nootka fault zone.

Rona, P.A., Davis, E.E. and Ludwig, R.J., 1998. Thermal properties of TAG hydrothermal precipitates, mid-Atlantic ridge, and comparison with Middle Valley, Juan de Fuca ridge; Proceedings of the Ocean Drilling Program: Scientific Results. Vol. 158, p. 329-335.

RSC Mining & Mineral Exploration (September 26, 2017). World's first success in continuous ore lifting test for seafloor polymetallic sulphides; Retrieved from: <http://www.rscmme.com/all-news/2017/9/26/worlds-first-success-in-continuous-ore-lifting-test-for-seafloor-polymetallic-sulphides> [accessed May 28, 2018]

Ryan, W.B.F., Carbotte, S.M., Coplan, J.O., O'Hara, S., Melkonian, A., Arko, R., Weissel, R.A., Ferrini, V., Goodwillie, A., Nitsche, F., Bonczkowski, J., and Zemsky, R., 2009. Global Multi-Resolution Topography synthesis, Geochemistry, Geophysics, Geosystems, Vol. 10, Issue 3 (March), Q03014, https://doi.org/10.1029/2008GC002332

Ryback, L., 2007. Geothermal sustainability; Geo-Heat Center Quarterly Bulletin Vol. 28, No. 3 (September), p. 2-7, https://www.oit.edu/docs/default-source/geoheat-center-documents/quarterly-bulletin/vol-28/28-3/28-3-art2.pdf

Satake, K., Wang, K., and Atwater, B. F., 2003. Fault slip and seismic moment of the 1700 Cascadia earthquake inferred from Japanese tsunami descriptions. Journal of Geophysical Research, Vol. 108, No. B11, ESE 7 P.1 7-17.

Scherer, F.C., 1981: Exploration in East Malaysia over the past decade; *in* Halbouty, M.T., (ed.), Giant oil and gas fields of the decade.1968-1978. AAPG, Memoir 30, p 423-440.

Scherwath, M., Riedel, M., Roemer, M., Juniper, K., Heesemann, M., Mihaly, S., Paull, C., Spence, G.D., and Veloso, M., 2017a. Continental shelf and slope gas venting off Cascadia; Geophysical Research Abstracts EGU General Assembly 2017 Vol. 19, EGU2017-10448.

Scherwath, M., Riedel, M., Roemer, M., Thomsen, L., Chatzievangelou, D., Juniper, S.K., Heesemann, M., and Mihaly, S., 2017b. Advantages of long-term multidisciplinary ocean observations for gas hydrate systems – Examples from Ocean Networks Canada; *in* EGU General Assembly 2017, (Vienna: European Geosciences Union).

Scherwath, M., Riedel, M., Spence, G.D., and Hyndman, R.D., 2006. Data report: seismic structure beneath the north Cascadia drilling transect of IODP Expedition 311; *in* Riedel, M., Collett, T.S., Malone, M.J., and the Expedition 311 Scientists, Proc. IODP, 311: Washington, DC (Integrated Ocean Drilling Program Management International, Inc.). doi:10.2204/iodp.proc.311.110.2006

Schneider, F., Dubille, M., and Montafert, L., 2016. Modeling of microbial gas generation: application to the eastern Mediterranean "Biogenic Play." Geologica Acta, Vol.14, No. 4 (December), p. 403-417, https://doi.org/10.1344/GeologicaActa2016.14.4.5

Schümann, T.K., Rohr, K.M.M., and Whiticar, M. J., 2013. 2D petroleum systems modeling of Queen Charlotte Basin, offshore British Columbia, Canada. Bulletin of Canadian Petroleum Geology, Vol. 61 (1), p. 65-82. http://bcpg.geoscienceworld.org/content/61/1/65.abstract

Schümann, T.K., Whiticar, M.J., and Rohr, K.M.M., 2008. Petroleum Resource Potential of the Tofino Basin. Report prepared by University of Victoria and the Ministry of Energy, Mines and Petroleum Resources (MEMPR). 60 p. Retrieved from http://bcpg.geoscienceworld.org/content/61/1/65.abstract

Scott, S.D., 2001. (Unpub.) Mineral Development Scoping Study for the Proposed Endeavour Hot Vents Marine Protected Area; Report prepared for Natural Resources Canada. April 1 2001.

Shaw, J., Stacey, C.D., Wu, Y., and Lintern, D.G., 2017. Anatomy of the Kitimat Fjord system, British Columbia; Geomorphology, Vol. 293, Part A (September), p.108-129, https://doi.org/10.1016/j.geomorph.2017.04.043

Shipboard Scientific Party, 1992a. Site 855; *in* Davis, E.E., Mottl, M.J., Fisher, A.T., et al., Proc. ODP, Init. Repts., 139: College Station, TX (Ocean Drilling Program), p. 101-160. doi:10.2973/odp.proc.ir.139.105.1992

Shipboard Scientific Party, 1992b. Site 856. In Davis, E.E., Mottl, M.J., Fisher, A.T., et al., Proc. ODP, Init. Repts., 139: College Station, TX (Ocean Drilling Program), p. 161-281. doi:10.2973/odp.proc.ir.139.106.1992

Shipboard Scientific Party, 1992c. Site 857. In Davis, E.E., Mottl, M.J., Fisher, A.T., et al., Proc. ODP, Init. Repts., 139: College Station, TX (Ocean Drilling Program), p. 283-429. doi:10.2973/odp.proc.ir.139.107.1992

Shipboard Scientific Party, 1992d. Site 858. In Davis, E.E., Mottl, M.J., Fisher, A.T., et al., Proc. ODP, Init. Repts., 139: College Station, TX (Ocean Drilling Program), p. 431- 569. doi:10.2973/odp.proc.ir.139.108.1992

Shipboard Scientific Party, 1994a. Site 888. In Westbrook, G.K., Carson, B., Musgrave, R.J., et al., Proc. ODP, Init. Repts., 146 (Pt. 1): College Station, TX (Ocean Drilling Program), p. 55–125. doi:10.2973/odp.proc.ir.146-1.007.1994

Shipboard Scientific Party, 1994b. Sites 889 and 890. In Westbrook, G.K., Carson, B., Musgrave, R.J., et al., Proc. ODP, Init. Repts., 146 (Pt. 1): College Station, TX (Ocean Drilling Program), p. 127-239. doi:10.2973/odp.proc.ir.146-1.008.1994

Shipboard Scientific Party, 1997a. Hydrothermal transition transect (Sites 1023, 1024, and 1025); *in* Davis, E.E., Fisher, A.T., Firth, J.V., et al., Proc. ODP, Init. Repts., 168: College Station, TX (Ocean Drilling Program), p. 49–100. doi:10.2973/odp.proc.ir.168.104.1997

Shipboard Scientific Party, 1997b. Rough basement transect (Sites 1026 and 1027). In Davis, E.E., Fisher, A.T., Firth, J.V., et al., Proc. ODP, Init. Repts., 168: College Station, TX (Ocean Drilling Program), p. 101–160. doi:10.2973/odp.proc.ir.168.105.1997

Shipboard Scientific Party, 1997c. Buried basement transect (Sites 1028, 1029, 1030, 1031, and 1032). In Davis, E.E., Fisher, A.T., Firth, J.V., et al., Proc. ODP, Init. Repts., 168: College Station, TX (Ocean Drilling Program), p. 161–12. doi:10.2973/odp.proc.ir.168.106.1997

Simoneit, B.R.T., 1994. Lipid/bitumen maturation by hydrothermal activity in sediments of Middle Valley, Leg 139. In Mottl, M.J., Davis, E.E., Fisher, A.T., and Slack, J.F. (Eds.), Proc. ODP, Sci. Results, 139: College Station, TX (Ocean Drilling Program), p. 447- 465. doi:10.2973/odp.proc.sr.139.237.1994.

Spence, G.D. and Riedel, M., 2014. Report of Cruise 2010005PGC, C.C.G. Vessel John P. Tully, 22 September - 2 October 2010, SeaJade-I Seafloor Earthquake Array Japan-Canada Cascadia Experiment, ocean bottom seismometer deployment and active-source airgun refraction and reflection program; Geological Survey of Canada, Open File 7558, 2014, 50 p., https://doi.org/10.4095/295546

Spence, G.D., Hyndman, R.D., Davis, E.E., and Yorath, C.J., 1991a. Seismic structure of the northern Cascadia accretionary prism: Evidence from new multichannel seismic reflection data; *in* Meissner, R., Brown, L., Durbaum, H. J., Franke, W. Fuchs, K. and Seifert, F. (Eds.), Continental Lithosphere: Deep Seismic Reflections, Geodynamics Series Vol. 22, p. 257-263, https://doi.org/10.1029/gd022p0257

Spence, G D., Hyndman, R.D., Langton, S., Yorath, C.J., and Davis, E.E., 1991b. Multichannel Seismic Reflection Profiles across the Vancouver Island Continental Shelf and Slope. Geological Survey of Canada, Open File 2391, 41 p. (12 sheets), https://doi.org/10.4095/132398

Spinelli G.A. and Fisher A.T., 2004. Hydrothermal circulation within rough basement on the Juan de Fuca Ridge flank. Geochemistry, Geophysics, Geosystems G^3, Vol. 5, Issue 2 (February), p. Q02001, https://doi.org/10.1029/2003GC000616

Srivastava, S., Barrett, D., Keen, C., Manchester, K., Shih, K., Tiffin, D., Chase, R., Thomlinson, A., Davis, E., and Lister, C., 1971. Preliminary analysis of geophysical measurements north of Juan de Fuca ridge; Canadian Journal of Earth Sciences, Vol. 8, No. 10, p. 1265-81.

Steel, R.R.R., 1998. Architecture of marine rift-basin successions, AAPG Bulletin, Vol. 82, No. 1, p. 110-146.

SubseaWorldNews (September 28, 2017). Japan starts Mining Hydrothermal Deposits. Retrieved from: https://subseaworldnews.com/2017/09/28/japan-starts-mining-hydrothermal-deposits/

Suess, E., Kulm, L.D., and Killingley, J.S., 2014. Coastal upwelling and a history of organic-rich mudstone deposition off Peru. From: Brooks, J. & Fleet, A. J. (eds) 1987, Marine Petroleum Source Rocks Geological Society Special Publication No. 26 p. 181-197.

Snowdon, L.R., Fowler, M.G., Osadetz, K.G., and Obermajer, M., 2002. Organic geochemical data from petroleum sources and shows in the Queen Charlotte Basin and adjacent areas of the Pacific margin of Canada. Geological Survey of Canada Open File Report 4367, https://doi.org/10.4095/213655

Su, X., Baumann, K.-H., and Thiede, J., 2000. Calcareous nannofossils from Leg 168: biochronology and diagenesis. In Fisher, A.T., Davis, E.E., and Escutia, C. (Eds.), Proc. ODP, Sci. Results, 168: College Station, TX (Ocean Drilling Program), 39-49. doi:10.2973/odp.proc.sr.168.015.2000.

Sun, Y.F., 2000. Core-log-seismic integration in hemipelagic marine sediments on the eastern flank of the Juan de Fuca Ridge. In Fisher, A.T., Davis, E.E., and Escutia, C. (Eds.), Proc. ODP, Sci. Results, 168: College Station, TX (Ocean Drilling Program), p. 21-35. doi:10.2973/odp.proc.sr.168.009.2000

Tipsword, H. L., F.M. Setzer, and F.L. Smith, Jr., 1966, Interpretation of depositional environment in Gulf Coast petroleum exploration from paleoecology and related stratigraphy: Transactions of the Gulf Coast Association of Geological Societies, Vol. 16, p. 119-130.

Tornos, F., Peter, J., Allen, R., Conde, C., 2015. Controls on the siting and style of volcanogenic massive sulphide deposits. Ore Geol. Rev. Vol. 68, p. 142-163. http://dx.doi.org/10.1016/j.oregeorev.2015.01.003

Triezenberg, P.J., Hart, P.E., and Childs, J.R., 2016. The National Archive of Marine Seismic Surveys (NAMSS): A USGS data website of marine seismic reflection data within the U.S. Exclusive Economic Zone (EEZ): U.S. Geological Survey Data Release, https://doi.org/10.5066/F7930R7P

Underwood, M.B. and Hoke, K.D., 2000. Composition and provenance of turbidite sand and hemipelagic mud in northwestern Cascadia Basin; *in* Fisher, A.T., Davis, E.E., and Escutia, C. (Eds.), Proceedings of the Ocean Drilling Program (ODP), Scientific Results, Vol. 168, College Station, Texas (Ocean Drilling Program), p. 51-65, doi:10.2973/odp.proc.sr.168.012.2000

Underwood, M.B., Hoke, K.D., Fisher, A.T., Davis, E.E., Giambalvo, E., Zühlsdorff, L., and Spinelli, G. A., 2005. Provenance, stratigraphic architecture, and hydrogeologic influence of turbidites on the mid-ocean ridge flank of northwestern Cascadia Basin, Pacific Ocean; Journal of Sedimentary Research, Vol. 75, No. 1 (January), p. 149-164, https://doi.org/10.2110/jsr.2005.012

Vellutini, D., 1988. Organic maturation and source rock potential of Mesozoic and Tertiary strata, Queen Charlotte Islands, British Columbia. University of British Columbia. Retrieved from https://circle.ubc.ca/handle/2429/28526

Vellutini, D. and Bustin, R.M., 1990. Organic maturation of Mesozoic and Tertiary strata, Queen Charlotte Islands, British Columbia. Bulletin of Canadian Petroleum Geology, Vol. 38 (4), p. 452-474.

Vellutini, D., Bustin, R.M., and Goodarzi, F., 1990. Source rock potential of Mesozoic and Tertiary strata, Queen Charlotte Islands, British Columbia; Bulletin of Canadian Petroleum Geology, Vol. 38 (4), p. 440–451.

Ventura, G.T., Simoneit, B.R.T., Nelson, R.K., and Reddy, C.M., 2012. The composition, origin and fate of complex mixtures in the maltene fractions of hydrothermal petroleum assessed by comprehensive two-dimensional gas chromatography; Organic Geochemistry, Vol. 45 (April), p. 48-65, https://doi.org/10.1016/j.orggeochem.2012.01.002

Walton, M.A.L., Gulick, S.P.S., Reece, R.S., Barth, G.A., Christeson, G.L., and Van Avendonk, H.J.A., 2014. Dynamic response to strike-slip tectonic control on the deposition and evolution of the Baranof Fan, Gulf of Alaska. Geosphere; Vol. 10; No. 4; p. 680–691; https://doi.org/10.1130/GES01034.1

Wang, K., He, J., and Davis, E.E., 1997. Influence of basement topography on hydrothermal circulation in sediment-buried igneous oceanic crust. Earth and Planetry Science Letters, Vol. 146, Issues 1-2 (January), p.151-164, https://doi.org/10.1016/S0012-821X(96)00213-0

Westbrook, G.K., Carson, B., and Shipboard Scientific Party, 1994. Summary of Cascadia drilling results; *in* Westbrook, G.K., Carson, B., Musgrave, R.J., et al.,Proceedings of the Ocean Drilling Program (ODP), Initial Reports, Vol. 146 (Part 1): College Station, TX (Ocean Drilling Program), p. 389-396, doi:10.2973/odp.proc.ir.146-1.012.1994

Wheat, C.G., Mottl, M.J., Fisher, A.T., Kadko, D., Davis, E.E., and Baker, E., 2004. Heat flow through a basaltic outcrop on a sedimented young ridge flank. Geochemistry, Geophysics, Geosystems, G^3, Vol. 5, Issue 12 (December), 18 p., https://doi.org/10.1029/2004GC000700

Whiticar, M.J., Faber, E., Whelan, J.K., and Simoneit, B.R.T., 1994. Thermogenic and bacterial hydrocarbon gases (free and sorbed) in Middle Valley, Juan de Fuca Ridge, Leg 139; *in* Mottl, M.J., Davis, E.E., Fisher, A.T., and Slack, J.F. (Eds.), Proc. ODP, Sci. Results, 139: College Station, TX (Ocean Drilling Program), p. 467-477, doi:10.2973/odp.proc.sr.139.241.1994

Whiticar, M.J., Hovland, M., Kastner, M., and Sample, J.C., 1995. Organic geochemistry of gases, fluids, and hydrates at the Cascadia accretionary margin. In Carson, B., Westbrook, G.K., Musgrave, R.J., and Suess, E. (Eds.), Proc. ODP, Sci. Results, 146 (Pt. 1): College Station, TX (Ocean Drilling Program), p. 385–397. doi:10.2973/odp.proc.sr.146-1.247.1995

Wilson, D.S., 1988. Tectonic history of the Juan de Fuca Ridge over the last 40 million years; Journal of Geophysical Research Solid Earth, Vol. 33, Issue B10 (October), p. 11863-11876, https://doi.org/10.1029/JB093iB10p11863

Wilson, D.S., 1993. Confidence intervals for motion and deformation of the Juan de Fuca Plate; Journal of Geophysical Research Solid Earth, Vol. 98, Issue B9 (September), p. 16053-16071, https://doi.org/10.1029/93JB01227

Wilson, D.S., 2002. The Juan de Fuca plate and slab: isochron structure and Cenozoic plate motions; *in* Kirby, S., Wang, K., Dunlop, S. (Eds.), The Cascadia subduction zone and related subduction systems - seismic structure, intraslab earthquakes and processes, and earthquake hazards; U.S. Geol. Survey Open-File Report 02-328 and Geological Survey of Canada Open File 4350, p. 9-12, https://doi.org/10.4095/222387

Yorath, C. and Hyndman, R., 1983. Subsidence and thermal history of Queen Charlotte Basin; Canadian Journal of Earth Sciences, Vol. 20, No. 1, p. 135-59, https://doi.org/10.1139/e83-013

Yorath, C.J., Clowes, R.M., Macdonald, R.D., Spencer, C., Davis, E.E., Hyndman, R.D., Rohr, K.M.M., Sweeney, J.F., Currie, R.G., Halpenny, J.F., and Seemann, D.A., 1987. Marine multichannel seismic reflection, gravity and magnetic profiles, Vancouver Island, continental margin and Juan de Fuca Ridge. Geological Survey of Canada, Open File 1661, 26 p. (7 sheets), https://doi.org/10.4095/122447

Yuan, T., Spence, G.D., Hyndman, R.D., 1994. Seismic velocities and inferred porosities in the accretionary wedge sediments at the Cascadia margin, Journal of Geophysical Research Solid Earth, Vol. 99, Issue B3 (March), p. 4413-4427, https://doi.org/10.1029/93JB03203

Zabanbark, A. and Konyukhov, A.I., 2005. Petroleum Potential of Continental Slopes in the World Ocean: Tectonic Aspect. Geotectonics, Vol. 39, No. 1, 2005, p. 87-93. Translated from Geotektonika, No. 1, 2005, p. 99–106.

Zühlsdorff, L. and Spiess, V., 2001. Modeling seismic reflection patterns from Ocean Drilling Program Leg 168 core density logs: Insight into lateral variations in physical properties and sediment input at the eastern flank of the Juan de Fuca Ridge; Journal of Geophysical Research Solid Earth, Vol. 106, Issue B8 (August), p. 16119-16134, https://doi.org/10.1029/2001JB900005

Zühlsdorff, L., Spiess, V., Huebscher, C., and Breitzke, M., 1999. Seismic reflectivity anomalies in sediments on the eastern flank of the Juan de Fuca Ridge: evidence for fluid migration?; Journal of Geophysical Research Solid Earth, Vol. 104, Issue B7 (July), p. 15351-15364, https://doi.org/10.1029/1999JB900061

LIST OF FIGURES

LIST OF TABLES